

**ISTANBUL TECHNICAL UNIVERSITY ★ GRADUATE SCHOOL OF SCIENCE**  
**ENGINEERING AND TECHNOLOGY**

**MECHANICAL ENHANCEMENT OF WOVEN COMPOSITE WITH VERTICAL  
ALIGNED CARBON NANOTUBES: INVESTIGATION OF INTERLAMINAR SHEAR  
STRENGTH PROPERTY OF NANO-STITCHED LAMINATED COMPOSITES**

**M.Sc. THESIS**

**İdris GÜRKAN**

**Department of Aeronautics and Astronautics Engineering**

**Aeronautics and Astronautics Engineering Programme**

**JANUARY 2015**



**ISTANBUL TECHNICAL UNIVERSITY ★ GRADUATE SCHOOL OF SCIENCE**  
**ENGINEERING AND TECHNOLOGY**

**MECHANICAL ENHANCEMENT OF WOVEN COMPOSITE WITH VERTICAL  
ALIGNED CARBON NANOTUBES: INVESTIGATION OF INTERLAMINAR SHEAR  
STRENGTH PROPERTY OF NANO-STITCHED LAMINATED COMPOSITES**

**M.Sc. THESIS**

**İdris GÜRKAN  
511111119**

**Department of Aeronautics and Astronautics Engineering**

**Aeronautics and Astronautics Engineering Programme**

**Thesis Advisor: Asst. Prof. Dr. Hulya Cebeci**

**JANUARY 2015**



**İSTANBUL TEKNİK ÜNİVERSİTESİ ★ FEN BİLİMLERİ ENSTİTÜSÜ**

**KARBON NANOTÜPLER KULLANILARAK KOMPOZİTLERİN MEKANİK  
ÖZELLİĞİNİN GELİŞTİRİLMESİ: NANO-DİKİŞLİ LAMİNE KOMPOZİTLERİN  
LAMİNELER ARASI KAYMA MUKAVEMETİNİN İNCELENMESİ**

**YÜKSEK LİSANS TEZİ**

**İdris GÜRKAN  
(511111119)**

**Uçak ve Uzay Mühendisliği Anabilim Dalı**

**Uçak ve Uzay Mühendisliği**

**Tez Danışmanı: Yrd. Doç. Dr. Hülya CEBECİ**

**OCAK 2015**



**İdris Gürkan**, a **M.Sc.** student of ITU **Graduate School of Science Engineering and Technology** student ID **51111119**, successfully defended the **thesis** entitled **“MECHANICAL ENHANCEMENT OF WOVEN COMPOSITE WITH VERTICAL ALIGNED CARBON NANOTUBES: INVESTIGATION OF INTERLAMINAR SHEAR STRENGTH PROPERTY OF NANO-STITCHED LAMINATED COMPOSITES”**, which he prepared after fulfilling the requirements specified in the associated legislations, before the jury whose signatures are below.

**Thesis Advisor :**     **Asst. Prof. Dr. Hulya CEBECI**                     .....  
İstanbul Technical University

**Jury Members :**     **Prof. Dr. Halit S. TURKMEN**                     .....  
İstanbul Technical University

**Asst. Prof. Dr. Nuri SOLAK**                     .....  
İstanbul Technical University

**Date of Submission :**   **15 December 2014**

**Date of Defense :**      **23 January 2015**





*To my family,*



## **FOREWORD**

This thesis is the last part of my three years graduate degree in Aeronautical Engineering at Istanbul Technical University. This research was executed as a project by collaboration of TUBITAK.

Firstly, I would like to show my special gratitude and appreciation to my supervisors, Assist. Prof. Dr. Hülya Cebeci, for contributing valuable and inspiring advices, and feedback on my works during the project term. Moreover, I would like to thank Assist. Prof. Dr. Fevzi Ç. CEBECİ, Dilek ÇAKIROĞLU and support of SUNUM Laboratory colleagues for giving me an opportunity using the devices for production and characterization of CNTs. Furthermore, I would like to thank Müslüm Çakır for helps to performed mechanical tests. Lastly, I would like to thank to office number 307 colleagues for always motivating and supporting me during project studies.

December 2014

İdris GÜRKAN  
(Project Engineer)



## TABLE OF CONTENTS

	<u>Page</u>
<b>FOREWORD</b> .....	<b>ix</b>
<b>TABLE OF CONTENTS</b> .....	<b>xi</b>
<b>ABBREVIATIONS</b> .....	<b>xiii</b>
<b>LIST OF TABLES</b> .....	<b>xv</b>
<b>LIST OF FIGURES</b> .....	<b>xvii</b>
<b>SUMMARY</b> .....	<b>xix</b>
<b>ÖZET</b> .....	<b>xxi</b>
<b>1. INTRODUCTION</b> .....	<b>1</b>
1.1 Nano-Engineered Composites Using Carbon Nanotubes .....	1
1.2 Motivation .....	2
<b>2. LITERATURE RESEARCH</b> .....	<b>3</b>
2.1 CNTs Fundamentals .....	3
2.1.1 Chemical structure .....	4
2.1.2 CNTs synthesis .....	5
2.1.3 Mechanical properties .....	9
2.2 Polymer Nano-Composites (PNCs) .....	10
2.3 Fiber Reinforced Plastic Composites (FRPs).....	10
2.4 Nano-Engineered Composites (NECs).....	11
2.4.1 CNTs as a nano-fillers (NFs) .....	13
2.4.2 Transfer of A-CNTs arrays onto prepreg lamina .....	15
2.5 CNTs for Aerospace Application .....	15
2.6 Optimization by Taguchi Method .....	17
<b>3. SYNTHESIS AND CHARACTERIZATION OF ALIGNED AND PATTERNED CNTs STRUCTURES</b> .....	<b>19</b>
3.1 Synthesis of CNTs.....	19
3.2 Characterization of CNTs.....	26
3.2.1 Scanning electron microscopy .....	26
3.2.2 Transmission electron microscopy.....	27
3.2.3 Raman spectroscopy .....	28
3.2.4 Thermal gravimetric analysis.....	28
3.3 Micro-Device Fabrication .....	31
<b>4. FABRICATION AND SHORT BEAM SHEAR TESTING (SBS) OF NF and STITCHED NANO-ENGINEERED COMPOSITES (S-NEC)</b> .....	<b>37</b>
4.1 Parametric Study of NF Prepreg Plies and S-NEC by Epoxy Types .....	37
4.1.1 Materials.....	38
4.1.2 Customized prepreg manufacturing of S-NEC .....	40
4.1.3 Fabricating of S-NEC laminates .....	44
4.2 Mechanical Properties Investigation of S-NEC with SBS .....	47
<b>5. RESULTS</b> .....	<b>51</b>
5.1 SBS Results .....	51
5.2 Electrical Conductivity Analysis.....	61

<b>6. CONCLUSIONS AND FUTURE WORK .....</b>	<b>63</b>
<b>REFERENCES .....</b>	<b>65</b>
<b>APPENDICES .....</b>	<b>69</b>
APPENDIX A : SBS results.....	69
<b>CURRICULUM VITAE.....</b>	<b>71</b>

## **ABBREVIATIONS**

<b>A-CNTs</b>	: Aligned Carbon Nanotubes
<b>AFM</b>	: Atomic Force Microscopy
<b>CF</b>	: Carbon Fiber
<b>CNTs</b>	: Carbon Nanotubes
<b>CVD</b>	: Chemical Vapor Deposition
<b>DWNTs</b>	: Double-Wall Carbon Nanotubes
<b>FRPs</b>	: Fiber Reinforced Plastics
<b>ILSS</b>	: Interlaminar Shear Strength
<b>IPA</b>	: Isopropyl Alcohol
<b>MWNTs</b>	: Multi-Wall Carbon Nanotubes
<b>NECs</b>	: Nano Engineered Composites
<b>NFs</b>	: Nano-Fillers
<b>OP</b>	: Optical Microscopy
<b>PA-CNTs</b>	: Patterned Aligned Carbon Nanotubes
<b>PDMS</b>	: Polydimethylsiloxane
<b>PNCs</b>	: Polymer Nano Composites
<b>PVD</b>	: Physical Vapor Deposition
<b>SBS</b>	: Short Beam Shear
<b>SCCM</b>	: Standard Cubic Centimeters per Minute
<b>SEM</b>	: Scanning Electron Microscopy
<b>S-NEC</b>	: Stitched Nano Engineered Composite
<b>SWNTs</b>	: Single-Wall Carbon Nanotubes
<b>SHM</b>	: Structural Health Monitoring
<b>TEM</b>	: Transmission Electron Microscopy
<b>TGA</b>	: Thermal Gravity Analysis
<b>UAVs</b>	: Unmanned Aerial Vehicles
<b>VIP</b>	: Vacuum Infusion Process





## LIST OF TABLES

<b>Table 2.1 :</b> Comparison of the established techniques for CNTs synthesis.....	6
<b>Table 2.2 :</b> Improvements in the interlaminar shear strength of CNT-based hierarchical composites .....	12
<b>Table 2.3 :</b> Some potential roles of CNTs in aeronautics.....	16
<b>Table 3.1 :</b> CNTs growth optimization parameters.....	21
<b>Table 3.2 :</b> An example A-CNTs growth protocol.....	22
<b>Table 3.3 :</b> Raman results of optimization design.....	28
<b>Table 3.4 :</b> TGA results of optimization study.....	30
<b>Table 4.1 :</b> Taguchi L8 orthogonal array parameters and levels.....	38
<b>Table 4.2 :</b> Taguchi L8 orthogonal array design.....	38
<b>Table 5.1 :</b> ILSS of CNTs/carbon/epoxy composites measured by SBS.....	51
<b>Table 5.2 :</b> SBS test results of Taguchi L8 orthogonal array design.....	54
<b>Table 5.3 :</b> Response table for signal to noise ratios (larger is better).....	58
<b>Table 5.4 :</b> Electrical conductivity results of Taguchi L8 orthogonal array design..	61



## LIST OF FIGURES

	<u>Page</u>
<b>Figure 2.1</b> : Trends in CNTs research and commercialization .	3
<b>Figure 2.2</b> : Typical carbon nanotube structures (a) SWNTs and (a) MWNTs.	4
<b>Figure 2.3</b> : Schematic diagram showing (a) a hexagonal graphite sheet, the atomic structure of (b) an armchair and (c) a zig-zag nanotube .	5
<b>Figure 2.4</b> : Schematic illustration of CVD.	7
<b>Figure 2.5</b> : Widely-accepted growth mechanisms for CNTs: (a) tip-growth model, (b) base-growth model.	8
<b>Figure 2.6</b> : Strategies to enhancement the properties of FRPs using CNT (a) in matrix, (b) fuzzy fiber, (c) bucky paper and nano-stitch.	13
<b>Figure 2.7</b> : Carbon nanotube publications with the keywords aerospace and aircraft, between the years 2000 and 2013.	16
<b>Figure 3.1</b> : A-CNTs growth by CVD method.	20
<b>Figure 3.2</b> : Picture of customized CVD system.	22
<b>Figure 3.3</b> : An example of pattern sketch.	23
<b>Figure 3.4</b> : Schematic illustration of chrome mask.	23
<b>Figure 3.5</b> : The mask treatment steps.	24
<b>Figure 3.6</b> : Patterned CNTs (a) Illustration of 4 inches photomask, (b) optical image of a fabricated photomask, (c) an optical image of PA-CNTs.	24
<b>Figure 3.7</b> : Schematic illustration of substrate preparation.	25
<b>Figure 3.8</b> : Coating steps for patterned samples.	26
<b>Figure 3.9</b> : An example SEM images of A-CNTs synthesized by CVD method.	27
<b>Figure 3.10</b> : An example TEM images of A-CNTs synthesized by CVD method.	27
<b>Figure 3.11</b> : Raman graphs of the optimization study.	29
<b>Figure 3.12</b> : TGA graphs of the optimization study.	30
<b>Figure 3.13</b> : Schematic view of micro device.	33
<b>Figure 3.14</b> : Image of prepared mold for isolating micro-device.	33
<b>Figure 3.15</b> : Adhesive testing between PDMS mold and substrate.	34
<b>Figure 3.16</b> : Nano-composite side-wall schematic illustration.	34
<b>Figure 3.17</b> : An example view of nano-composite side-wall molding.	35
<b>Figure 3.19</b> : Display of the processed substrate using laser.	35
<b>Figure 4.1</b> : An example of different length A-CNTs SEM image (a) short CNTs (b) long CNTs.	39
<b>Figure 4.2</b> : Stages of magnetic stirrer process.	40
<b>Figure 4.3</b> : Illustration of RTM 6 dispersion.	41
<b>Figure 4.4</b> : Schematic view of CNTs prepreg manufacturing.	42
<b>Figure 4.5</b> : An example illustration of CNTs transfer-printed on commercial prepreg.	42
<b>Figure 4.6</b> : An optimization study for fully transferring A-CNTs on customize prepreps.	43
<b>Figure 4.7</b> : A view of patterned nano-stitch on customize prepreg ply.	43

<b>Figure 4.8</b> : Schematic illustration of manufacturing methods of laminates (a) vacuum infusion (b) hand lay-up [6].	44
<b>Figure 4.9</b> : Schematic illustration of modified hand lay-up method.	45
<b>Figure 4.10</b> : Schematic illustration of vacuum infusion process.	46
<b>Figure 4.11</b> : Bottom surface view of poor wetted composite using VIP.	46
<b>Figure 4.12</b> : Schematic visualization of resistance measurement.	47
<b>Figure 4.13</b> : SBS test specimen being tested under load.	48
<b>Figure 4.14</b> : Typical failure modes in short beam shear test	49
<b>Figure 4.15</b> : Typical time-short beam strength graph.	49
<b>Figure 5.1</b> : SB strength versus displacement for laminated composites samples.	52
<b>Figure 5.2</b> : An example view of crack propagation of S-NEC with 200 $\mu$ m long A-CNTs after SBS test.	52
<b>Figure 5.3</b> : Chart of ILSS of the NECs.	53
<b>Figure 5.4</b> : SB strength versus time for NECs samples.	54
<b>Figure 5.5</b> : SBS fracture surface image of (a) marine epoxy and (b) aerospace epoxy NECs using optical microscopy.	55
<b>Figure 5.6</b> : SBS fracture surface of aerospace laminates, (a) epoxy fracture along tows, (b) low and (c) high magnification of pulled out of fracture surface in NECs laminates.	56
<b>Figure 5.7</b> : SBS fracture surface of marine laminates, (a) epoxy fracture along tows, (b) low and (c) high magnification of pulled out of fracture surface in NECs laminates.	57
<b>Figure 5.8</b> : Pull-out mechanism of S-NECs.	59
<b>Figure 5.9</b> : Main effects plots for S/N ratios.	60
<b>Figure 5.10</b> : SB strength versus time for ninth experiment.	60
<b>Figure 5.11</b> : Chart illustration of results of Taguchi L8 orthogonal array design.	61
<b>Figure 5.12</b> : Electrical conductivity through the thickness.	62
<b>Figure 6.1</b> : Fuzzy fiber SEM image.	64
<b>Figure A.1</b> : Aerospace type epoxy experimental design results (a)First. (b)Second. (c)Third. (d)Fourth.	69
<b>Figure A.2</b> : Marine type epoxy experimental design results (a)Fifth. (b)Sixth. (c)Seventh. (d)Eighth.	70

# **MECHANICAL ENHANCEMENT OF WOVEN COMPOSITE VERTICAL ALIGNED CARBON NANOTUBES: INVESTIGATION OF INTERLAMINAR SHEAR STRENGTH PROPERTY OF NANO-STITCHED LAMINATED COMPOSITES**

## **SUMMARY**

Vertically aligned carbon nanotubes (A-CNTs) that are added into carbon fiber reinforced polymer matrix composite can significantly improve not only mechanical but also electrical properties of composites and called as hybrid or nano-engineered composite. Three common methods such as dispersion of CNTs into the polymer matrix, stitching them onto carbon fibers and synthesis CNTs onto fibers (fuzzy) are used to produce hybrid composites. In this study, A-CNTs which are synthesized using thermal chemical vapor deposition (CVD) are integrated by stitching directly onto carbon fiber surface after fabrication of custom made prepreg layers with carbon fibers. The custom made prepreg layers are made of nanotube reinforced epoxy matrix and carbon fibers. At the same time in this project, instead of performing higher number of experiments, experimental design which is called Taguchi L<sub>8</sub> orthogonal array is preferred and also only 8 experiments (each experiment is repeated at least 5 times) are performed according to Taguchi design. At this design 7 different parameters which has 2 levels of each one are examined. Manufacturing method, epoxy type, dispersion solvent type, dispersed amount of CNT in epoxy and stitch types are selected as parameters.

A-CNTs are synthesized on a Si substrate using CVD of C<sub>2</sub>H<sub>4</sub>/H<sub>2</sub> at atmospheric pressure. The length of A-CNTs which is used to fabricate hybrid composites are around 80 μm with Raman measurements of (G/D ratio) about 2. During the hybrid composite fabrication A-CNTs are removed from the substrate without any damage with an easy delamination growth protocol and fully transferred onto the middle bidirectional carbon fiber ply. Three most important steps of the study can be summarized as the transfer printing of CNTs from substrate to reinforcement ply without disturbing orientation, homogeneous distribution of A-CNTs into epoxy and application of the mixture into the system. In our earlier studies, unmodified A-CNTs are dispersed using homogenizer and tip types ultrasonication in epoxy and alcohol (IPA, acetone etc.) respectively. After removed alcohol (if necessary) all dispersed CNTs are mixed using mechanical mixer in a low viscosity thermosetting resins which are consisted two components and a high viscose thermosetting resin (has a component). But some agglomerations are seen in these methods, so in this project magnetic stirrer is used for dispersion and achieved CNTs which is also called as bucky paper and this paper can be easily disperse to individual CNTs. This approach generally has the advantages of simplicity and high amount of CNTs can be dispersed on the contrary tip sonicator. A uniform distribution of CNTs during wetting is critical for composite properties. Samples are produced using hand lay-up/vacuum, and vacuum infusion process (VIP). Hand lay-up/vacuum and vacuum assisted resin

infusion molding are a very attractive, cost effective and environmentally friendly method of processing composites. Experiments are performed to compare fracture behavior of the hierarchical composite with and without A-CNT.

For the mechanical properties interlaminar shear strength (ILSS) of the samples are measured by short beam shear (SBS) test. In earlier reports it is stated that carbon nanotube reinforced composites have showed an improvement of 8-30% interlaminar shear strength by short beam tests. The addition of A-CNTs onto the carbon nanotube reinforced matrix and fiber composite is expected to show higher interlaminar shear strength properties. On the other hand before the experiments, the electrical conductivity of all samples are measured, to assess the potential as sensors for strain sensing for structural health monitoring (SHM). The stitch A-CNTs effects is investigated on the mechanical and electrical properties of composite as well as dispersed CNTs in epoxy.

In the other section of thesis, vertically aligned multi walled carbon nanotubes (A-MWNTs) are synthesized with CVD method to create small dimension pore sized ultra narrow nano-exchangers for nano-particle and gas transfer through channels. As-grown A-MWNTs would have <2% volume fraction after the growth procedure and the rest is air (~98%). These structures would have high porosity and high permeability due to their structures with the CNT-CNT spacing between 80-100 nm depending on the catalyst and precursor system coupling. A micro device are fabricated with this A-MWNT and the nano-particle and gas exchange transfer will be studied with this context. The growth of A-MWNTs will be either in a continuous fashion as arrays or templated pillars that will help to characterize the effects of morphology on the efficiency of micro-device.

# **KARBON NANOTÜPLER KULLANILARAK KOMPOZİTLERİN MEKANİK ÖZELLİĞİNİN GELİŞTİRİLMESİ: NANO-DİKİŞLİ LAMİNE KOMPOZİTLERİN LAMİNELER ARASI KAYMA MUKAVEMETİNİN İNCELENMESİ**

## **ÖZET**

Fiber takviyeli polimer matrisli kompozit malzemeler otomotiv, denizcilik ve havacılık gibi bir çok sektörde önemli ölçüde kullanılmaktadır. Özellikle havacılık sektöründe kullanım oranları her geçen gün artarken buna bağlı olarak özellikleri de gelişim göstermektedir. Yüksek mekanik özellikleri ve hafifliği, kimyasal ve çevre koşullarına gösterdiği direnç gibi üstün özellikleri bu malzemeleri giderek daha da çekici hale getirmektedir. Bütün avantajlarına rağmen, basma kuvvetlerine karşı nispeten daha zayıf özellikler sergilemesi ve arayüzey özelliklerinin yetersiz olması kompozit malzemelerin en büyük sorunları olarak görülmektedir. Polimer matriste oluşan çatlak veya hasar hızlı bir şekilde ilerleyip genişlerken, arayüzey özelliklerini ve dolayısıyla kompozitin bütün mekanik özelliklerini olumsuz yönde etkilemektedir. Havacılık sektöründe üreticiler tarafından takviye malzemelerini örme, yükseklik yönünde işleme gibi çeşitli modifikasyonlar yapılarak arayüzey özelliklerini geliştirmek istenmiştir.

Bu proje kapsamında kompozit malzemelere nano mertebesinde takviyeler (karbon nanotüp) yapılarak arayüzey özellikleri iyileştirilmeye çalışılırken, aynı zamanda yalıtkan özelliğe sahip olan epoksi matrise iletkenlik kazandırılarak havacılık sektöründe önemli yer teşkil eden buzlanma ve yıldırım çarpması sonucu oluşabilecek olası kaza ve hasarları minimize etmek istenmiştir. Ayrıca polimer matrisli kompozitlerin tahribatsız muayene testleri oldukça zorlu işlemlerdir. Kompozite iletkenlik özelliği vermek, anlık yapısal durumunu inceleyebilmek anlamına da gelmektedir. Bu kavram yapısal sağlık taraması olarak bilinmektedir.

Karbon nanotüpler sadece karbon atomlarından oluşan içi boş silindirik yapılardır. Bu tüplerin çapları nano mertebesindeyken uzunlukları santimetre mertebesine kadar çıkabilmektedir. Yüksek yüzey alanı ve en boy oranı, gibi üstün özellikleri karbon nanotüpleri havacılık endüstrisi dahil bir çok alanda ileri teknoloji uygulamaları için ümit vaat etmektedir. Nano tüpler birbirleri içerisine geçerek birden fazla duvarlara sahip olabildikleri gibi tek duvarlı yapıda da olabilirler. Genellikle çok duvarlı yapıların çapları 5nm ile 20 nm arasında değişim gösterirken tek duvarlı yapıya sahip karbon nano tüplerin çapları 0.8 ile 2 nm arasındadır. Bu iki tip nanotüpün elektriksel ve mekanik özellikleri de farklılık göstermektedir.

Karbon nanotüpler kusursuz moleküler yapısı ve kuvvetli C-C bağlarından dolayı çok yüksek mekanik özelliklere sahiptir. Tek duvarlı bir nanotüp yaklaşık 1TPa'lık elastik modüle sahip iken çok duvarlı nanotüpler 1.8TPa elastik modüle sahip olabilmektedir. Bu değer yaklaşık olarak çeliğin 5 katına eşit olmaktadır. Nanotüplerin bu üstün özellikleri sayesinde, kompozit malzemelerin özelliklerini nanotüpler kullanarak geliştirmek, oldukça ilgi gören konular arasındaki yerini almıştır ve bu konuda yapılan

çalışma sayısı her geçen gün artmaktadır. Bu tarz kompozitler nano-mühendislik kompozitleri veya hibrit kompozitler olarak adlandırılmaktadırlar. Nanotüpler bireysel olarak çok yüksek mekanik özelliklere sahip olmalarına rağmen, kompozit içerisinde kullanıldıklarında aynı ölçüde gelişime neden olamamaktadırlar. Bunun en temel sebebi, karbon nanotüplerin polimer matrisli kompozitlere entegrasyonu sırasında karşılaştıkları homojen dispersiyon, dağılım, hasar alması ve oryantasyonunu kaybetmesi gibi kritik konulardır.

Karbon nanotüpler polimer matrisli kompozit malzemeler içerisinde genel olarak 4 farklı şekilde entegre edilebilmektedirler. En genel olarak kullanılan yöntemde, nanotüpler polimer matris içesine çeşitli yöntemler kullanarak dağıtılır ve matris ile fiber arayüzey özellikleri geliştirilmek istenir. Bu yöntem basittir ve büyük ölçekli üretim açısından oldukça elverişlidir. Diğer yandan nanotüpü matris içesine homojen bir şekilde entegre etmek oldukça zorlu bir işlemdir. Düşük miktarlarda nanotüp takviyesi bu sistemde verimli çalışırken, yüksek yüzey alanı, çok yüksek boy en oranı ve çok küçük çaplarından dolayı yükselen nanotüp miktarı ile karbon nanotüpler topaklaşma eğiliminde bulunmakta, viskoziteyi çok fazla artırmakta ve yapının mekanik özelliklerinin düşmesine neden olabilmektedir. Bu sistemde ki en büyük problem kompozit içerisinde kullanılacak karbon nanotüp miktarının sınırlı olması olarak görülmektedir. Bu sorunu çözmek için yapılan fazla sayıda çalışma literatürde mevcuttur ve en genel olarak bilinen nanotüplere çeşitli kimyasal işlemler uygulanarak yapının fonksiyonlaştırılmasıdır. Ayrıca bu yöntemin verimi kompozit üretim metoduna bağlı olarak ta değişebilmektedir.

'Fuzzy' fiber yöntemi diğer çalışılan yöntemlerden bir tanesidir. Bu yöntemle karbon nanotüpler, direk olarak kompozit için kullanılacak takviye malzemesi üzerinde sentezlenerek homojen, kontrollü ve yönelimli olarak kompozit içine entegre edilirler. Bu yöntemdeki en büyük problem yüksek sıcaklıklarda nanotüp sentezi ile fiberlerin zarar görmesidir. Başka bir yöntem olarak 'Nano-stitch' nano dikiş kullanılmaktadır. Bu yöntemde nanotüp yönelimlerine zarar verilmeden homojen şekilde takviye malzeme üzerine transfer edilmesi amaçlanır. Transfer edilen nanotüplerin yükseklikleri çok önemlidir ve transfer için yapışkan bir yüzeye ihtiyaç duyulmaktadır. Son olarak ise 'Bucky paper' yönteminde nanotüpler bir çözücü içerisinde dağıtılır ve daha sonra çözücü uzaklaştırılarak ince bir kağıt gibi nanotüp tabakası elde edilir. Bu kağıt matris içerisinde daha kolay ve homojen karbon nanotüp dağılmasına olanak sağlamaktadır. Bu yöntemin dezavantajı ise karbon nanotüpler ilk olarak havacılık sektöründe çok fazla istenmeyen uçucu organik bileşenler içerisinde dağıtılmaktadır. Tez kapsamında 'fuzzy' fiber yöntemi hariç diğer yöntemler farklı aşamalarda kullanılmıştır ve ayrıca 'fuzzy' fiber sentezi gerçekleştirilmiştir, ve gelecek uygulamalarda kullanılacaktır.

Bu tezde kullanılmak üzere farklı yüksekliklerde dikey yönelimli karbon nanotüpler kimyasal buhar biriktirme yöntemi kullanılarak sentezlenmiştir. Sentezlenen nanotüpler epoksi matris içerisinde dağıtılarak, nano-dikiş uygulamaları için elle yatırma yöntemi ile özel karbon nanotüplü 'prepreg'ler hazırlanmıştır. Daha sonra bu prepregler üzerine nanotüpler nano-dikiş yöntemi ile transfer edilmiştir. Arica üretim yönteminin etkisi incelenmek için vakum infüzyon yöntemi de kullanılmıştır. Bu yöntemde yapışkan yüzey bulunmadığı için nano-dikiş yapılacak yüzey hazırlanan prepreglerden temin edilmiştir. Epoksi içerisinde dağıtılarak ve nano-dikiş yapılarak kompozit içine daha fazla miktarda karbon nanotüp entegre edilmek istenmiştir ve elektriksel ve mekanik özelliklerde daha fazla iyileştirme olacağı öngörülmüştür. Ayrıca fazla sayıda deney yapmamak ve en iyi deney seviyelerini elde edebilmek için



Taguchi  $L_8$  ortogonal dizi yönteminden faydalanarak daha az sayıda deney ile daha fazla parametre incelenmiştir. Bu deneysel tasarım, sadece 8 deney yaparak 7 farklı parametrenin ikişer farklı seviyede incelenmesine olanak sağlamaktadır. Daha sonra sonuçlar analiz edilerek bu parametreler arasından en iyi sonucu verecek seviyeleri belirlenmektedir. Taguchi deney tasarımında 3 farklı yaklaşım bulunmaktadır ve bizim için uygun olanı ‘higher the better’ olanıdır ve bu yaklaşım ile en yüksek tabakalar arası kayma mukavemeti ve elektriksel iletkenliğin elde edilebileceğimiz seviyeler analiz sonucu olarak verilecektir. Diğer yaklaşımlar ayrıca literatür kısmında detaylandırılmıştır. Her deney en az 5 kez tekrar edilerek ortalamaları alınmıştır.

Deney parametreleri olarak epoksi çeşiti (RTM 6 havacılık ve West System 105/206 denizcilik epoksileri), üretim yöntemi (vakum infüzyon ve elle yatırma), nanotüp dağıtma yöntemi (izopropil ve aseton içerisinde), nano dikiş ve nanotüp miktarları seçilerek etkileri incelenmiştir. Kalan son iki parametre için de farklı nanotüp miktarları seçilerek daha farklı oranlardaki karbon nanotüp değerleri incelenmiştir.

Numuneler mekanik test ile deformasyona uğratılmadan önce iki prob yöntemi kullanılarak iletkenlik değerleri ölçülmüştür. Bu yöntemde numunelere sabit bir voltaj uygulayarak direnç değerleri elde edilmiştir ve elde edilen veriler sayesinde kalınlık ve fiber oryantasyonları boyunca iletkenlik hesaplanmıştır.

Tabakalar arası kayma mukavemeti belirlemek için numunelere ‘short beam shear’ kısa kiriş kayma testi uygulanmıştır. İki destek üzerine konulan numunenin üst orta yüzeyine belli bir hızla ilerleyen yük uygulamış ve deformasyona uğratılmıştır. Test esnasında yük değişimi ve deplasmanlar zamanın fonksiyonu olarak kayıt edilmiştir. Daha sonra standartta belirtilen formül kullanılarak kısa kiriş mukavemeti hesaplanmıştır. Bu test oldukça basit olup 3 nokta eğme testine çok benzemektedir.

Nanotüpler tek kristal silikon altlık üzerinde etilen gazı kullanılarak atmosferik basınç altında kimyasal buhar biriktirme yöntemi ile sentezlenmiştir. Sentezlenen nanotüpler, taramalı elektron mikroskobu, geçirimli elektron mikroskobu, Raman spektroskopisi ve termogravimetrik analiz yöntemleri kullanılarak karakterizasyonları hakkında bilgiler edinilmiştir. Kompozit uygulamalarında kullanmak için sentezlenen nanotüplerin yükseklikleri yaklaşık olarak 100 mikron civarında iken Raman ölçümlerinden elde edilen G/D oranları yaklaşık 2 olarak belirlenmiştir. Bu oran oldukça yüksek saflıkta nanotüp sentezlediğimizi göstermektedir. Ayrıca nano mühendislik kompozitlerinde kullanacağımız karbon nanotüplere üretim aşamasında hidrojen gazı uygulayarak altlıktan deforme olmadan kolay bir şekilde ayrılmasını sağlayacak reçeteler oluşturulmuş ve özellikle non-dikiş aşamasında nanotüplerin yönelimleri bozulmadan ‘prepreg’ üzerine tamamen aktarılmasını sağlanmıştır. Karbon nanotüplerin epoksi içerisinde homojen bir şekilde dağıtılması, nano dikiş esnasında nanotüplerin zarar göremeden altlıktan karbon fiber üzerine aktarılması ve hazırlanan nanotüp/epoksi karışımının kompozite homojen şekilde dağıtılabilmesi çalışmanın en önemli üç aşamasını oluşturmaktadır.

Tez kapsamında ayrıca çok duvarlı karbon nanotüplerin sıralı ve dizile halinde ve örüntülü olarak sentezlenmesi ve bunları kullanılarak gaz veya sıvı gibi akışkan ortamlarda madde aktarımını sağlayacak mikro akışkan cihazlar üretilecektir. Üretilen nanotüplerin hacim fraksiyonları yaklaşık olarak %2 değerindedir ve geri kalan %98’lik kısım havadır. Bu durum gözenekli ve geçirgen bir yapıya sahip olmalarını sağlamaktadır. Ayrıca nano tüperlin arasındaki mesafeler 80-100nm arasında olup üretim ve katalist parametrelerine bağlı olarak değişim göstermektedir. Üretilen nanotüpler kullanılarak mikro akışkan cihaz üretilecek ve bu cihaz akışkanlar arasında

nano-madde transferi ve deęişimi açısından test edilecektir. Çok duvarlı nanotüpler hem diziler hem de kolonlar halinde sentezlenerek bu farklı morfolojilerin mikro akışkan cihaz üzerinde ki etkileri gözlemlenecektir. Ayrıca bu proje TÜBİTAK tarafından desteklenmektedir.

## **1. INTRODUCTION**

### **1.1 Nano-Engineered Composites Using Carbon Nanotubes**

Conventional continuous fiber-reinforced polymer composites have made a huge impact over the past half-century, particularly in the aerospace industry. Their superior mechanical properties and low weight, combined with their chemical and environmental resistance, make them ideal for many structural applications, including sporting equipment, aircraft, automotive, civil and marine structures, and the relatively weak compression and interlaminar properties of these composites remain major issues [1].

A carbon nanotube (CNT) is a tubular structure made of carbon atoms, although having nanometer order diameter, length of CNTs can be several micrometers. Since they were first described by Iijima [2], CNTs researches have been shown a dramatic increase because of advanced electrical, thermal, mechanical and optical properties [3, 4]. CNTs have shown great potential for use in a variety of applications, such as electrodes, actuators, filters, ultrafast photonics, structural fibers, and so forth [5]. In addition CNTs possess low density, well alignment, huge aspect ratio, a large surface area to volume ratio and low coefficient of thermal expansion. While the individual CNT shows excellent mechanical properties (Young's modulus of individual CNT over 1TPA and the strength between 11-63GPA), on the large scale composites which made using CNTs have shown some improvement not only in mechanical properties [6], and also electrical [7, 8] and thermal properties, making them attractive for enhancing a variety of matrices. The main motivation for adding CNTs to conventional fiber composites is to overcome the existing limitations associated with the matrix dominated properties. For example, CNTs could offer both intralaminar and interlaminar reinforcement, thus improving delamination resistance and through-thickness properties, without compromising in-plane performance [1]. These type composites could be called as hybrid, hierarchical or nano-engineered composites (NECs).

## 1.2 Motivation

Motivation of this thesis is to improve interlaminar shear strength (ILSS) of conventional composites using CNTs. High purity vertical aligned carbon nanotubes up to 2.2 mm length are synthesized using thermal chemical vapor deposition (CVD). In this study, two common methods;

- Dispersion of CNTs into the polymer matrix
- Stitching of them between customized prepreg plies

are used to produce nano-engineered composites to exploit their multi-functional properties for improve traditional composite properties. Dispersion of CNTs into a polymer matrix provides transferring the matrix loads to fibers and also to block crack propagation along crack route is an advantage of using CNT due to the high aspect ratio of them with minimal weight addition. In this method, most critical point is dispersion amount of CNTs without functionalization is too limited, because of CNTs agglomeration and this type defects cause a decrease in mechanical properties of composites. In addition, the agglomeration of CNTs depends on matrix viscosity during composite production as well as dispersion method. Due to there is no commercial prepreps with CNTs loading, it is decided to produce custom-made prepreps with CNTs fillers. The second method is focused on stitching CNTs between the plies to reinforce the interlaminar properties of nano-engineered composites. This method has two important parameters;

- Removing A-CNTs from substrate
- Length effect of A-CNTs (should be about 20 $\mu$ m to be wetted by epoxy prepreg and penetrate the ply structure 10–20 $\mu$ m).

It is expected that simultaneously applying both methods at once, it can be shown more ILSS improvement. Besides, in order to determine best production parameters and levels such as dispersion method or amount of CNTs, Taguchi L<sub>8</sub> orthogonal array (7 different parameters which have 2 levels each one) is used to study the influence of various combinations of process parameters on ILSS. To determine interlaminar shear strength short beam shear (SBS) tests are performed.

## 2. LITERATURE RESEARCH

### 2.1 CNTs Fundamentals

Carbon nanotubes are a hollow cylinder structure made of carbon atoms, while having nanometer order diameter, length of CNTs can be several micrometers. Even though CNTs were synthesized, studied and reported by several researchers, Iijima detailed and reported analysis of carbon atom structures in 1991 [2]. Ever since, CNT has remained a thrilling material and number of CNT-related journal publications and patents continue to grow as shown in **Fig. 2.1**. It has remarkable properties: many-fold stronger than steel, harder than diamond, electrical conductivity higher than copper, thermal conductivity higher than diamond, etc. set off a considerable interest subject in academic and industrial laboratories all over the world to find out practical application of CNTs. Thousands of publications and patents have been germinated on innumerable potential applications of CNTs in nearly all the walks of life; media, entertainment, communication, Transport and health and environment [9].

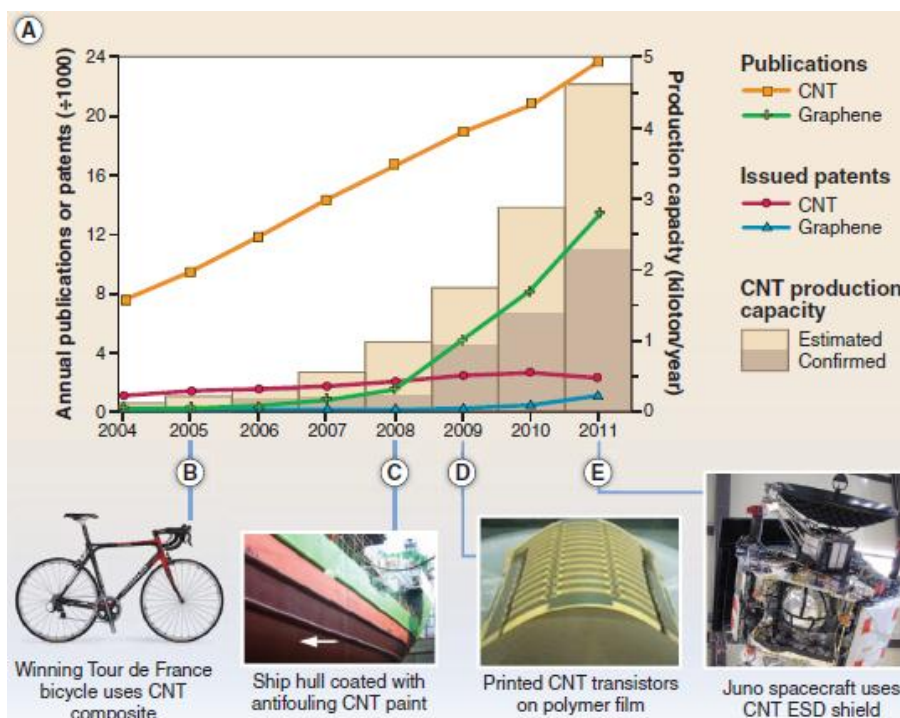


**Figure 2.1** : Trends in CNTs research and commercialization [10].

### 2.1.1 Chemical structure

Carbon nanotube is a graphite layer that has been rolled into a tubular structure. Carbon nanotubes are considered as almost unidimensional structures in respect of their high aspect ratio (length to diameter ratio). There are two types of CNTs structures depending on number of walls, single-walled nanotubes (SWNTs) and multi-walled nanotubes (MWNTs) as shown in **Fig. 2.2**. A SWNT is considered as a tubular structure with one wrapped graphene layer, while the multi-walled nanotubes consist of two or more graphite layer cylinders. The diameter and length of these structures are different and their properties are also very different [11]. Diameters of SWNTs and MWNTs are usually 0.8 to 2 nm and 5 to 20 nm, respectively, and also MWNTs diameters can surpass 100 nm. CNTs can be synthesized in lengths range from less than 100 nm to several centimeters, so that bridging molecular and macroscopic scales [10].

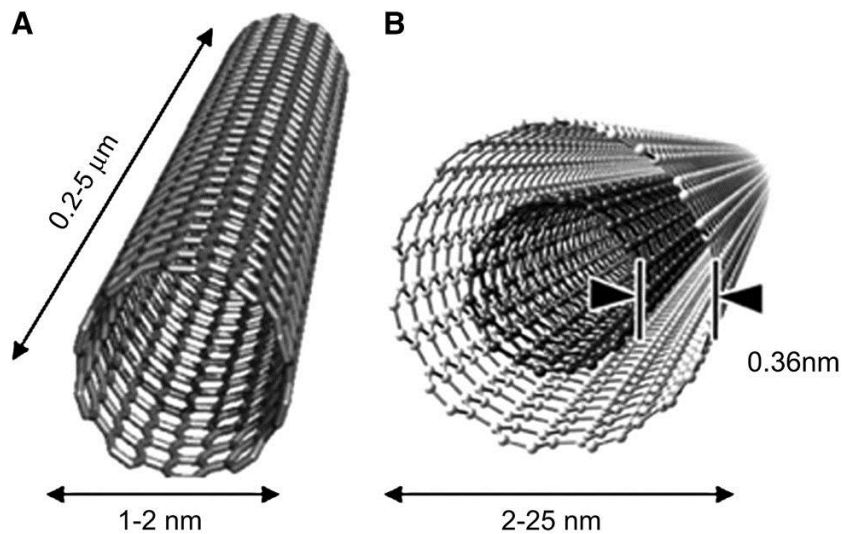


**Figure 2.2 :** Typical carbon nanotube structures (a) SWNTs and (a) MWNTs.

Helicity of CNTs is one of their most important characteristics and is defined as the deviation from the parallel and normal orientations of the ring arrays with respect to the tube axis. The helicity of the CNTs has a strong influence on their electrical properties. SWNTs are completely defined, apart from their length, by a single vector  $\vec{C}$  (called chiral vector). Two atoms in a planar graphene layer are selected and one is determined as origin. The chiral vector  $\vec{C}$  is pointed from the first atom toward the second atom as shown in **Fig. 2.3a** and is described by the relation (2.1);

$$\vec{C} = n \vec{a}_1 + m \vec{a}_2 \quad (2.1)$$

where  $\vec{a}_1$  and  $\vec{a}_2$  are unit cell vectors, of the two-dimensional lattice formed by the graphene sheets,  $n$  and  $m$  are integers. The direction of the nanotube axis is perpendicular to this chiral vector [11]. The chiral angle ( $\theta$ ) determines the twisting in the tube where the limit cases are termed zig-zag ( $\theta=0^\circ$ ) and armchair ( $\theta=30^\circ$ ). Schematics of zig-zag and armchair nanotubes are shown in **Fig. 2.3b-c**.

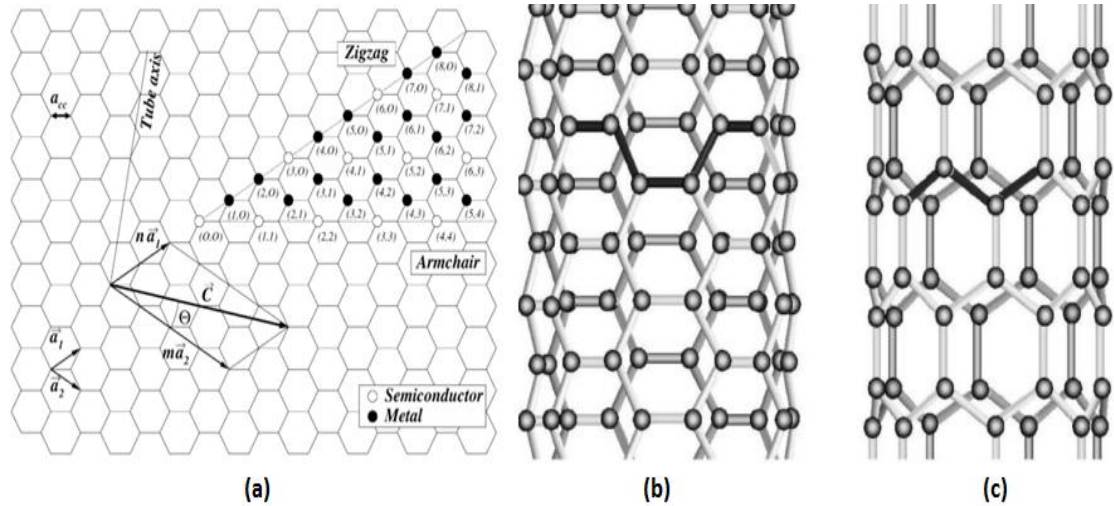


**Figure 2.3** : Schematic diagram showing (a) a hexagonal graphite sheet [11], the atomic structure of (b) an armchair and (c) a zig-zag nanotube [12].

### 2.1.2 CNTs synthesis

The most used CNTs synthesis methods can be group;

- Arc discharge
- Laser ablation[2]
- Chemical vapor deposition.

In all synthesis techniques, product purification is a necessary element that effects on the overall cost and quality [13]. For industrial applications, large quantities of CNTs are required to be incorporated into macroscopic composite systems. Both laser ablation and arc discharge methods need a further purification step which is usually carried out in a multi-step process, involving the controlled oxidation of amorphous carbon, followed by removal of catalyst particles with mineral acids and CVD has offered new opportunities for large-scale synthesis by allowing an ability to control the morphology and orientation of CNTs. Comparison of established techniques is given in **Table 2.1**.

**Table 2.1** : Comparison of the established techniques for CNTs synthesis.

Method	Arc discharge	Laser ablation	Chemical vapor deposition
Description	Arc evaporation of graphite in the presence of inert gas; CNTs formed on electrodes during quenching	Vaporization of graphite target by laser; CNTs formed on receiver during quenching	Decomposition of hydrocarbons over transition metal catalyst to form CNTs
Operating temperature	>3000°C	>3000°C	<1200°C
Operating pressure	50-7600 Torr generally under vacuum	200-700 Torr generally under vacuum	760-7600 Torr
Advantages	Good quality CNTs	Good quality CNTs, single conformation SWNTs formed	Easy scale up; aligned synthesis on templates possible
Disadvantages	Difficult to scale up	Difficult to scale up, expensive	Quality of CNTs not as good

**Arc discharge and laser ablation;**

The principle of the arc-discharge method is the production of an electric arc between two closely separated graphite rods (<1 mm apart) as anode and cathode under an inert atmosphere of helium or argon, and generally under decreased pressures of between 50 and 700mbar. A direct current carried by a driving potential of ~30 V creates a high-temperature plasma (>3000°C) between the electrodes. In the inter-electrode plasma region, the carbon electrodes sublime and condense rapidly to form CNTs and other carbonaceous byproducts.

The principle of the laser-ablation method is similar. High temperature is achieved on a carbon target using laser source. The vaporized carbon rapidly cools in a carrier gas stream, e.g., helium, and forms CNTs and other carbonaceous byproducts.

Arc discharge or laser ablation have the advantage of better quality CNTs, compared to synthesized CNTs using CVD. Most commercially available CNTs are synthesized using the arc-discharge method as a reconciliation between cost and quality. However, the natural design of arc-discharge exhibits limitations to the large-scale production of CNTs [14].



### Chemical vapor deposition;

One of the most popular method of producing CNTs is chemical vapor deposition. In this method, hydrocarbon vapor is decomposed in the metal catalyst by the effect of temperature. Therefore, it is also called as thermal CVD or catalytic CVD [9]. The process requires passing a hydrocarbon vapor along a tubular reactor in which a catalyst material is present at enough high temperature (600–1200 °C) to decompose the hydrocarbon. CNTs grow on the catalyst in the reactor. Schematic illustration of CVD is given in **Fig. 2.4**. CNTs growth mechanism of CVD has been arguable right from its discovery. The common accepted mechanism can be described as follows. When hydrocarbon vapor comes in contact with the hot catalyst in which is generally a metal nano-particles;

- Firstly hydrocarbon source decomposes into carbon and hydrogen molecules; hydrogen flies away and carbon gets dissolved into catalyst
- After catalyst is reached carbon-solubility limit at that temperature, dissolved carbon going out from catalyst in a crystal form of a cylindrical network having without idle bonds, so energetically stable.

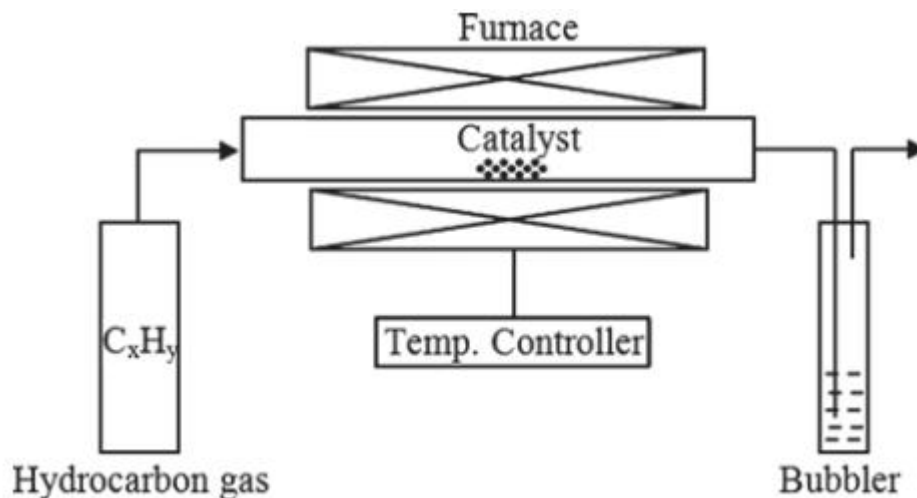


**Figure 2.4** : Schematic illustration of CVD [9].

There are two widely-accepted growth mechanisms for CNTs (**Fig. 2.5a**). If the catalyst–substrate interaction is weak (metal has an acute contact angle with the substrate);

- i. Firstly hydrocarbon decomposes on the top surface of the catalyst, carbon diffuses along the catalyst, and CNTs precipitates out from the catalyst bottom surface, pushing the catalyst off the substrate

- ii. CNT continues to grow as long as the catalyst's surface is open for fresh hydrocarbon decomposition
- iii. Once the catalyst surface is exactly covered with excess carbon, the catalyst becomes inactive and the CNT growth is stopped.

This is known as tip-growth model. In the other condition (**Fig. 2.5b**), when the catalyst–substrate interaction is strong (metal has an obtuse contact angle with the substrate), hydrocarbon decomposes on the top surface of catalyst and diffuses down through the catalyst particles, then the CNT precipitation fails to separate the catalyst particle up; so the precipitation is forced to come out from the metal's peak (farthest from the substrate, having minimum interaction with the substrate).

- i. First, carbon emerge out as a crystal hemispherical dome (the most favorable closed-carbon network on a spherical nano-particle) which then extends up in the form of uninterrupted graphitic cylinder
- ii. Following hydrocarbon deposition takes place on the lower peripheral surface of the catalyst, and as-dissolved carbon diffuses upward.

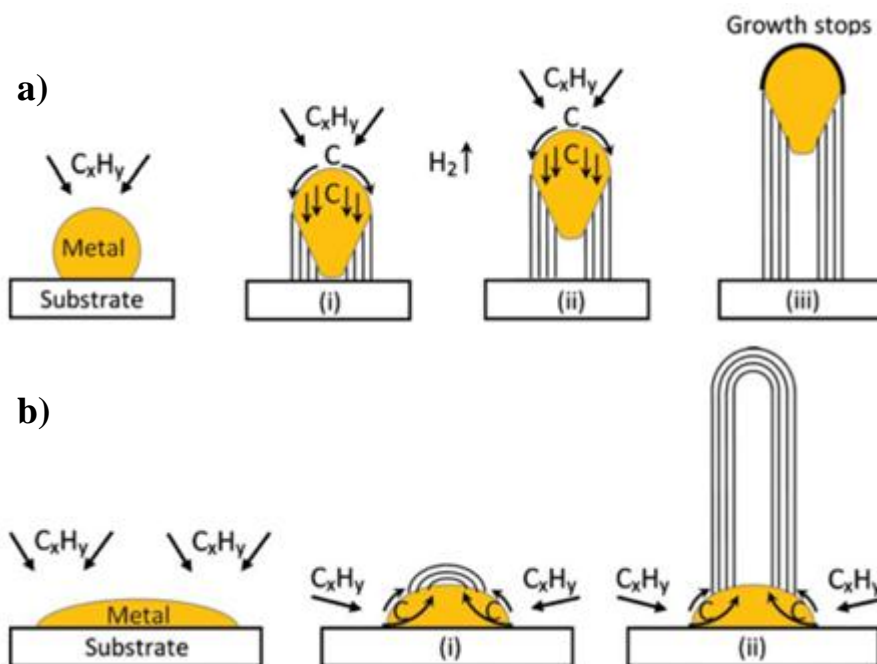


**Figure 2.5 :** Widely-accepted growth mechanisms for CNTs: (a) tip-growth model, (b) base-growth model [9].

Thus CNT grows up with the catalyst particle rooted on its base; hence, this is known as base-growth model. Generation of multi or single wall is determined by the catalyst particle size.

### 2.1.3 Mechanical properties

The properties of CNTs depend on several parameters such as diameter, chirality, and purity. Although Young's modulus depends on tube diameter and wall purity, it is independent of tube chirality. The presence of defects in CNT wall makes them weaker and it is a stress concentration point. Direct measurements of individual CNTs are limited due to the difficulty of handling individual CNTs and because of this, it shows a variation in a broad range of parameters in the experimental studies. Treacy et al. [15] reported on the elastic modulus of arc-grown MWNTs by measuring the amplitude of their intrinsic thermal vibration in a TEM. Due to the experimental uncertainties such as CNT length, the averaged value for 11 samples was calculated as 1.8TPa. In 1997 Wong et al. [16] measured the mechanical properties of arc-grown MWNTs attached to a substrate using atomic force microscopy (AFM). The AFM tip loaded the side of the CNT in order to apply a perpendicular load, and bending force-displacement was recorded to investigate the mechanical properties. The obtained elastic modulus was 1.26TPa and bending strength was measured as  $14.2 \pm 8$ GPa.

In another study, stress-strain measurements on CVD grown MWNTs were performed, and a modulus of 450 GPa and tensile strength of 4GPa were reported [17]. When the results of arc and CVD-grown MWNTs were compared, the much larger variation of values in CVD-grown MWNTs suggest that modulus is highly dependent on defect concentration and CNT type. While the arc-grown MWNTs are expected to have a lower defect density and therefore be stronger than the CVD-grown MWNTs, it has been hypothesized that defect induced ripples in the sidewalls of MWNTs improved stress transfer through the structure and thereby increased the strength [17].

The first direct measurements on mechanical properties of SWNTs that have between 1 and 2 nm diameter are found to have a very high Young's modulus more than 1TPa, while MWNTs having as high as 1.8TPa, whereas Young's modulus of steel is only about 0.21TPa. MWNT's Young modulus is generally higher than SWNT's due to bond acting (van der Waals forces) between the tubes, and diameters differences included coaxially in the MWNTs. The tensile strength of individual MWNTs is measured about 50GPa. In comparison, they are about 20 times stronger than steel [18]. Difficulties in direct measurements of CNT properties due to small sizes and handling have led researchers to investigate the mechanical properties by theoretical and modeling studies as well.

## **2.2 Polymer Nano-Composites (PNCs)**

Advanced polymer composites, such as carbon fiber reinforced plastics have shown efficient reinforcement and are usually manufactured using simple methods. Homogeneous mixing fillers or fibers evenly into liquid or molten matrices before curing or solidifying to create isotropic composites. These materials are increasingly being used in aerospace and other advanced composite industries due to their high specific mechanical properties [19]. It is well known that the additive of inorganic fillers into a polymer matrix can bring to the development of composites with improved properties as well as the introduction of new ones. The main aim is the development of mechanical performance by keeping at the same time the good processability properties of the polymer matrix. Fillers such as carbon fibers, carbon black and more recently carbon nanotubes and graphene in polymer composites, have been broadly studied for the improvement of the mechanical properties [7]. There are many issue to be overcome and improvement have been limited by several key processing issue. The first major issue is dispersion of CNTs uniformly in the matrix. CNTs tends to agglomerate into bundles, and techniques to separate the CNTs by sonication, surface modification, or mixing easily damages the CNTs. The CNTs are only able to reinforce the matrix if the adhesion between the CNTs and polymer is strong enough to facilitate load transfer.

## **2.3 Fiber Reinforced Plastic Composites (FRPs)**

Aerospace structural components are increasingly being made of fiber reinforced plastics owing to their great specific mechanical properties obtained in excellent specific stiffness and strength [6]. Even though excellent in-plane tensile properties (strong, stiff, and tolerable) achieved using various configurations of fiber architectures, including unidirectional tapes or two-dimensional woven fabrics, the relatively weak compression and interlaminar properties of these composites which lead to failure due to delamination and other damage modes remain main issues and [1]. Because of their anisotropic structure, FRPs fail in a complex behavior [20].

To address these deficiencies at the interlaminar interface, several architectures have been developed. Z-pinning, stitching, and 3-D weaving are most used methods to improve strength and/or toughness in the through thickness direction of the laminate. These processes result in a important reduction in in-plane properties of the laminate

owing to damage from insertion of through-thickness direction reinforcements that are hundreds of microns in diameter, and loss of micro-fiber volume fraction in the in-plane direction. Alternative routes to increasing interlaminar toughness include modification of matrix properties through added toughening agents, compliant or reinforced interlayers or nano-particles [6].

#### **2.4 Nano-Engineered Composites (NECs)**

Laminated composites cannot get the heat out of the structure and with stand high temperature due to poor thermal conductivity transversely. Advanced composites are not electrically conductive enough to discharge static electricity or lightning strikes, and they have brittle structure and sensitive to impact damage and delamination also. These are limiting the flight envelope of aircraft or are requiring retrofit of materials to enhance properties of composites; however, this offsets the main benefit of weight reduction obtained from using the composite material in the first place [21]. As nano-scale material, CNTs offer possibility to solve these problems discussed above benefiting from their exceptional multi-functional specific properties. Application of new nano-engineered, multi-scale, multi-functional CNT composites can be extended to system health monitoring with electrical or thermal resistance change induced by damage, fire-resistant structures among other multi-functional features [22].

The introduction of CNTs in interface of composites lamina can improve the bonding between fiber and matrix. Interfacial reinforcing mechanisms are explained by several types, such as rising of fiber surface roughness and creation of chemical bond between fiber and CNTs [23]. Mechanical tests of nano-engineered composites have approved that, the fiber dominant in-plane properties are not importantly affected by the CNTs loading (up to 2 wt%). Whereas, matrix-dominant properties, particularly the interlaminar shear strength (ILSS), are improved by about 8–30% [1]. On the other hand, while CNTs possess significant potential for composite reinforcement, only small improvements in composite properties can be observed due to difficulties in processing and controlling CNT orientation during manufacturing [6].

There are several methods CNT can be integrated into composites and this is a continuing area of investigation. The combination of CNTs with conventional fiber reinforcements in polymer composites has been achieved predominantly through four

different routes, and in **Fig. 2.6** schematic illustration of these strategies to improve the properties of FRP methods are listed;

- a) Dispersing CNTs entirely throughout the composite matrix [24, 25],
- b) Growing (fuzzy) CNTs on fiber [22],
- c) Interleaving bucky papers made from CNTs at certain laminar interfaces [26],
- d) Stitching CNTs directly onto primary reinforcing fiber.

Interlaminar shear strength of epoxy matrix composites, containing CNTs in the interlaminar region, can be increased by 2–20%. The ILSS increase depends on the several parameters such as, fiber type, content, surface chemistry of CNTs and integrated method into the composite system as given in **Table 2.2**.

**Table 2.2** : Improvements in the interlaminar shear strength of CNT-based hierarchical composites.

Fiber	Matrix	Nano-filler	Nano-filler reinforced region	Test method	ILSS improvement	Ref.
glass	epoxy	0.1-0.3 wt% functionalized DWNTs	entire matrix	SBS	15.7 – 19.8% (0.1 -0.3 wt%)	[29]
glass	epoxy	0.3 wt% DWNTs	entire matrix	SBS	16%	[30]
glass	epoxy	0.1–1 wt% carbon nano-fibers	entire matrix	SBS	23% (0.1 wt%)	[31]
glass	epoxy	1 wt% functionalized MWNTs	entire matrix	SBS	7.9%	[32]
carbon	epoxy	SWNTs, MWNTs	around fibers	SBS	27%	[33]
carbon	epoxy	0.1, 0.2 and 0.3 wt.% CNT functionalized	entire matrix	SBS	10%	[34]
carbon	epoxy	bucky paper	mid ply	SBS	31%	[26]
carbon	epoxy	20 $\mu$ m A-CNTs	between each ply	SBS	50%	[21]

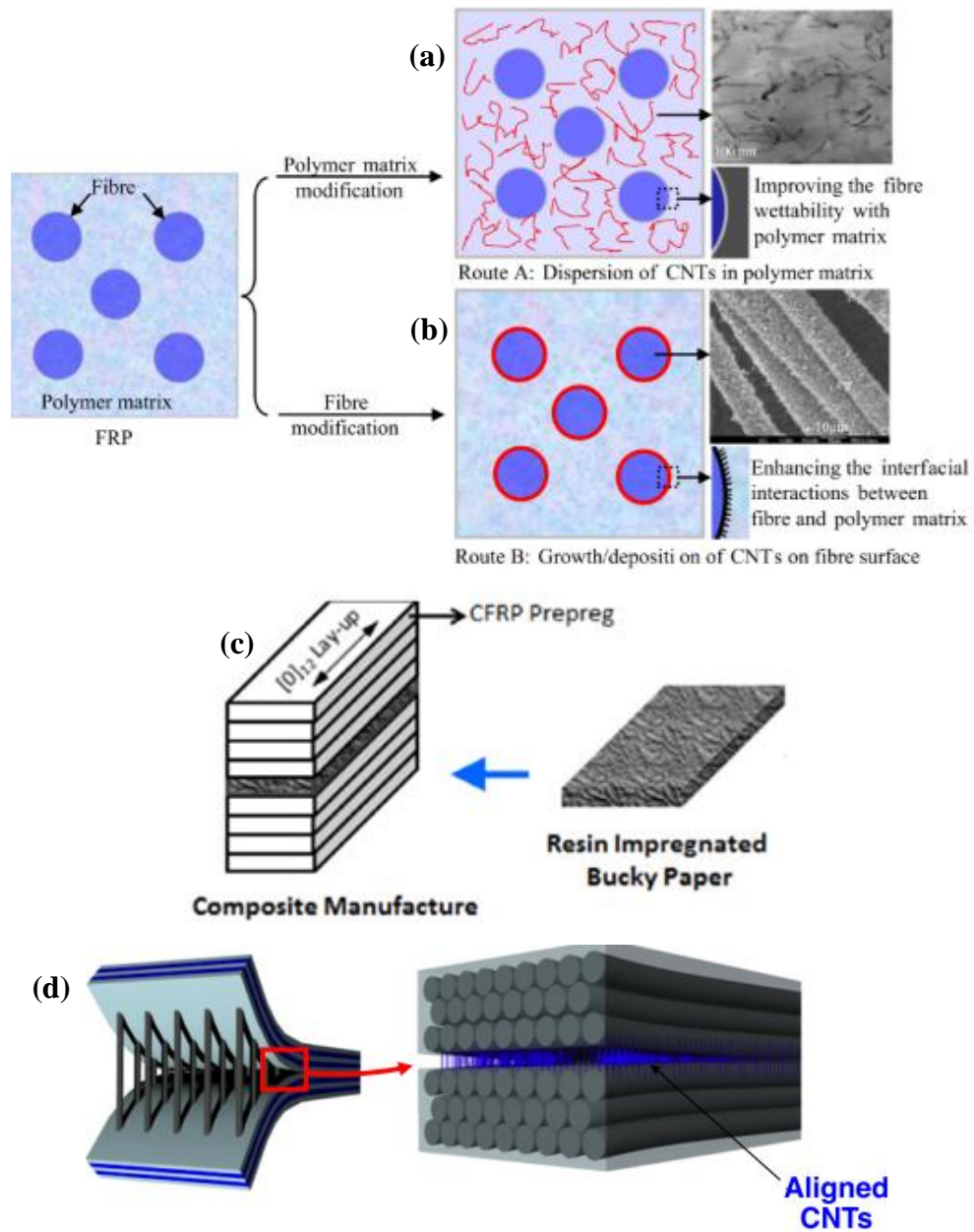


**Figure 2.6 :** Strategies to enhancement the properties of FRPs using CNT (a) in matrix, (b) fuzzy fiber [27], (c) bucky paper [26] and nano-stitch [28].

#### 2.4.1 CNTs as nano-fillers (NFs)

Pure epoxy matrix has poor electrical conductivity, strength and/or toughness compared to fiber. Whereas, volume percent of epoxy is as high as 30–50% in composite. The epoxy resin is not easy to combine with fibers strongly because of original carbon fibers possess inert surface. As a result of this, weak interface exists in fiber/epoxy composite. Weak interface leads to serious physical defects on a micro level and as well as low electrical conductivity through thickness direction and modest

mechanical performances of composite such as interlaminar shear strength in macro scale due to large interface resistance. The use of nano-fillers in epoxy improves matrix properties and can add new functionalities.

Modifying the matrix resin by dispersing CNTs in the polymer offers the most conventional, easy and industrially compatible technique due to their high modulus, aspect ratios, and thermal/electrical conductivity. The existence of CNTs in matrix has direct effects on crosslinking density, toughness, stiffness and electrical conductivity of matrix [20].

Several methods have been invented for homogeneous CNT dispersion into a polymer matrix, which includes shear mixing, calendaring, extrusion, ultrasonication and ball milling, either in the matrix or solvents [21]. For effective CNT reinforcement, four system requirements have been specified;

- Large aspect ratio
- Good dispersion
- Alignment
- Interfacial stress transfer.

Achieving the full potential of CNTs as a mechanical reinforcement in matrix depends on the ability to disperse and distribute the CNTs uniformly through the polymer matrix without any damage to their integrity. By good dispersion and distribution, effective load transfer can be achieved, minimizing the formation of stress concentration in the matrix. The main mechanisms of load transfer from CNTs nano-filler to matrix are chemical and van der Waals bonding. Strong bonding between filler and matrix provides well adhesive properties and pull out mechanism.

The dispersed amount of CNTs is a critical issue. If dispersed amount of CNTs is too much, it tends to agglomerate resulting from their characteristics of small diameter in nanometer scale with high aspect ratio and large surface area. Besides, when CNT loading is low, thus could not improve properties of matrix and interface between fiber and matrix simultaneously.

In a study, It was found that the the compression modulus is higher than the tension modulus indicating a more effective load transfer mechanism in compression for MWNT/epoxy nano-composites due to only the outer layers of MWNTs carried the stresses for tension, whereas in compression all of the layers participated [35].



In this thesis, A-CNTs were used as nano-filler to improve interlaminar shear strength using their effective compression load transfer mechanism.

#### **2.4.2 Transfer of A-CNTs arrays onto prepreg lamina**

The development of composites with CNTs is prevented by difficulties in dispersing CNTs in matrix at high weight fractions while obtaining uniform and strong interactions with the polymer matrix. Randomly oriented CNTs reinforcement NECs studies report only some mechanical property improvements at low CNTs loadings. To transfer A-CNTs on fiber surface helps to improve properties of composites due to controlled morphology and orientation. Wardle et al. reported that stitched A-CNT forests into composites improve interlaminar strength and toughness due to bridge and strengthen this interlaminar region [28].

Transfer of A-CNT arrays on the prepreg is a critical step of the process since the applicability and scale-up of this process is highly dependent on the height of the A-CNTs array and scaling up CNTs production. Long height CNTs arrays could result in imperfect resin infiltration on a prepreg laminate and reduce overall performance of the nano-engineered composite. In a study, it was reported by Yi Song et al., introduction of the 20 $\mu$ m long CNTs array between each ply leads to about 50% increase of the short beam shear strength while increasing the sample thickness about 9% [18]. Another critical step of stitch process is transferring CNTs on prepreg without damaging orientation. In order to solve this problem, the easy delamination recipe is used during CNTs synthesis. On the other hand this technique can be used on a adhesive surface as prepreg surface.

#### **2.5 CNTs for Aerospace Application**

The interest for applications of carbon nanotubes has since their scientific introduction increasingly increased due to the extraordinary properties. The potential applications of CNTs have extended in different scientific disciplines, such as in energy storage, mechanical systems, sensing, biological applications, and field emission. As aerospace engineering is imagined to be one of the most important disciplines of the future, and these materials will play a game-changing act for aerospace industry. Literature research on CNTs clearly shows that the number of scientific publications on this topic has increased considerably since the year 2000, as shown in **Fig. 2.7**. In this context,

an interesting explanation is that the number of articles including the keyword aerospace has increased from less than 0.25% to 1.8% in 2013. This figure shows a continued brilliant possibility of CNTs application in aerospace sciences. Equally, it is clear that there is a diverse distinction in the number of publications related to CNTs only with the keyword “aircraft” versus “aerospace”, as shown in the **Fig. 2.7**.

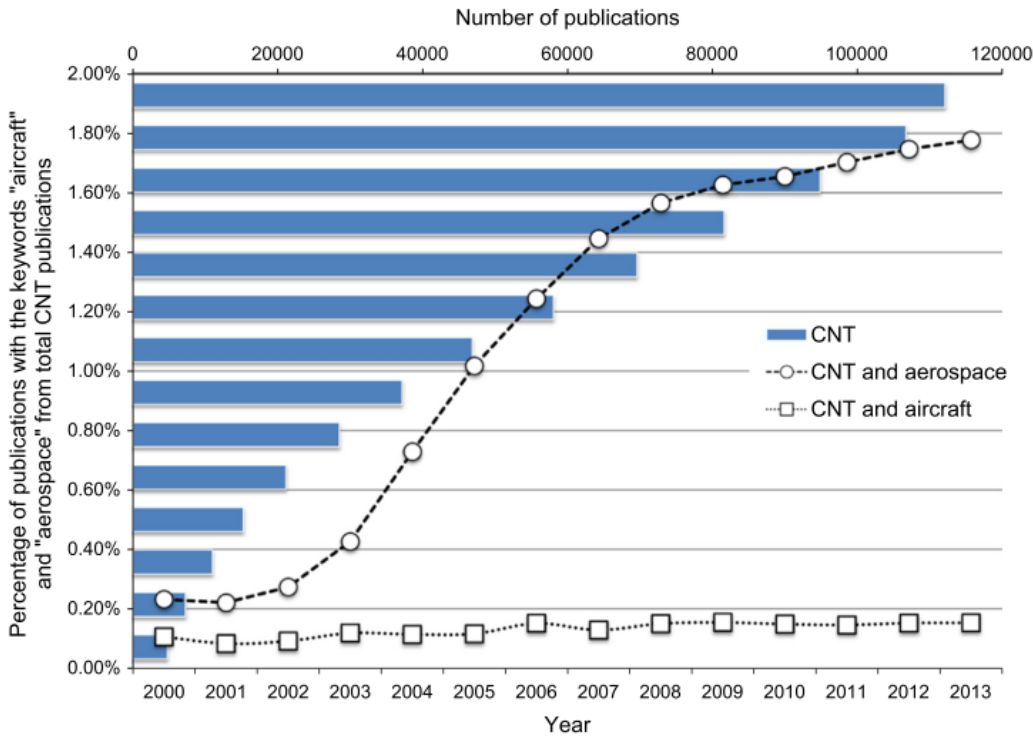


**Figure 2.7 :** Carbon nanotube publications with the keywords aerospace and aircraft, between the years 2000 and 2013 [36].

Some potential roles of CNTs in aeronautics are given **Table 2.3**.

**Table 2.3 :** Some potential roles of CNTs in aeronautics.

Commercial Aircraft	Military Aircraft	UAV	Rotorcraft	Morphing Aircraft
Airframe	Stealth	Electric UAVs	Structural	
Wiring	Aircraft	Mitigation of Aircraft	Monitoring,	
Aircraft icing	Icing	Icing Related	Icing on	
Propulsion			Rotorcraft	
Lightning Protection				
Electromagnetic Interference				
Shielding Sensing				
Safety				

Next generation aircraft, rotorcraft, unmanned aerial vehicles, and missiles will have stricter requirements in terms of lightweight, visual and thermal signature, increased speed, and maneuverability. These requirements, however, incite a need for advanced materials and systems that can combine these functionalities. CNTs are ideal material to meet these claims, as they can be incorporated in distinct technologies [36].

## 2.6 Optimization by Taguchi Method

The Taguchi method uses orthogonal arrays from design of experiments theory to study a large number of variables with a small number of experiments. The experimental results are then converted into a signal-to-noise (S/N) ratio. It uses the S/N ratio as a measure of quality characteristics deviating from or oncoming to the desired values. There are three categories of quality characteristics in the analysis of the S/N ratio, i.e. the lower the better, the higher the better, and the nominal the better. The formula used for calculating S/N ratio is given below. Smaller the better (2.2): It is used where the smaller value is desired [37].

$$\frac{S}{N} \text{ ratio}(\eta) = -10 \log_{10} \frac{1}{n} \sum_{i=1}^n y_i^2 \quad (2.2)$$

where  $y_i$  = observed response value and  $n$  = number of replications.

Nominal the best (2.3): It is used where the nominal or target value and variation about that value is minimum.

$$\frac{S}{N} \text{ ratio}(\eta) = -10 \log_{10} \frac{\mu^2}{\sigma^2} \quad (2.3)$$

where  $\mu$  = mean and  $\sigma$  = variance. Higher the better (2.4): It is used where the larger value is desired.

$$\frac{S}{N} \text{ ratio}(\eta) = -10 \log_{10} \frac{1}{n} \sum_{i=1}^n \frac{1}{y_i^2} \quad (2.4)$$

where  $y_i$  = observed response value and  $n$  = number of replications.

Taguchi suggested a standard procedure for optimizing any process parameters.

The steps involved are;

- Determination of the quality characteristic to be optimized

- Identification of the noise factors and test conditions
- Identification of the control factors and their alternative levels
- Designing the matrix experiment and defining the data analysis procedure
- Conducting the matrix experiment
- Analyzing the data and determining the optimum levels of control factors
- Predicting the performance at these levels.

### **3. SYNTHESIS AND CHARACTERIZATION OF ALIGNED AND PATTERNED CNTs STRUCTURES**

In this section, A-CNTs and patterned carbon nanotubes (PA-CNTs) are synthesized using chemical vapor deposition. While the A-CNTs synthesis are being on entire substrate surfaces, for PA-CNTs synthesis the growth is occurred by coating on specific substrate surface. This project is consisted of two part. It is synthesized A-CNTs for composite application and PA-CNTs to fabricate of 3D ultra porous micro and nano-structures for nano-particle exchangers. In this chapter the following topics will be covered;

- a) Photolithography method is used for create selected coating surface
- b) Customized thermal CVD system is used for the both types CNTs growth
- c) Morphology will be characterized by imaging and other techniques
- d) Micro-device fabrication will be describe.

#### **3.1 Synthesis of CNTs**

Although there are many different CNTs synthesis methods, only CVD method provides control on the CNTs orientation. CVD is a simple and low cost process, in which CNTs grow at low temperature and ambient atmosphere pressure, with usually moderated quality. One disadvantage of CNTs is supported-catalyst growth that eventually, the catalyst is coated by pyrolyzed hydrocarbons and becomes deactivated [38] and the growth ends. In the CVD method <100> silicon wafer was used as substrate material, due to having high melting temperature, do not interaction with gases at high temperature and should be have strong physical bond between substrate and catalyst for base growth. Fe, Co and Ni are most popular catalyst elements due to having high C solubility and high C diffusion rate at high temperature. In this thesis, Fe was selected as catalyst and was coated 2nm thickness on alumina support using physical vapor deposition method (PVD). Catalyst coating thickness plays significant role in CVD process. CNTs diameters depends on this thickness and with the increasing thickness also CNTs diameters grow and it ends after a while. Alumina was

coated 10nm length on Si wafer to create porous interface between the substrate and catalyst using PVD.

### A-CNTs;

For the A-CNTs growth all substrate surface are coated with catalyst and growth occurs on each region and are given in **Fig. 3.1**. This type synthesis cheaper and easier than PA-CNTs which needs extra processing to occur specific areas on Si wafer. Thus all optimization stages were done on forest CNTs such as determination of growth recipes. Although there are many articles in literature, CNTs growth can be show differences between the different systems and the recipe should be optimized. Optimization parameters such as amount of gases and time, growth temperature and time were optimized using an experimental design in **Table 3.1** and an example recipe which is obtain resulting form this study is given in **Table 3.2**.

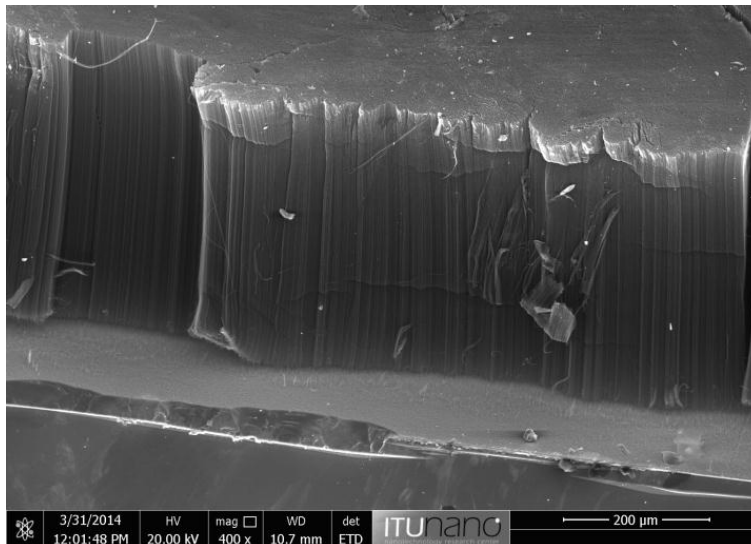


**Figure 3.1** : A-CNTs growth by CVD method.

An example of CNTs growth recipe can be given as below;

1. Purging (He,Ar... etc.): In this step the purpose is that to remove all the ambient gases like O<sub>2</sub> from the quartz tube.
2. Nucleation : Second step is heating the tube for activation of catalyst materials. While heating the tube, He and H<sub>2</sub> gases are flew throughout the tube channel.
3. Growth : When the tube come to stable temperature, besides H<sub>2</sub> and He, ethylene (C<sub>2</sub>H<sub>4</sub>) gas is also added as a hydrocarbon source.
4. Easy delamination: After growth procedure is done, in order to remove (easily and without any deformation) the CNTs, only H<sub>2</sub> gas is sent for a minute.

5. Cooling : In the last step just He gas is flew for high purity until about room temp.

**Table 3.1** : CNTs growth optimization parameters.

Experiment Number	Step	He (sccm)	H <sub>2</sub> (sccm)	C <sub>2</sub> H <sub>4</sub> (sccm)	Time (min.)	Temperature (°C)
1	Nucleation	2400	1000	0	15	750
	Growth	2400	1000	400	13	750
2	Nucleation	1600	1000	0	15	680
	Growth	1600	500	400	15	680
3	Nucleation	1600	1000	0	15	750
	Growth	1600	500	300	15	750
4	Nucleation	1600	1000	0	10	790
	Growth	1600	500	400	15	790
5	Nucleation	1600	1000	0	10	750
	Growth	1600	500	400	15	750
6	Nucleation	1600	1000	0	15	750
	Growth	1500	400	400	15	750
7	Nucleation	1600	1000	0	15	750
	Growth	1200	400	400	15	750
8	Nucleation	1600	1000	0	15	750
	Growth	1500	400	400	20	750

An example recipe are given in **Table 3.2**. Using this recipe CNTs can be synthesized up to 2mm length by changing growth time. In custom made CVD system (see in **Fig. 3.2**), a single zone Lindberg Blue M series tube furnace (max. temp. 1200°C), is used with a quartz tube of 2 inches diameter. Larger quartz tubes allows to produce greater amount of CNTs, larger fuzzy fiber or stitch sample for composite application. On the other hand as a drawback, larger tube consumes more amount of gases. To control of gas flow rate, time and furnace temperature, a software were customized by A. F. Ergenc. By this software and control system the furnace can easily be automated for control over parameters and can be created a protocol for production.

**Table 3.2 :** An example A-CNTs growth protocol.

Step	Gases	SCCM	Time (min.)	Temperature(°C)
1	He	2000	5	23
2	He, H <sub>2</sub>	1600,1000	15	750
3	He, H <sub>2</sub> , C <sub>2</sub> H <sub>4</sub>	1000,600,300	20	750
4	H <sub>2</sub>	1000	1	750
5	He	1000		<100



**Figure 3.2 :** Picture of customized CVD system.

### **Patterned CNTs;**

Photolithography is a method used to pattern on substrate. It uses light to transfer a geometric pattern from a photomask to photoresist coated substrate surface. There are many advantages of photolithography. It can create a pattern which has extremely small dimensions about nm, it provides full control over the shape and size of the sketch. Its main drawbacks are that it can require extremely clean operating conditions and it needs a flat surface to begin.

In this project, a predetermined geometric pattern is formed on the silicon wafers by masking and carbon nanotubes synthesis takes place in only the specified pattern area. These may be referred to as specific architectural structures. To make the production of patterned special architectural structure (given an example **Fig. 3.3**), it is necessary to do some pre-processing to the substrate material. In this project for this step would



prefer a process which called "lift-off". Briefly this process consists of three parts listed in below.

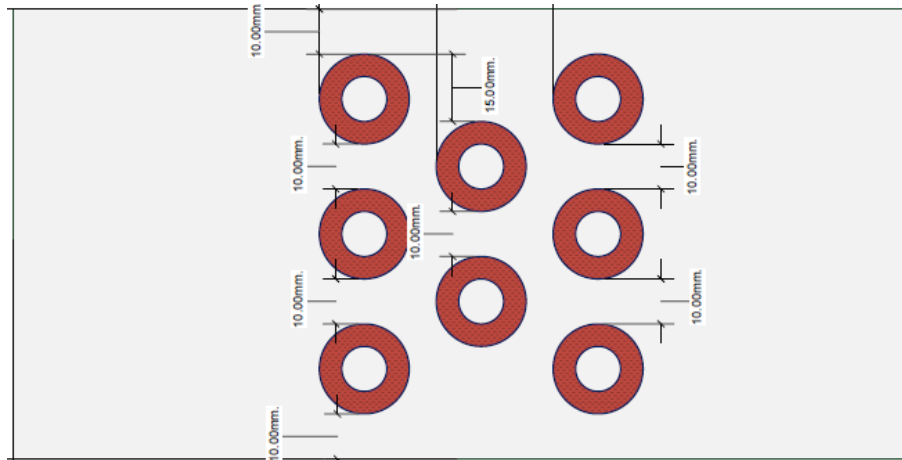


**Figure 3.3 :** An example of pattern sketch.

**i. Photomask treatment;**

Mask treatment is the first stage of the production and one of the most used photomask is chrome mask. There are three layers in photomask. First layer (base layer) is glass material light transmission, glass is coated with chrome and the last coating is photoresist material on chrome layer (shown in **Fig. 3.4**).

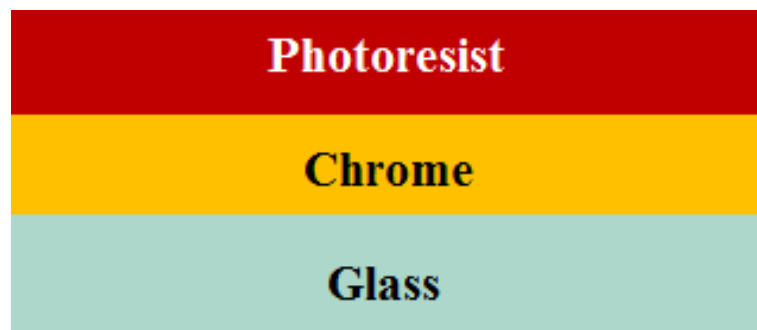


**Figure 3.4 :** Schematic illustration of chrome mask.

In the first step, the photomask is placed on the bed of the photomask-writer and be exposed to laser beam (**Fig. 3.5a**). The light particles on the resist absorb the laser, and it forms a hidden image in the photoresist layer.

The second step of photomask treatment is development. The developer of photoresist is applied and the resist removes photoresist which is exposed the light (**Fig. 3.5b**).

The next stage of photomask fabrication is etching. The etching is a chemical process to picky remove the chrome parts which is appearing under photoresist layer (**Fig. 3.5c**). It is one of the most critical step, and requires inspection during this step.

The final chemical step of the photomask treatment is to remove remain photoresist particles using acetone on the chrome layer (**Fig. 3.5d**). This provides us with chrome on quartz pattern (**Fig. 3.5e**).

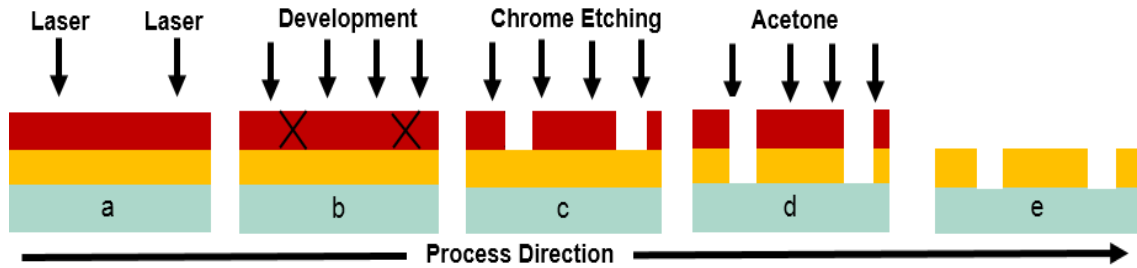


**Figure 3.5 :** The mask treatment steps.

In this project the photomask was prepared using HEILDELBURG brand mask writer in ITU-Nano laboratory. The prepared mask image and the geometric sketch is given in **Fig. 3.6**.

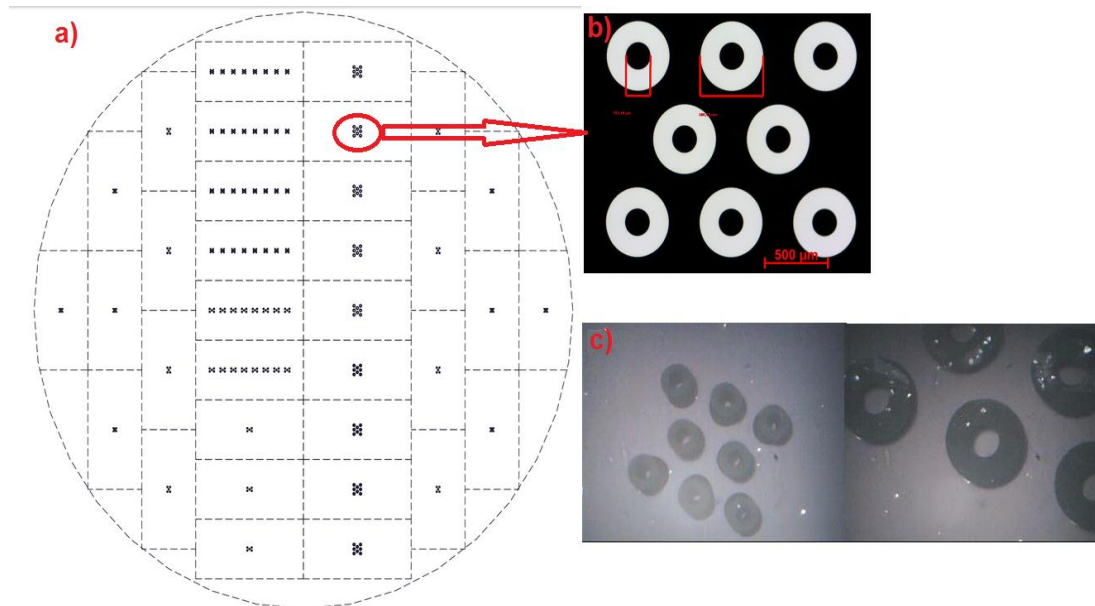


**Figure 3.6 :** Patterned CNTs (a) Illustration of 4 inches photomask, (b) optical image of a fabricated photomask, (c) an optical image of PA-CNTs.

### ii. Preparation of substrate.

After the mask preparation, substrate needs to be prepared as next step. Spin coating is one of the most used method for creating thin photoresist layer on substrate. In this method the wafer is placed on a rotating disk for homogeneous coating distribution. After to load the mask an amount of adhesion promoter such as HDMS is applied to support adhesion of the photoresist to the silicon wafer. The silicon wafer covered with a viscous liquid photoresist solution by spin coating (**Fig. 3.7b**). Disk rotation speed

and time determines to the thickness and homogeneity of the coating. The photoresist thickness is a critical parameter and it should be thicker than catalyst layer. AZ1500 series photoresist liquid was used and the coating was done at 3000 rpm in 30 seconds. Under these parameters about 0.5 micron thick coating was obtained. The coating process was performed under N<sub>2</sub> inert environment for adversely affected by atmospheric conditions. Later pre-baking was done at 100 °C in 50 sec. for increase viscosity of photoresist. After pre-baking, the photoresist was exposed to a pattern of intense light and it is shown in **Fig. 3.7c**. SUSS brand MA/BA6 mask aligner was used in ITU Nano laboratory and a UV beam which has 405 nm wavelength was send on the coated wafer surface in 6 sec. The exposure to light causes a chemical change (**Fig. 3.7d**) as photomask treatment step. It lets some of the photoresist to be removed by the developer of photoresist (**Fig. 3.7e**). The developer process time and dilute are important parameters and is given by manufacturer. In this application, 1 ml developer to 7 ml distilled water ratio was selected and applied in 5 sec. After control of pattern under the microscopy, post-bake was performed at 110 °C in 50 sec. (**Fig. 3.7f**).

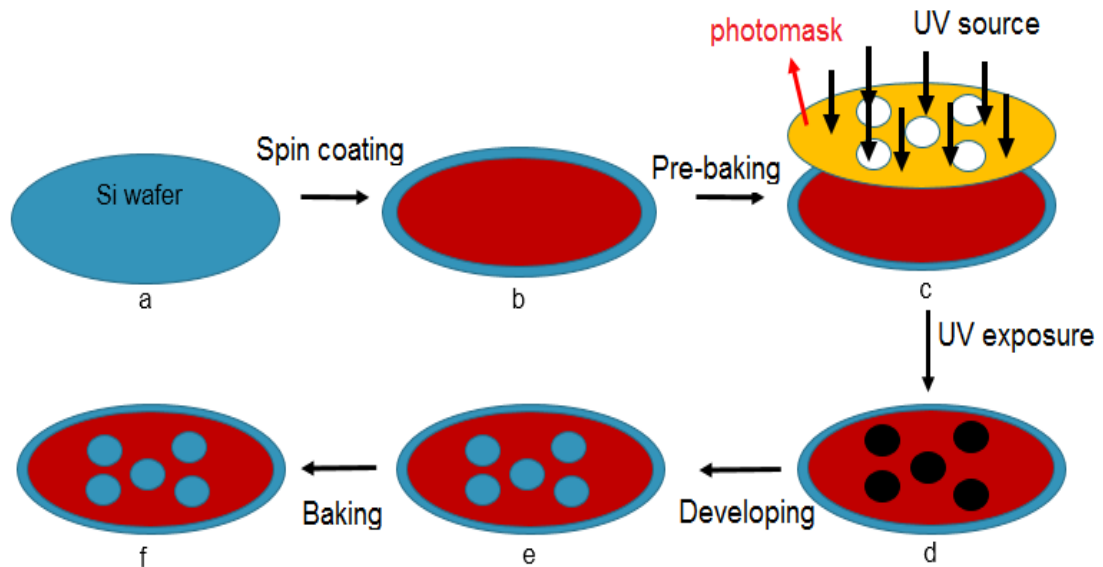


**Figure 3.7 :** Schematic illustration of substrate preparation.

### iii. Catalyst coating.

The catalyst particle size and properties effects the CNTs properties during growth, so coating method is a very important part of the production. Base and tip growth which are determined in CVD method also depends on coating method. For the base growth the bond which is between catalyst and substrate must be strong. Alumina is a way for improve adhesion between catalyst and iron particles. An coating steps for patterned

samples are shown in **Fig. 3.8**. For the base growth the substrate was firstly coated with 10nm alumina (**Fig. 3.8b**) and 1nm iron particles (as catalyst) were coated on alumina surface (**Fig. 3.8c**) by physical vapor deposition (PVD) or e-beam evaporation method. At the end of the step excess of photoresist particles were removed from Si wafer substrate using acetone and the substrate is now ready to PA-CNTs growth. PA-CNTs can be easily synthesized using the same recipe with A-CNTs.

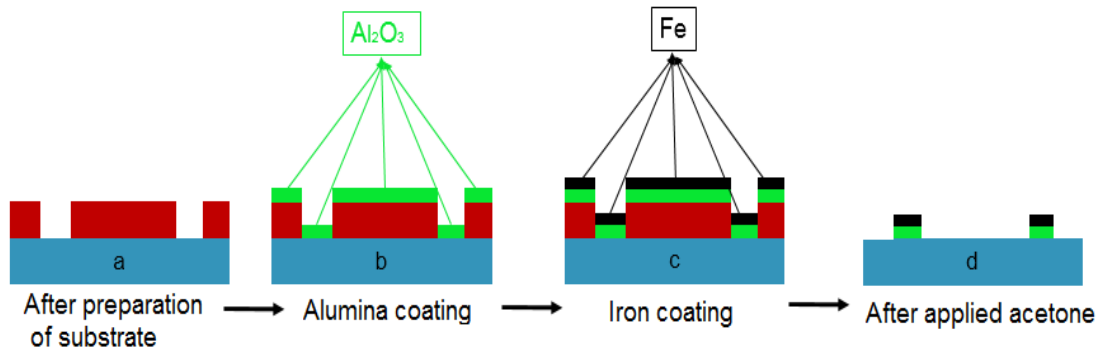


**Figure 3.8** : Coating steps for patterned samples.

## 3.2 Characterization of CNTs

CNTs can be characterized by several methods to determine their morphological, thermal properties. Scanning electron microscopy (SEM), transmission electron microscopy (TEM), Raman spectroscopy and thermal gravimetric analysis (TGA), are the ones which were used most commonly and along this thesis.

### 3.2.1 Scanning electron microscopy

In order to investigate the orientation and the length of CNTs SEM is used for morphological characterization. The SEM images were taken in the ITU Nano laboratory and an example of A-CNTs SEM image is given in **Fig. 3.9**. The image shows the appearance of vertically aligned CNTs and also right figure is taken at higher magnifications and reveals wavy view of individual CNTs. It can be seen easily the porous structure and interact with each other. As-grown A-CNTs would have <2% volume fraction after the growth procedure and the rest is air (~98%).

In thesis, long A-CNTs (<2mm), and PA-CNTs were synthesized for micro device fabrication, while short CNTs (<90 $\mu\text{m}$ ) were synthesized for nano-stitch composite application.



**Figure 3.9** : An example SEM images of A-CNTs synthesized by CVD method.

### 3.2.2 Transmission electron microscopy

In order to determine types of CNTs TEM is used. The measurement of outer and inner diameter and linear electron absorption coefficient are provide. A-CNTs TEM image is given in **Fig. 3.10**. In this figure number of walls are 5 and outer diameter about 10nm, and there is no any nano-particle, so there is no evidence to determine growth mechanism ‘tip or base growth’.

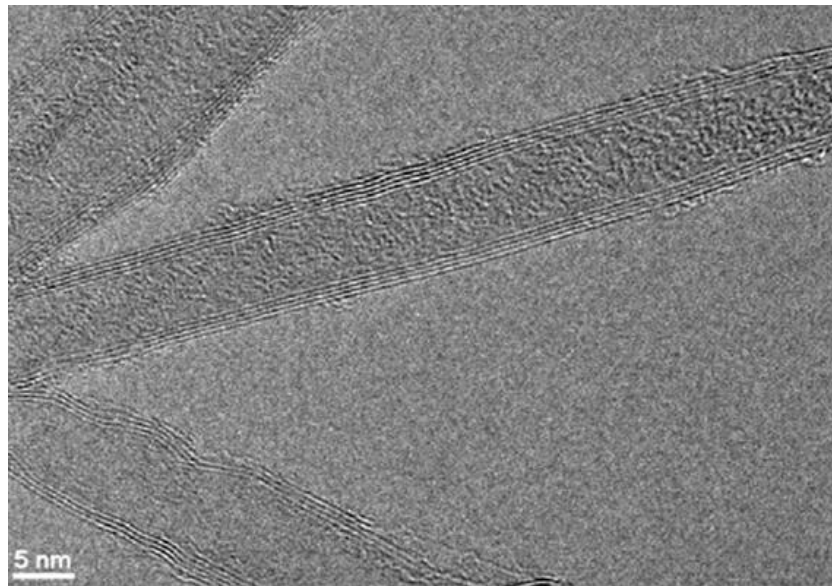


**Figure 3.10** : An example TEM images of A-CNTs synthesized by CVD method.

### 3.2.3 Raman spectroscopy

Raman spectroscopy is one of the most strong method for characterization of CNTs. Non-destructive and fast analysis is possible without specimen preparation. Fullerenes, carbon nanotubes, amorphous carbon etc. all carbon allotropes are active in Raman. According to carbon form, peak position and intensity of bands are changed. In MWNTs generally appear two peaks are observed, (i) large structure ( $1340\text{cm}^{-1}$ ) assigned to residual ill-organized graphite so-called D-line (disorder) and (ii) a large structure bunch (between  $1500\text{-}1600\text{ cm}^{-1}$ ) called G band also characteristic of nanotubes [11]. It is desired that the G peak intensity must be higher than D peak intensity for CNTs. These two intensity ratio is a kind of degree of purity and shows as  $I_G/I_D$ . In this study Raman spectroscopy was employed to investigate the effect of temperature, grow time and gas flow rates on the quality of CNTs arrays for two CNTs synthesis stage which named pre-heating tube and growth. Mean  $I_G/I_D$  ratios of optimization design is exhibited in the **Table 3.3** and also the optimization study Raman spectroscopy figures (a figure from each sample) are given below as **Fig. 3.11**. The highest  $I_G/I_D$  ratio is obtained as 2 in third experiment and this growth recipe is used for all CNTs synthesis.

**Table 3.3** : Raman results of optimization design.

Experiment number	#1	#2	#3	#4	#5	#6	#7	#8
$I_G/I_D$ (mean)	1,25	1,49	2,01	1,13	1,65	1,00	1,21	1,3

### 3.2.4 Thermal gravimetric analysis

Thermogravimetric analysis (TGA) is a thermal analysis technique that measures the weight loss of the material at depending on the temperature at desired atmospheric conditions. Especially it is widely used to measure the oxidation resistance of carbon-based materials. Oxidation resistance of the CNTs is an indication of its quality, so the thermogravimetric analysis was carried out at room temperature until  $900^\circ\text{C}$  using TA Instrument brand SDT Q600 DSC-TGA. Result of synthesized CNTs TGA graph which is the best result from optimization design is given in **Fig. 3.12** and the all TGA results are shown in **Table 3.4**. The decomposition temperature of CNTs is about  $650^\circ\text{C}$  at 5% weight loss and it shows as  $T_{d(5\%)}$ .

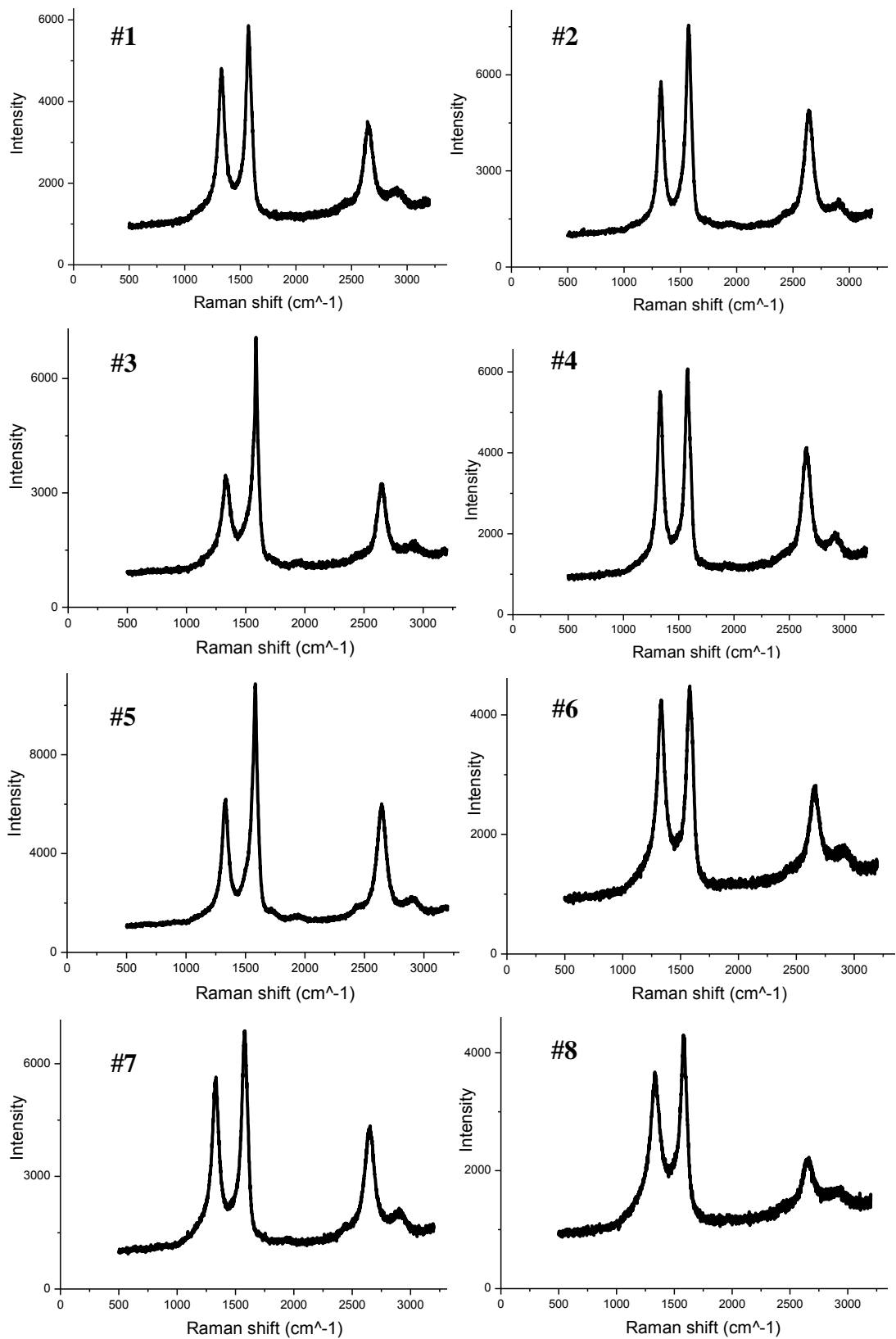


**Figure 3.11** : Raman graphs of the optimization study.

**Table 3.4 : TGA results of optimization study.**

Experiment number	#1	#2	#3	#4	#5	#6	#7	#8
$T_d(5\%)(^{\circ}\text{C})$	600	600	650	600	250	650	600	600

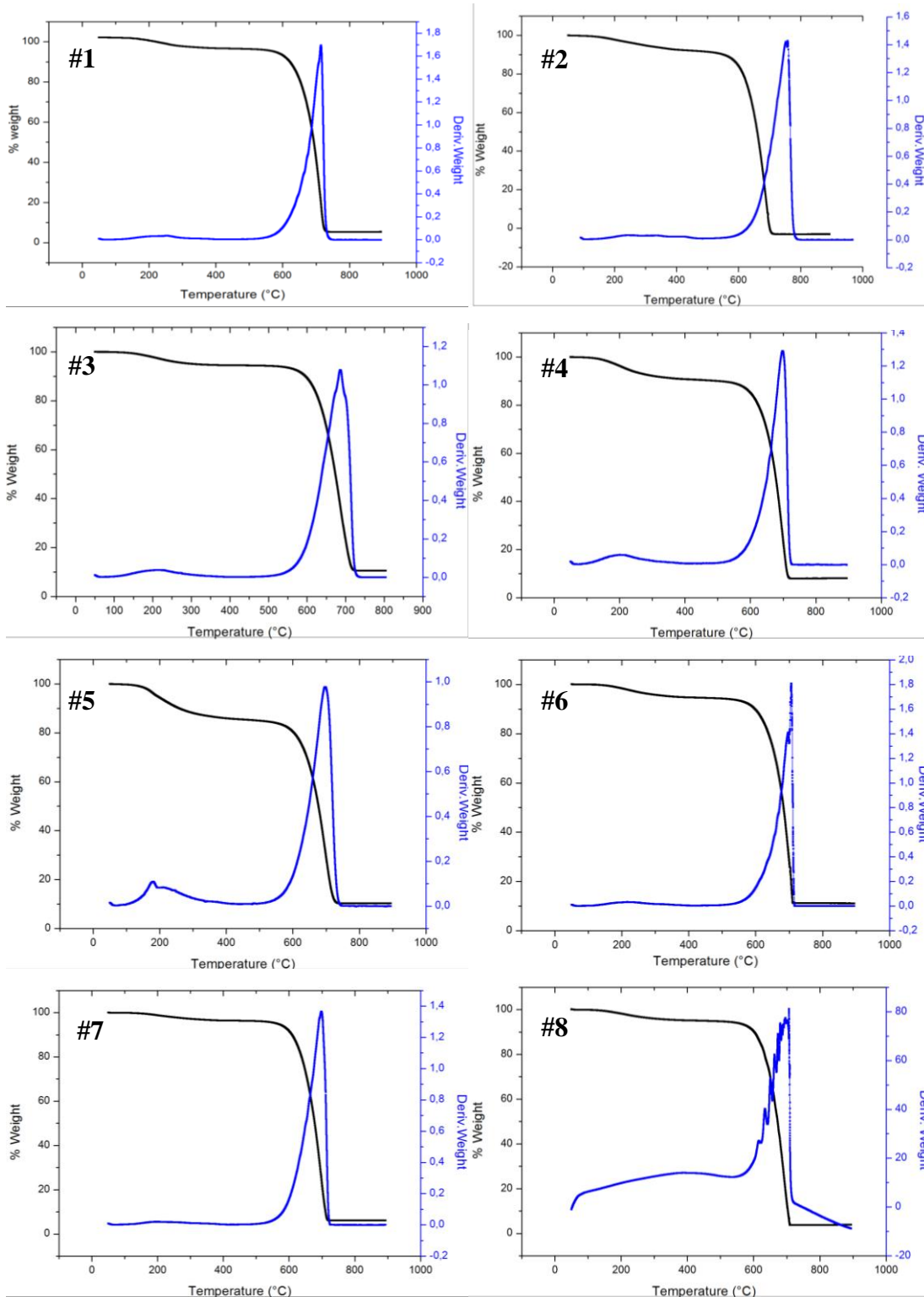


**Figure 3.12 : TGA graphs of the optimization study.**



### 3.3 Micro-Device Fabrication

Three dimensional micro and nano-porous structures are widely investigated for various applications since many improvements on the nanotechnology and micro-fabrication have been achieved recently. Carbon based micro and nano-devices are being studied and found applications in a diverse fields such as biomedical, aerospace and energy areas. Among those carbon nano-materials, carbon nanotubes achieved considerable interest with their high aspect ratio, high surface area and intrinsic mechanical, electrical and thermal properties for nanoscience research as a popular material.

Considering the micro and nano-effects, the synthesis method of CNTs is one of the most important steps in controlling its structure, morphology and orientation. Because it is possible to grow CNTs either in a random or aligned fashion even the efficiency is higher in randomly orientated CNTs, when micro and nano-device fabrication are taken into account the preferential orientation and alignment are necessary.

CNTs can also be thought as nano-pipes with their nano-scale dimensions, smooth and graphitic walls, showing an extreme compatibility and great environment to transfer and exchange nano-materials e.g. like nano-particles in the fluids. Nanometer scale inner diameter and millimeter long CNTs heights achieved by CVD methods enable to have very high aspect ratios of these ultra narrow nano-pipes that will act as channels for the transport and exchange phenomenon. In the literature there are many studies related to use of CNTs in membranes, besides filtering none of them really considers nano-material exchange along the CNTs channels. As similar to biological principles in human body, material exchange through fluids can be mimicked to tailor and design new nano-materials in a diverse field. The proposed water and air transport mechanism can be orders of magnitude faster compared to other channel types. The ultra porosity and permeability of CNTs can have a distinct effect on increasing the efficiency of these CNTs nano-pipe channels.

In this project, vertically aligned multi-walled carbon nanotubes (A-MWNT) were synthesized with CVD method to create small dimension pore sized ultra narrow nano-exchangers for nano-particle and gas transfer through channels. As-grown A-MWNT would have <2% volume fraction after the growth procedure and the rest is air (~98%). These structures would have high porosity and high permeability due to their structures with the CNT-CNT spacing between 80-100 nm depending on the catalyst and

precursor system coupling. A micro device was fabricated with this A-MWNT and the nano-particle and gas exchange transfer will be studied with this context. The growth of A-MWNTs will be either in a continuous fashion as arrays or templated pillars that will help to characterize the effects of morphology on the efficiency of micro device. Along the project, the parametric study of exchange and transport of nano-particles and gases will be also investigated. Within this project, the outcome as an application can found a lot of novel areas from biomedical to aerospace and energy with the advanced characterization and testing methods that will also help to identify new models to explain the transport mechanism of fluids in the nano-channels compared to existing models.

Schematic illustration of the micro-device is presented in the **Fig. 3.13**. For the micro-device manufacturing, after A-CNTs synthesis are optimized and characterized, the next step is to isolate the flow channel. After synthesized CNTs, the substrate was covered with polymer for isolation. And then small holes were created to sent different nano-particles towards vertical and horizontal direction. Then the out put value of flows and mixing ratio will be measured with sensors.

The flow channel dimensions vary depending on CNTs height. In the first stage, long CNTs were used due to the mold manufacturing is cheaper than micro mold that has micro channel by photolithography technique and easily handling. The mold was designed according to four diverse A-CNTs length, which can be synthesized, and it was produced using 3D-printer method as shown in the **Fig. 3.14**. Polydimethylsiloxane (PDMS) was used as mold materials due to some properties;

- Non-toxic
- Chemically inert
- Flexible in a wide temperature range
- Bio-compatible
- Thermally stable
- Having a low glass transition temperature.

After casting PDMS mixture (with hardener) in the mold, degas process was performed in a desiccator about 1 hour and then PMDS was waited at least 48 hours at the room temperature for curing due to low glass transition temperature of mold polymer.

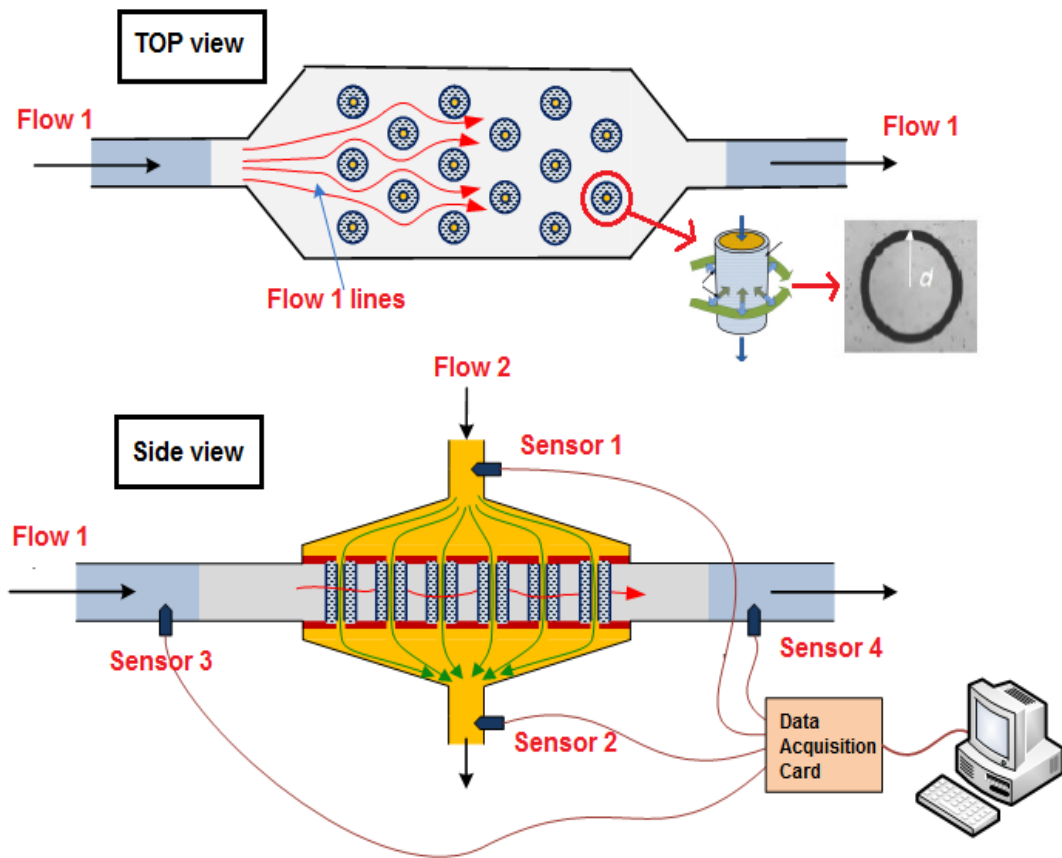


**Figure 3.13 :** Schematic view of micro device.

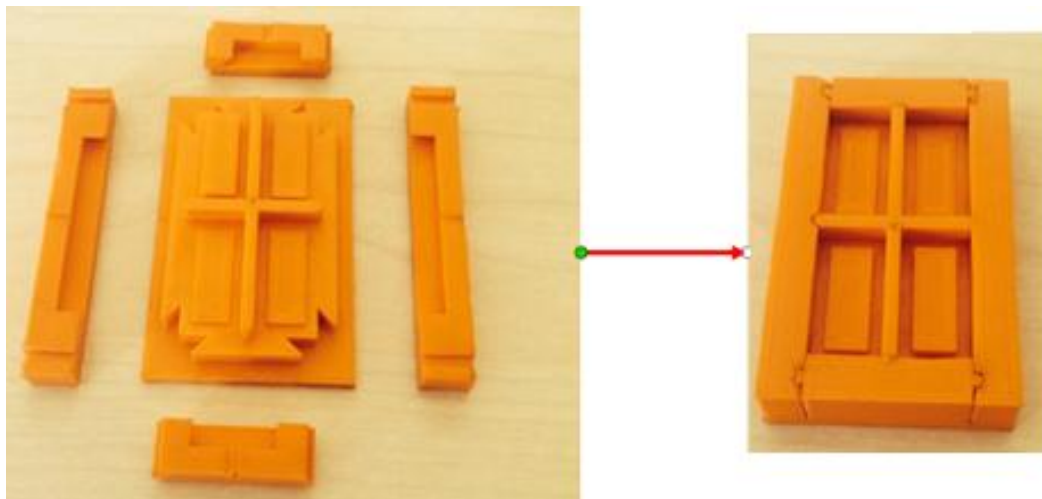


**Figure 3.14 :** Image of prepared mold for isolating micro-device.

Adhesive property of PDMS that is between mold and substrate was investigated. In order to obtain highest adhesive property three different methods were tried to cover A-CNTs with PDMS mold and are listed in below;

- I. A-CNTs corner surfaces were removed using razor and created contact surface for the mold (Fig. 3.15). This system is simplest, easy and cheap method for produce a micro device, but at the same time it had worst adhesion property.

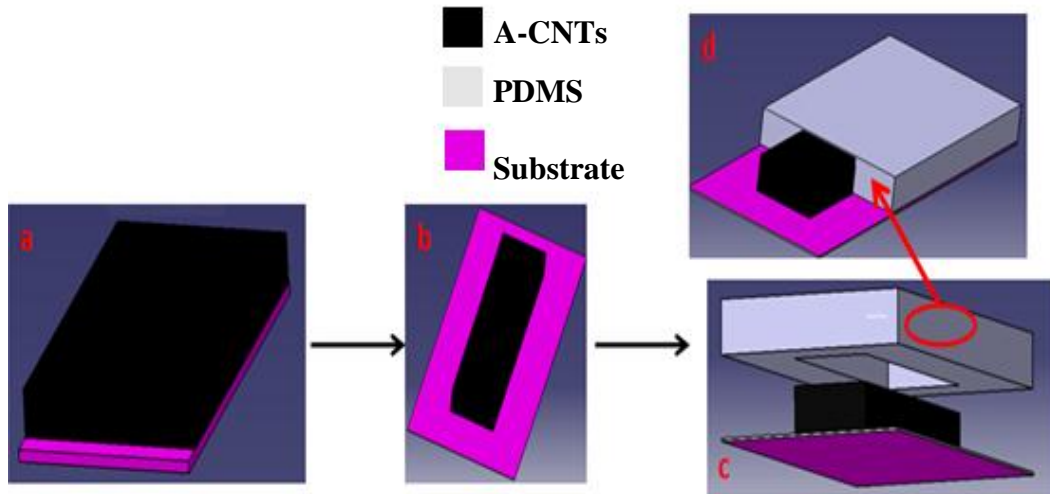


**Figure 3.15 :** Adhesive testing between PDMS mold and substrate.

- II. In the second system, a channel was created using razor and the outer CNTs regions were wetted with PDMS to use as a nano-composites walls and then a PDMS roof are placed top of the nano-composite (Fig. 3.16 and Fig. 3.17). In this method, the adhesion properties are limited to nano-composite bonding with substrate, difficult to set uniform roof height and the channel width. On the other hand, it showed better adhesion properties than first system

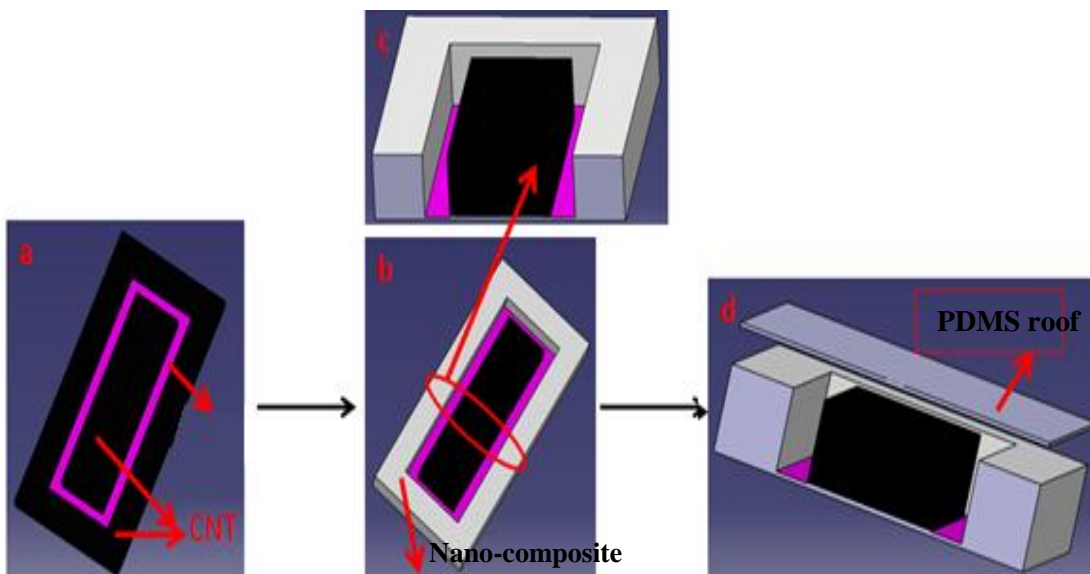


**Figure 3.16 :** Nano-composite side-wall schematic illustration.

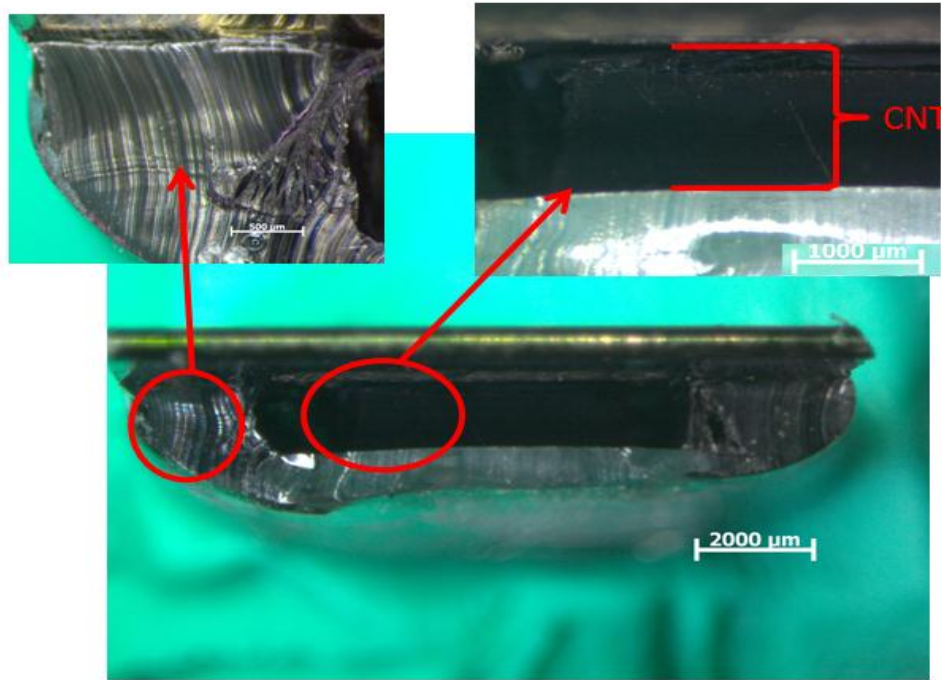


**Figure 3.17** : An example view of nano-composite side-wall molding.

- III. At the last method, the substrate was processed using laser as shown in **Fig. 3.18**. In this method, the contact surfaces showed the best adhesion feature due to increasing porosity of substrate, but it is too difficult to keep clean substrate and laser also affects some coating areas for A-CNTs synthesis.

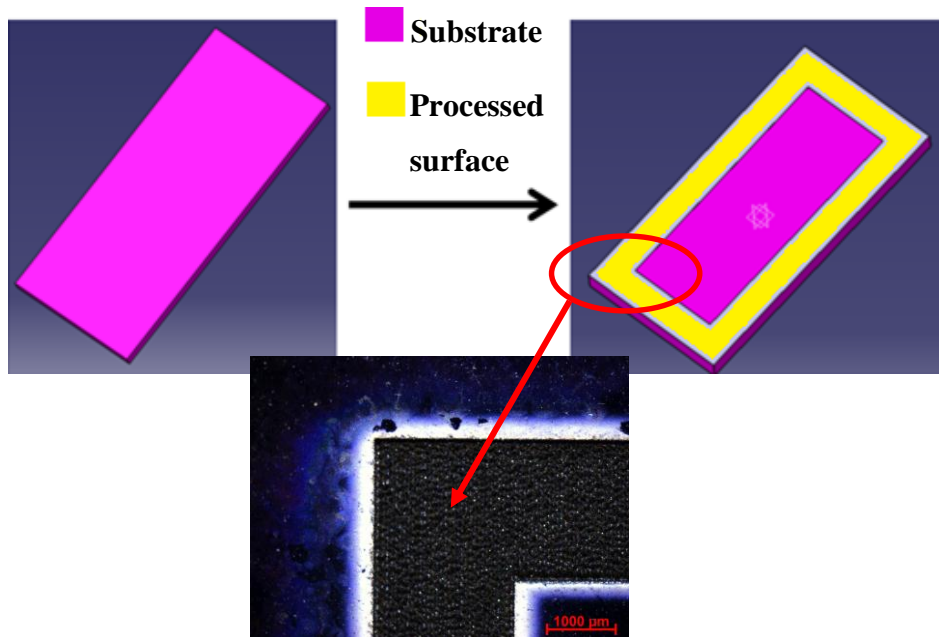


**Figure 3.18** : Display of the processed substrate using laser.

Next steps of the project can be listed as follows;

- Mold design and manufacturing for two different flow direction,
- Connecting to collector,
- Connect the test setup,
- Flow optimization,
- Testing of nano-particle exchangers.

## **4. FABRICATION AND SHORT BEAM SHEAR TESTING (SBS) OF NF and STITCHED NANO-ENGINEERED COMPOSITES (S-NEC)**

In this chapter, fabrication of nano-engineered composite laminates with nano-filler and stitched CNTs and following short beam testing are defined.

### **4.1 Parametric Study of NF Prepreg Plies and S-NEC by Epoxy Types**

In this chapter, the carbon nanotubes are synthesized using chemical vapor deposition method as explained in chapter 3. By using Taguchi L<sub>8</sub> orthogonal array, lower number of experiments are studied to achieve the test results related to experiments. The parameters and levels are shown in the **Table 4.1**.

The effective parameters related to this chapter studies were determined by previous and literature studies about NECs.

- Both matrix system were epoxy and they have very different characteristic. RTM6 is a highly crosslinked polymer and has better mechanical properties compared to West System 105 due to different chemical structure. Besides RTM6 is a mono-component system, while the marina type epoxy is bicomponent system.
- For the dispersion magnetic stirrer method was used and 2 different solvent effect were investigated.
- To manufacturing laminates, vacuum infusion and hand lay-up method were used. Both manufacturing method were asked to investigate efficiency depending on increasing CNTs loading.
- CNTs loading is a critical parameters in the system. When too much CNTs tend to agglomerate, and when the it low the improvement does not appear. CNTs loading were done between 0 and 0.11wt% range in epoxy.
- Nano stitch was used for some experiment according to array, and A-CNTs length were about 80 $\mu$ m.

The experimental design set-up was given in **Table 4.2** and results were investigated by Minitab 17 software. The first column shows experiment numbers, while the other showing parameter levels as 1 and 2 first and second level respectively.

**Table 4.1 :** Taguchi L8 orthogonal array parameters and levels.

Parameters	Level 1	Level 2
Epoxy type	Aerospace Epoxy (RTM 6)	Marina Epoxy (West System 105/206)
Fabrication method	Vacuum infusion	Hand lay-up
Nano-stitch	Not Available	Available
Dispersion alcohol	IPA	Acetone
	0	0,01
Amount of CNTs (wt%)	0	0,04
	0	0,06

The experiments were performed according to their rows. For example, forth experiment was carried out 0,01 wt% CNTs dispersed in acetone and RTM6 epoxy respectively with stitched ply was manufactured using hand lay-up method.

**Table 4.2 :** Taguchi L8 orthogonal array design.

Number of Experiment	Epoxy Type	Fabrication Method	Nano-Stitch	Dispersion Method	Amount of CNTs		
1	1	1	1	1	1	1	1
2	1	1	1	2	2	2	2
3	1	2	2	1	1	2	2
4	1	2	2	2	2	1	1
5	2	1	2	1	2	1	2
6	2	1	2	2	1	2	1
7	2	2	1	1	2	2	1
8	2	2	1	2	1	1	2

#### 4.1.1 Materials

All necessary materials in order to produce NEC which fabricated under the project are given in this topic.

##### CNTs;

Carbon nanotubes were grown for NF and nano-stitch application. Differently from section 3 the easy delamination CNTs growth procedures were used. Easy to remove CNTs from substrate without any damage is one of the most critical steps especially



during the nano-stitch process. In order to easy delamination, after growth step in recipe the H<sub>2</sub> gas was added as we said before. CNTs length for the nano-stitch is recommended about 20μm [28] because would introduce no additional thickness to ply interlayer and in this step shortest CNTs were used shown in the **Fig. 4.1a**. In order to synthesize short CNTs, the growth time was changed as 30sec. and the CNTs was synthesized about 50μm length.

In nano-filler application longer CNTs was grown about 2mm to required in large amounts of CNTs and for testing new dispersion method by changing growth time at 20min. and the SEM image is given in **Fig. 4.1.b**.

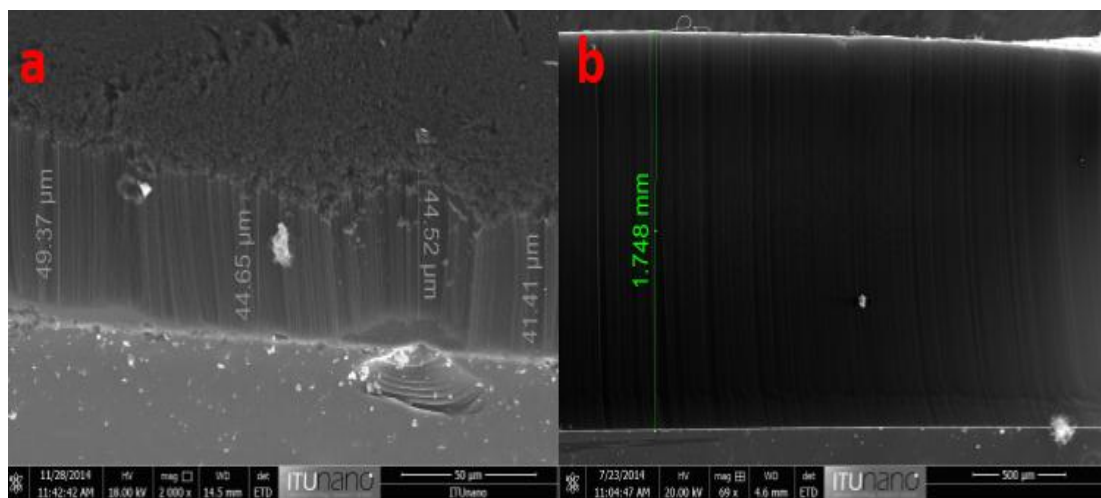


**Figure 4.1** : An example of different length A-CNTs SEM image (a) short CNTs (b) long CNTs.

### **Carbon Fiber (CF);**

According to ASTM D2344 multi-directional or pure unidirectional laminates can be tested as long as have at least 10% 0° direction. In the project the bidirectional (0°/90°) carbon fiber cloth with density of 370 g/m<sup>2</sup> was used as reinforcement and each tow of the carbon fiber consists of 12000 fibers.

### **Epoxy;**

Including aerospace (Hexcel RTM 6) and marina (west system 105/206) type epoxy were used. The aerospace resin is a extremely crosslinked polymer class with the marine epoxy because of the chemical structure, and the differing chemical structure causes to diverse mechanical properties, where RTM 6 has a tensile strength of 75MPa with a strain to failure of 3.4%, while the west system 105/206 has a tensile strength of 50MPa and a strain to failure of 4.5%.

#### 4.1.2 Customized prepreg manufacturing of S-NEC

Dispersion process is one of most important part of adding nano-fillers. Carbon nanotubes have to disperse very well in an epoxy, otherwise, it can be play adverse role and decreasing is observed in mechanical properties. Some of the reasons and dispersion technics are mentioned in the literature section.

In earlier studies, homogenizer and tip sonicator were used for dispersion of CNTs in epoxy and IPA respectively. Homogenizer method showed well CNTs dispersion, while the sonicator was indicating agglomerate with high CNTs loading. In this thesis differently from these method, magnetic stirrer dispersion method was used for dispersion of CNTs in IPA or acetone solvent. The solvent type was accepted as a parameter. A magnetic stirrer device that employs a rotating magnetic field to cause a stir bar immersed in a liquid to spin very quickly. As a first level of dispersion parameter, magnetic stirrer process are summarized in **Fig.4.2**.

In this method CNTs are dispersed in an alcohol such as IPA or acetone due to their low viscous properties and viscous epoxies which are used are not eligible.

- Firstly all components (two magnetic stir bars and solvent) were mixed and they were milled by hitting each other at 1200 rpm at least 2 hours as a small grinder.
- Secondly solvent was removed from CNTs using a small space mesh.
- At the end of the process the CNTs is dried in 30 °C at least 8 hours due to evaporation of remain alcohol.

The last image (numbered 7) shows to achieved CNTs which is also called as bucky paper and this paper can be easily disperse to individual CNTs.

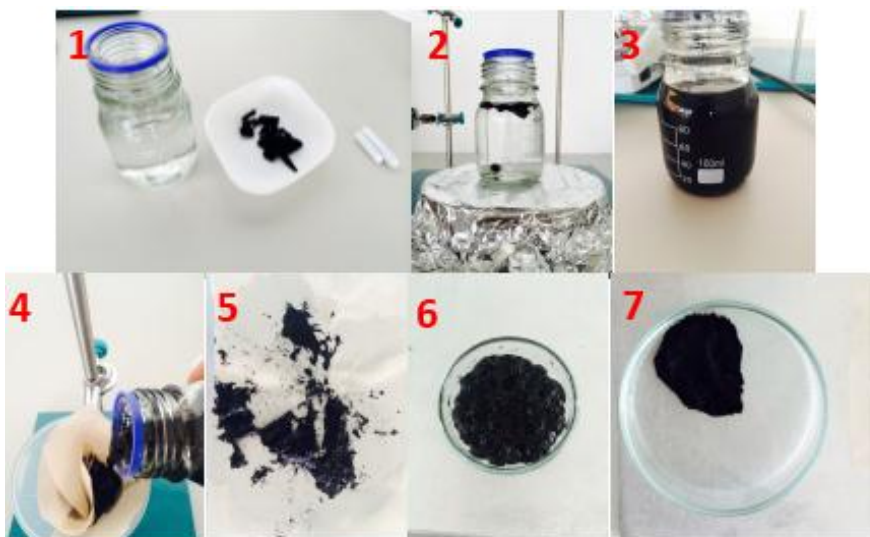


**Figure 4.2 :** Stages of magnetic stirrer process.

After dispersion, the obtained CNTs paper was dispersed in the viscous epoxies using mechanical mixer at about 1800 rpm at least 2 hours. These times were changed according to amount of CNTs to achieve homogeneous CNTs distribution. West System epoxy was dispersed at the room temperature, while the RTM6 was being dispersed at 80 °C on a hot plate (**Fig. 4.3**).

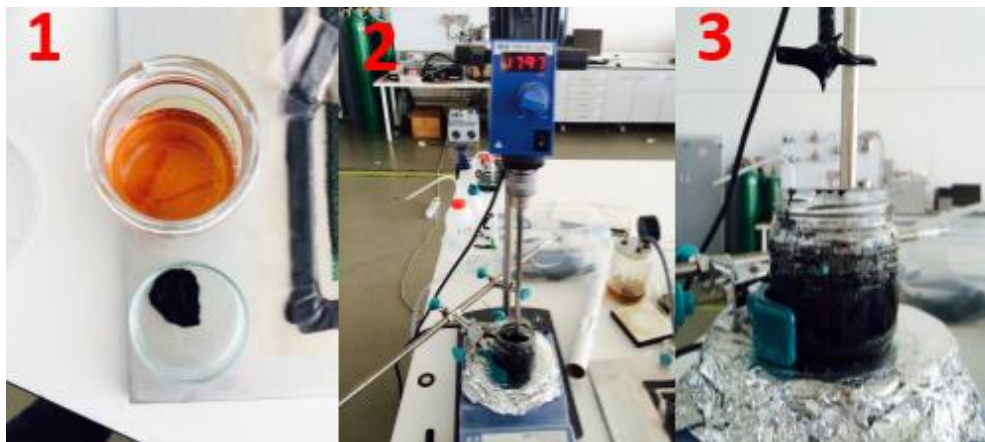


**Figure 4.3 :** Illustration of RTM 6 dispersion.

In literature, there are very few studies about prepreg with CNTs loading [39-41] and for the stitch application prepreps are provided great convenience [28]. In this project, firstly CNTs prepreg plies were produced for easy stitch application and to manufacture customize prepreg layers hand lay-up method was used and an example of schematic view is shown in **Fig. 4.4**. Detailed information about hand lay-up method will be given in next topic. Firstly the epoxies which have homogeneous CNTs distribution were prepared and the carbon fibers wetted with the epoxy contents. The prepreg plies were produced in the previously mentioned epoxy types and after manufacturing, RTM6 prepreps (between prepreg release film) were stored in fridge at -30 °C until the laminate production, while the west system prepreps were used immediately. Besides, during to do prepreg using West System epoxy must be fast due to short curing time.

Joining prepreg composite interfaces is the second main aim of this thesis. Short height A-CNTs (<80µm) were transferred on the customize carbon prepreps. This method provides homogeneous CNTs alignment in the through thickness direction. Stitched A-CNTs forests into composites improve interlaminar strength and toughness due to bridge and strength, and electrical conductivity of composite through thickness.

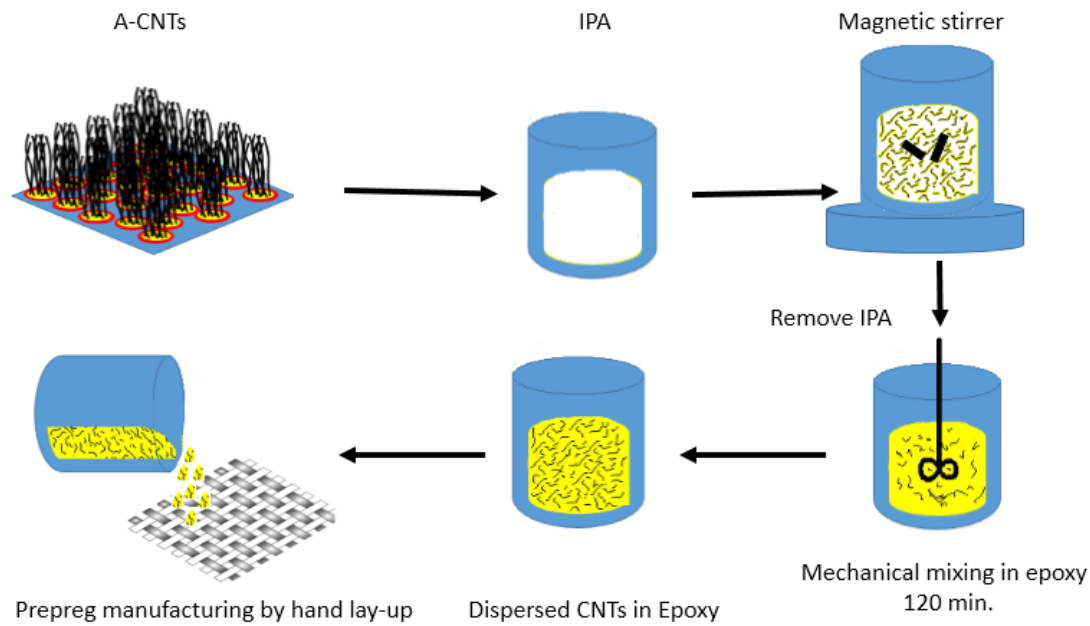


**Figure 4.4 :** Schematic view of CNTs prepreg manufacturing.

In this method the growth recipe is the most critical parameters. The carbon nanotubes have to be short length and have to remove easily from substrate for full transferred and to exhibit similar properties through thickness. A transfer printed on commercial carbon prepreg illustration is given in **Fig. 4.5**. Easy delamination recipe was used in this step like as CNTs prepreg preparation step. Firstly the CNTs was put on the customize prepreg and apply uniform pressure on substrate using a roller. The the wafer was removed slowly and carefully.

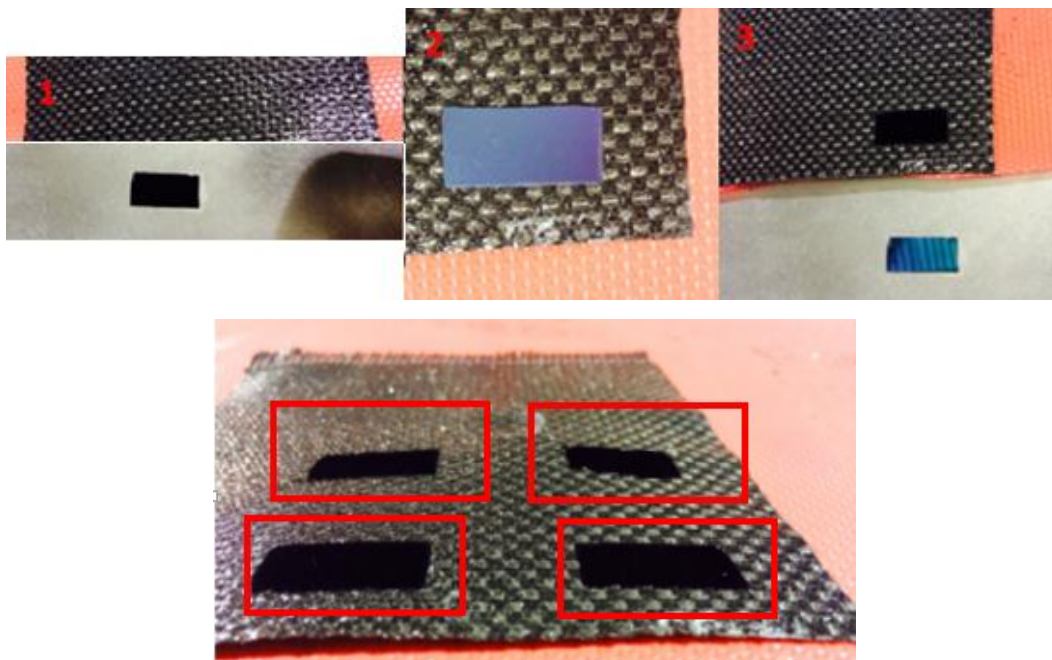


**Figure 4.5 :** An example illustration of CNTs transfer-printed on commercial prepreg.

While the transferring short height CNTs on the commercial prepregs did not experience any transfer problem due to well adhesion and smooth surface, transferring short height CNTs on customize prepreg surface is too difficult. The A-CNTs were not transferred fully, some A-CNTs areas remained on substrate due to bidirectional woven surface, and in order to obtain best transferring results (in minimum CNTs height), different recipes were used and obtained CNTs were applied as shown in **Fig. 4.6**. The best CNTs height result was determined as 80 $\mu$ m and all stitched CNTs were synthesized in this height.

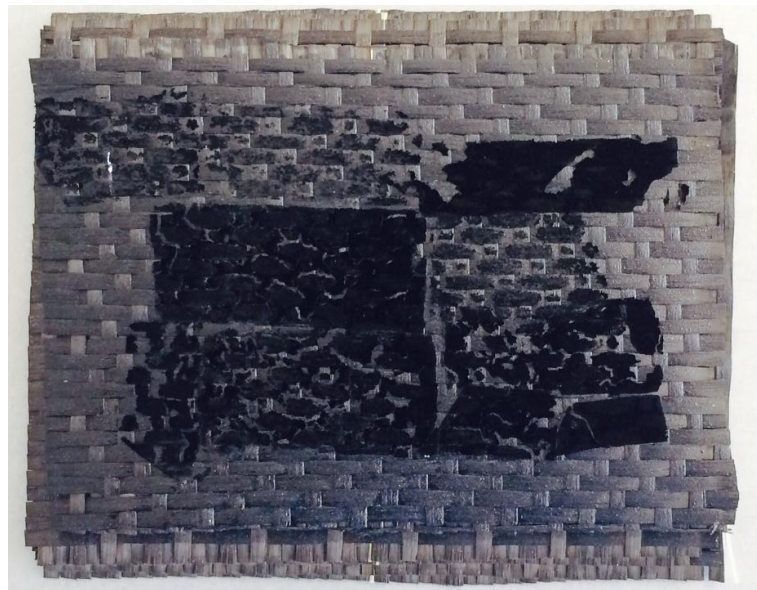


**Figure 4.6** : An optimization study for fully transferring A-CNTs on customize prepregs.

Instead of producing separately, nano stitch samples were produced as one large sample shown in **Fig. 4.7** and then the specimens were cut from this samples using dremel saw.



**Figure 4.7** : A view of patterned nano-stitch on customize prepreg ply.

### 4.1.3 Fabricating of S-NEC laminates

For the manufacture of laminates were studied on two different production methods as called hand lay-up and vacuum infusion process (VIP) and the schematic illustration is given **Fig. 4.8**. Both production methods have some advantages and drawbacks.

In hand lay-up method (**Fig. 4.8b**), selected reinforcements are cut to the required size and are provided full wet with resin. The prepared ply is immediately can be available or store between prepreg release films in the fridge for later use. Firstly a mold release material is applied on the mold surface to avoid the sticking of polymer to the mold. Then the plies are placed on the mold of the desired thickness and are cured according to resin materials. Hand lay up method is the simplest and minimum equipment required technique of composite manufacturing. There are many drawbacks of this technique and some of them are;

- Quality and resin/reinforcement mixing ratio is very depend on employee skills
- Health and safety consideration of resin
- Resin need to be low viscosity to be workable by hand.

The vacuum infusion process is a technique that uses vacuum pressure to drive resin into a laminate (**Fig. 4.8a**). Reinforcements are laid into the mold and the vacuum is applied before resin is transferred. After a complete perfect vacuum is obtained, resin is sucked into the laminate via carefully placed tubing. In vacuum infusion process, higher fiber and lower void content laminates can be achieved, better fiber wet-out because of pressure and the vacuum bag reduces the amount of volatiles emitted during cure. On the other hand, the extra process adds cost in labor and materials. A higher level skill is required by working.

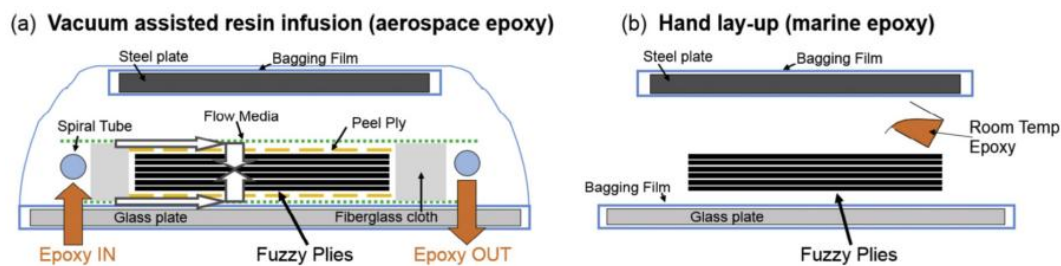


**Figure 4.8 :** Schematic illustration of manufacturing methods of laminates (a) vacuum infusion (b) hand lay-up [6].

For the laminate product, the hand lay-up method is not enough by itself due to lack of quality. When performed alone, the fiber-resin ratio is too low and amount of void

is increasing, so after each prepreg laid, the vacuum was applied during the curing time and excessive resin was removed from laminate using tubing as vacuum infusion method which is given in **Fig. 4.9**. After laid customized prepregs, a peel ply layer was laid on prepreg to obtain homogeneous surface and a mesh was placed on peel ply for easily flow of resin and then this system was covered with vacuum bag and lastly was cured under vacuum. During West system epoxy laminates curing, the samples were placed at least 24 hours under vacuum and the vacuum pump or the tubing system had never been closed. In similarly, while the RTM 6 samples curing at 160 °C in 75 min. in furnace, the pump always was worked in this method. After producing all RTM 6 specimens the post cure was performed at 180 °C in the furnace without vacuum and before the test specimens were waited at least a weak for post cure of west system samples. The 3,4,7 and 8 numbered experiments (is given in **Table 4.2**) were manufactured using this modified hand lay-up method. 3 and 4 numbered experiments also have stitched CNTs layer in the mid ply.

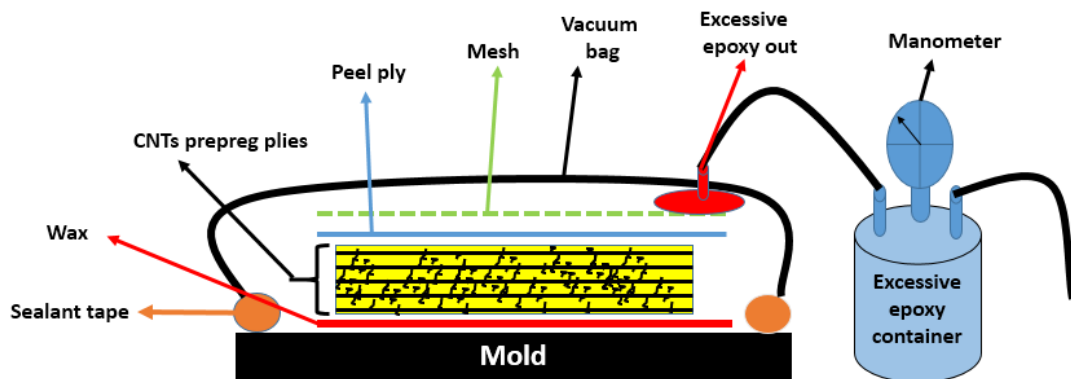


**Figure 4.9 :** Schematic illustration of modified hand lay-up method.

In vacuum infusion method (**Fig. 4.10**) the biggest issue is placed the stitch CNTs due to there is no adhesive surface on carbon fiber and small length CNTs remove from substrate without any damage are too difficult, so the mid ply of laminate would preferred as CNTs prepregs (numbered 5 and 6 experiments and take notice CNTs content is given in **Table 4.2**) to obtain sticky surface as in the **Fig 4.10**. The second main problem is homogeneous distribution of CNTs in laminates. The CNTs can be accumulate on mesh, peel ply or upper plies. Small length and well dispersed CNTs can be solve this problem. In this method, during to ly the RTM 6 epoxy the mold and epoxy were heated at 90 °C and 80 °C respectively. The wetting process was done under a 740mm Hg vacuum for straight and without tripping wetting while the west

system epoxy laminates production were being done at room temperature. In order to obtain well wetted homogenous composite, the wetting process have to done very slowly. Otherwise high viscosity epoxy which is increased by A-CNTs causes poor wetting samples (**Fig. 4.11**). After all plies are fully wetted, the tubing system were closed at the both end with the help of tubing clamps and the vacuum was kept during the curing time according to epoxy types. This method is easier and faster than modified hand lay-up method. In both method 12 plies carbon fiber and same curing conditions were used and the thickness and voids were investigated using optical microscopy.

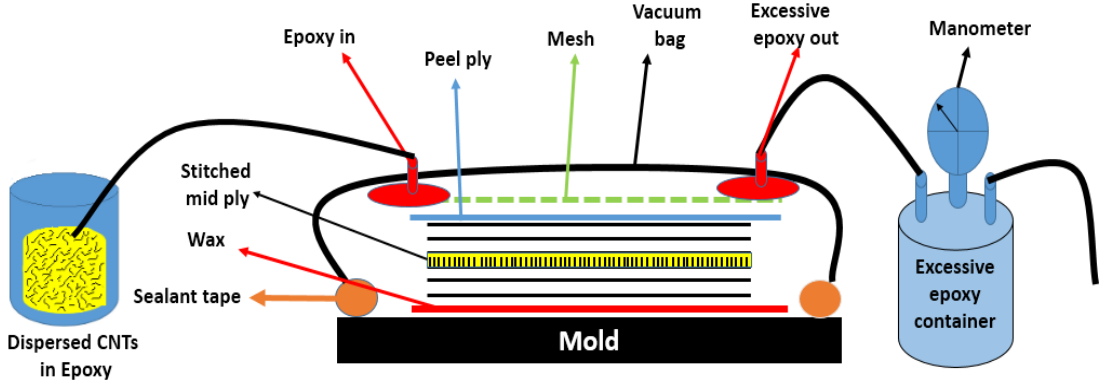


**Figure 4.10** : Schematic illustration of vacuum infusion process.

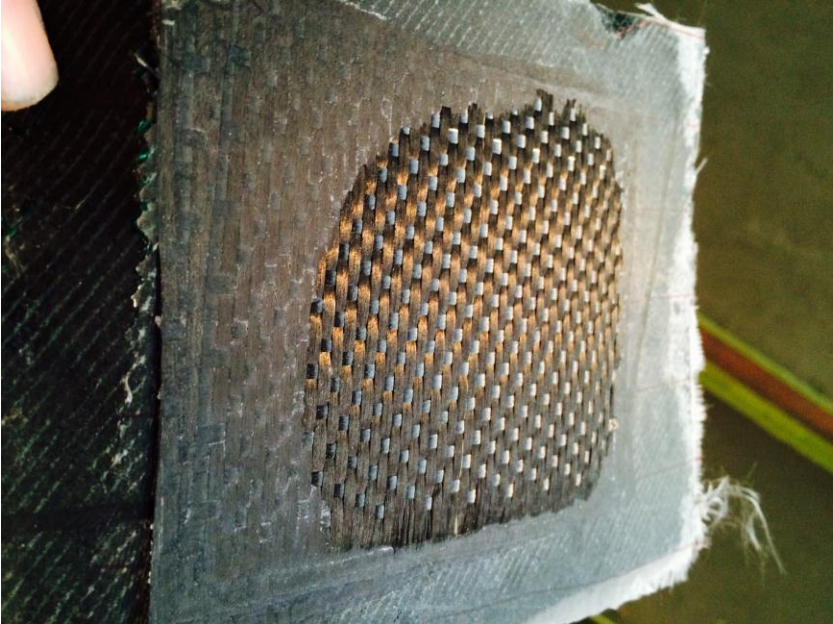


**Figure 4.11** : Bottom surface view of poor wetted composite using VIP.



## 4.2 Mechanical Properties Investigation of S-NEC with SBS

Electrical resistance was measured through thickness. The visual information about direction is exhibited in **Fig. 4.12**. The resistance measurement is provided to calculate electrical conductivity of NECs for structural health monitoring application.

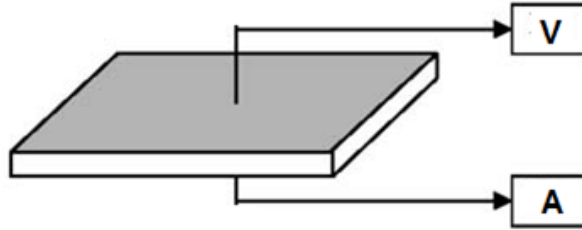


**Figure 4.12 :** Schematic visualization of resistance measurement.

The DC electrical conductivity of the composites was measured by a standard two-probe electrode using a digital multimeter in dry air at ambient temperature. Silver paste was applied on probe contact surface and then the samples were placed between two electrodes through which current was passed and the resistance was measured directly from the instrument. The conductivity of the samples was calculated using the formula (4.1);

$$\sigma(S/cm) = \frac{l}{\Omega \times A} \quad (4.1)$$

where ‘ $\sigma$ ’ is the electrical conductivity, ‘ $\Omega$ ’ is resistance, ‘ $l$ ’ is the distance between probes in centimeters and ‘ $A$ ’ is the area of contact of the electrodes with the sample in centimeter square.

The short beam shear mechanical testing method was performed in our investigation to determine interlaminar shear strength of nano-engineered composites according to ASTM D2344 [42]. The main advantage of the SBS is simplicity.

The specimen thickness determines to the other geometries. For the flat specimen, length and width are 6 and 2 times bigger than specimen thickness respectively. The specimens are placed on two cylindrical support and the other cylindrical head is moved -z direction speed of 1.0 mm per minutes until applied load dropped by 30% or the cross-head travel exceeded the specimen nominal thickness. The image of test system, sample position on support and cross section view of sample are shown in **Fig. 4.13**. The support span is set span-to-measured thickness ratio is 4.0 to an accuracy of  $\pm 0.3$ .

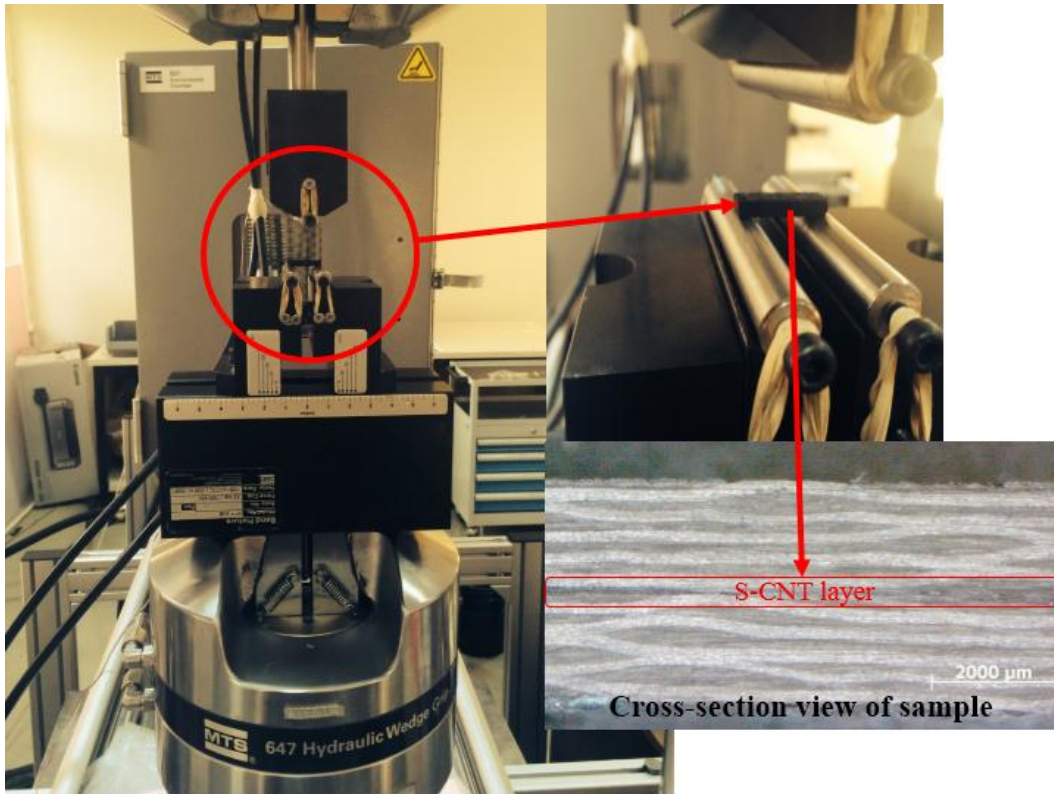


**Figure 4.13** : SBS test specimen being tested under load.

In the SBS test, the determination of ILSS is based on classical (Bernoulli–Euler) beam theory. The maximum interlaminar shear stress occurs at the mid-thickness of the beam between the center and end supports and is calculated using **Eq. 4.2**.

$$F^{SBS} = 0.75 \times \frac{P_m}{b \times h} \quad (4.2)$$

Where;

F sbs = short-beam strength, MPa (psi);

Pm = maximum load observed during the test, N (lbf);

b = measured specimen width, mm (in.), and

h = measured specimen thickness, mm (in.).

There are three kind of failure modes in this test. In the first case, the crack is occurred by max. stress in mid ply of the specimen and crack propagation continuous along the mid ply. In the second instance, the crack is emerged on the top-mid or bottom-mid surface which are called compression and tension failure respectively due to flexure load. In the last case, the specimen shows inelastic deformation. All failure mode figures are shown in **Fig. 4.14**.

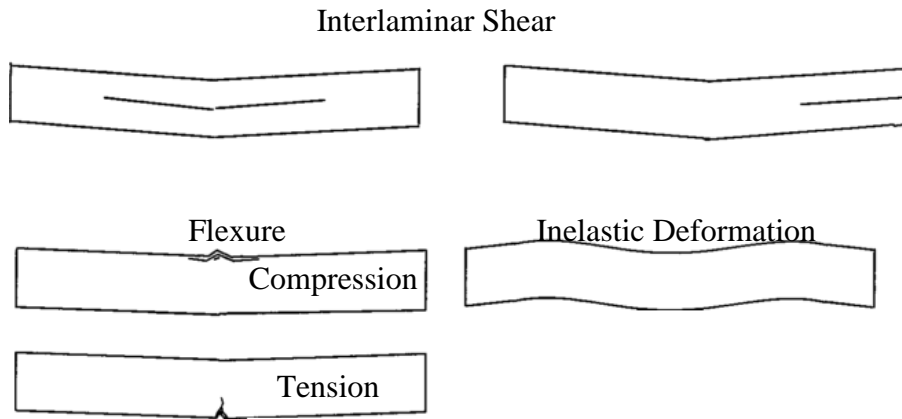


**Figure 4.14 :** Typical failure modes in short beam shear test [42].

The experiments were performed using MTS test machine. The displacements and loads as a function of time were recorded. The maximum load was reading at the moment of crack start. Data were used to determine short-beam strength and an example graph is given in **Fig. 4.15**. A max. load is occurred by cylinder movement and load begins to decrease. Beside the ILSS decreases with decreasing load. Also specimen fracture surfaces were characterized by optical and scanning electron microscopy.

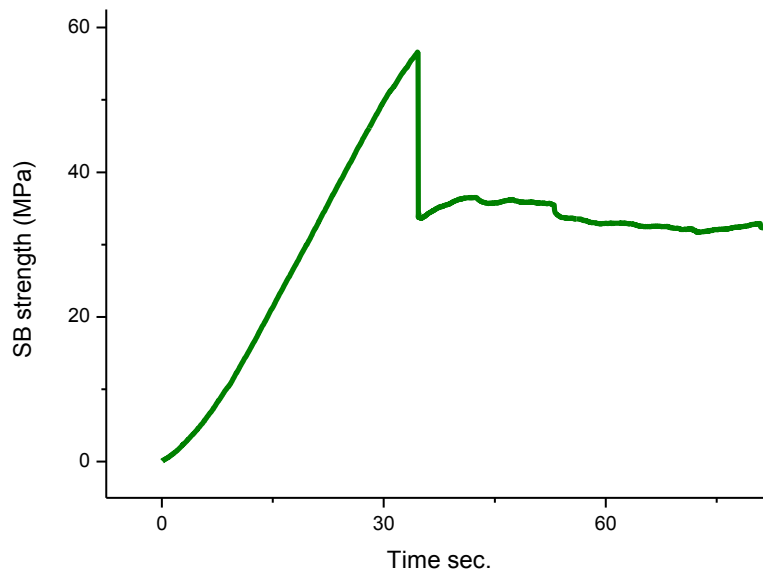


**Figure 4.15 :** Typical time-short beam strength graph.



## 5. RESULTS

In this chapter the data which are obtained from test results, followed by an investigation of interlaminar shear strength properties and electrical conductivity of NEC.

### 5.1 SBS Results

Two different studies were performed to improve ILSS.

In the first study results are given in **Table 5.1** and an example graph from each experimental group is shown in **Fig. 5.1**. All specimens were manufactured customized prepregs (A-CNTs/10plies carbon fiber/RTM6) using customized hand lay-up method. CNTs was dispersed in RTM6 epoxy 30min. and 2 hours using homogenizer and mechanical mixer respectively. Stitch-CNTs length were about 200  $\mu\text{m}$ .

**Table 5.1** : ILSS of CNTs/carbon/epoxy composites measured by SBS.

Specimen Number	ILSS (MPa)					
	0%	0.1%	0.15%	0% + Stitch	0.1% + Stitch	0.15% + Stitch
1	47	55,93	50,19	33,66	34,4264	38,76
2	44,1	54,75	46,27	35,76	34	36,8
3	45,95	53,1	48,9	34,56	34,99	37,53
4	46,3	53,59	46,54	33,94	36,81	35,5
5	46,69	54,85	47,3	33,86	36,27	35
average	46,01	54,44	49,84	34,356	35,3	36,72

This study was conducted to determine effects of A-CNTs and stitched CNTs in composites. Although the A-CNTs in epoxy caused ILSS improvement, the middle stitched CNTs layer exhibited negative effect. Two typical SB strength-deformation behaviors are shown in the **Fig. 5.1**. In **Fig. 5.1A** max. short beam strength rises gradually and the strength drops suddenly to begin crack. Then the specimen continuous to load bearing and load continuous to increase until second crack begins

and this time the load decreases less than the first dropped load value . In **Fig.5.1B** the curve rises a peak and shows a small drop. Then the load continuous to increase until interlaminar shear failure occurs. This type failure can be occurred by resin micro cracks [43].

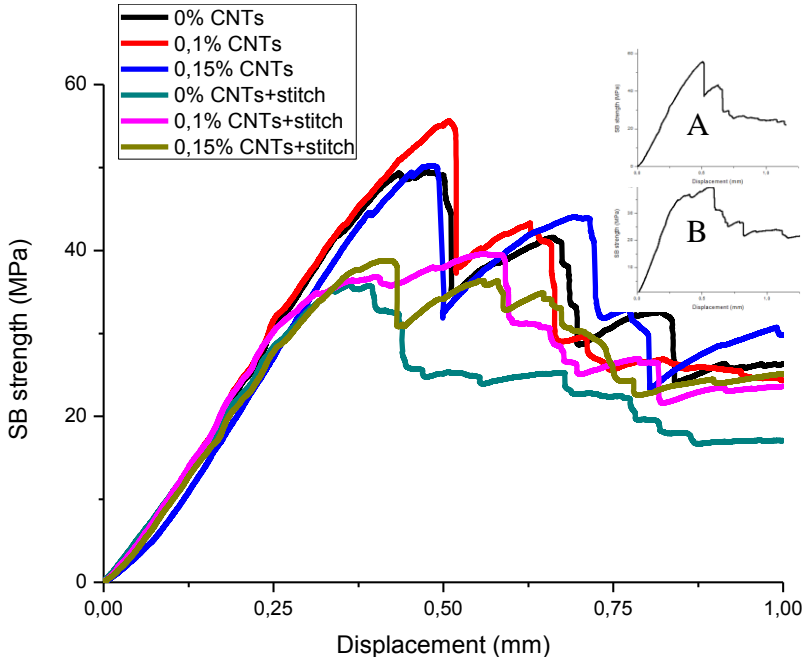


**Figure 5.1 :** SB strength versus displacement for laminated composites samples.

High length stitched CNTs were caused wetting problem and increased to specimen thickness. An example of fracture figure of this study is shown in **Fig. 5.2**. First crack was occurred in middle ply and crack propagation was easily continued throughout this layer until it reaches the midpoint and then the other cracks were occurred.

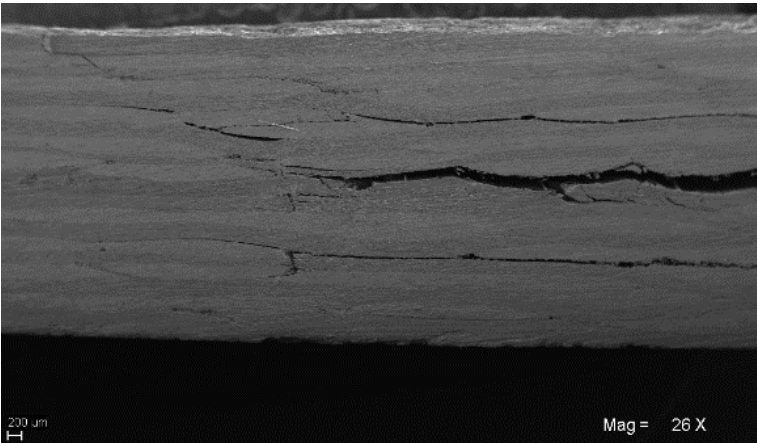


**Figure 5.2 :** An example view of crack propagation of S-NEC with 200µm long A-CNTs after SBS test.

The ILSS of the composite most improved 18.3 % by adding 0.1 wt% A-CNTs in epoxy, and 8.3% for 0.15 wt% A-CNTs. On the other hand the average ILSS of

composites worsened -25.3% , -23.3% and -20.2% for baseline, 0.1 wt% and 0.15 wt% in epoxy respectively as shown by error bars in **Fig. 5.3**.

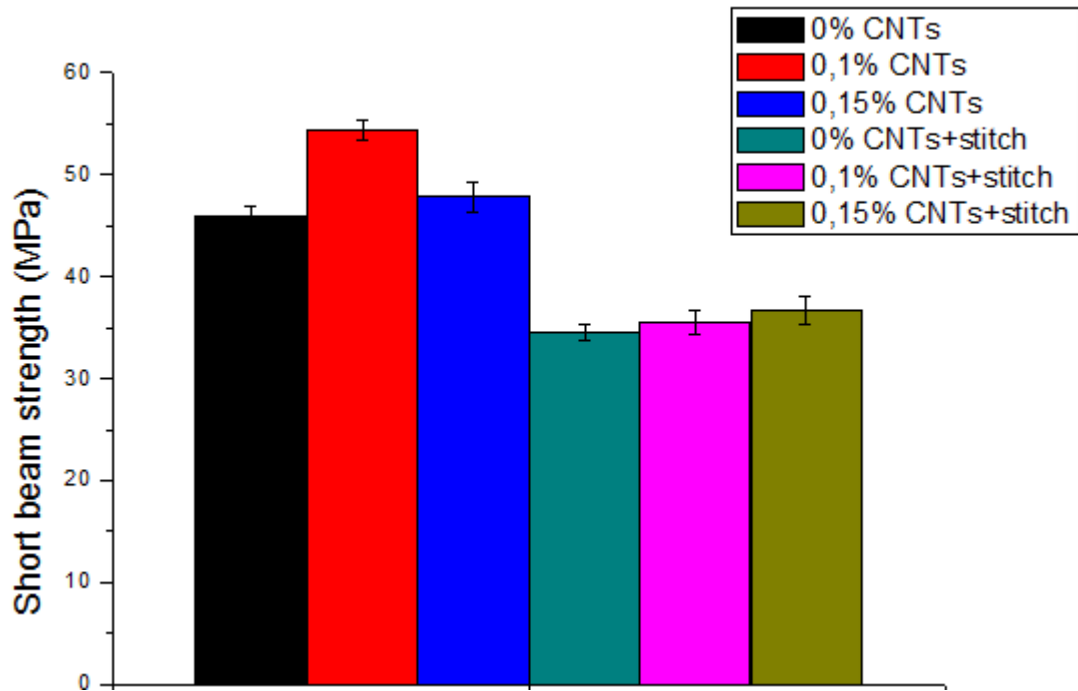


**Figure 5.3** : Chart of ILSS of the NECs.

In the second study, in order to achieve highest ILSS and effects of factors, Taguchi  $L_8$  orthogonal array design was used and **Table 5.2** presents the mean interlaminar shear strength results of Taguchi  $L_8$  orthogonal array design. Numbered as 1 and 2 are levels of factors which are given in the table and section 4. The biggest improvement shows at the maximum amount of CNTs with 0.11 wt% CNTs in aerospace epoxy. According to table it is seen clearly, interlaminar shear strength has shown the greatest decline with the change of epoxy type. For the aerospace epoxy, results of second and third experiment shows 13% and 7.5% improvement ILSS. In contrast, fourth experiment results shows -4.44% decline, and it can be explain that amount of CNTs is too little with 0,01wt% and the production method is hand lay-up. When the compare marine type epoxy, the amount of CNTs are very close for each experiment number. It seems that the effective parameters are fabrication method and nano-stitch.

When the graphs are plotted, results show two typical SB strength-deformation behaviors which are given in the **Fig. 5.4**. In **Fig. 5.4A** curve rises gradually and then drops suddenly showing a distinct failure load developed in the sample (same behaviors with the first study), while in **Fig. 5.4B** the curve rises, flattens for some time and then shows a drop gradually after begin crack. The reason of these behaviors

is different matrix properties. The RTM6 aerospace epoxy has brittle structure unlike marine type epoxy has ductile structure properties. The other experiment results are given in **Fig. A.1** and **Fig. A.2**.

**Table 5.2 : SBS test results of Taguchi L8 orthogonal array design.**

Experiment #	Epoxy Type	Fabrication Method	Nano-Stitch	Dispersion Method	Amount of CNTs	Average ILSS (MPa)
1	1	1	1	1	1 1 1	<b>55,18</b>
2	1	1	1	2	2 2 2	<b>62,42</b>
3	1	2	2	1	1 2 2	<b>59,34</b>
4	1	2	2	2	2 1 1	<b>52,73</b>
5	2	1	2	1	2 1 2	<b>30,07</b>
6	2	1	2	2	1 2 1	<b>29,02</b>
7	2	2	1	1	2 2 1	<b>27,23</b>
8	2	2	1	2	1 1 2	<b>25,42</b>

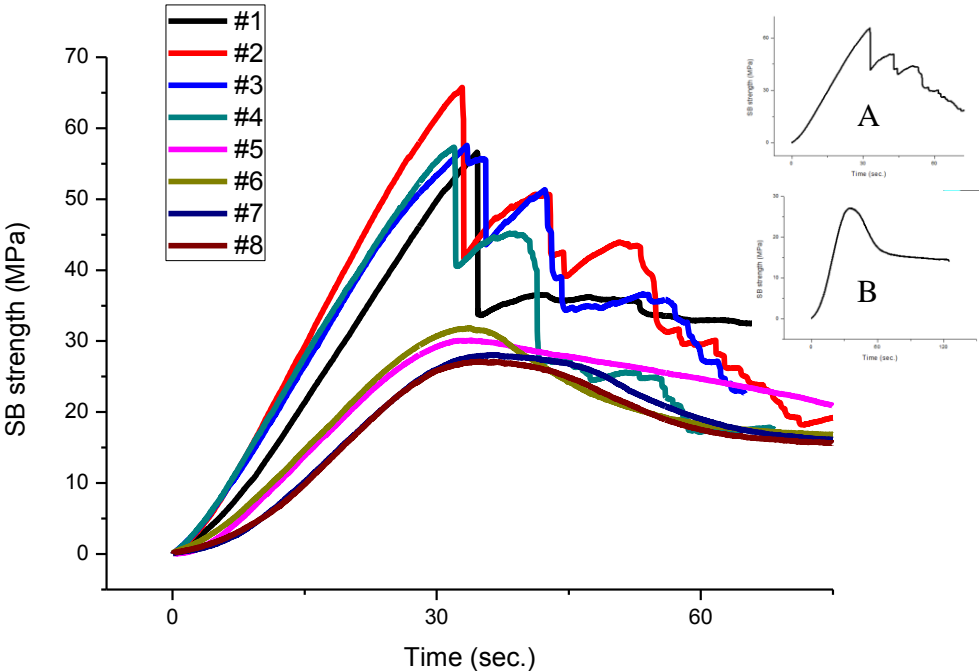


**Figure 5.4 : SB strength versus time for NECs samples.**

In order to determine crack mechanism of NECs, the SEM and OP images were investigated and some pulled out behaviors were observed.



Marine epoxy laminates surfaces (**Fig. 5.5a**) showed more micro-fiber-matrix interface adhesive failure and exposed fibers than aerospace epoxy (**Fig. 5.5b**). Besides, in marine type epoxy, too many resin rich clusters which independent from fiber were shown as in the **Fig. 5.5a**. This structures can be caused to poor adhesive property between matrix and reinforcement.

SEM fractography of the fractured laminates shows that the A-CNTs in matrix stimulate micro-scale changes to the fracture surface. In the aerospace epoxy NECs laminates, as given in **Fig. 5.6**, the fracture surfaces showed residual micro-fibers from other laminate due to high adhesive of laminates with matrix cohesive failure and CNTs were pulled out during crack propagation. The same pulled out CNTs system was also shown in marine type epoxy as shown in **Fig. 5.7**.

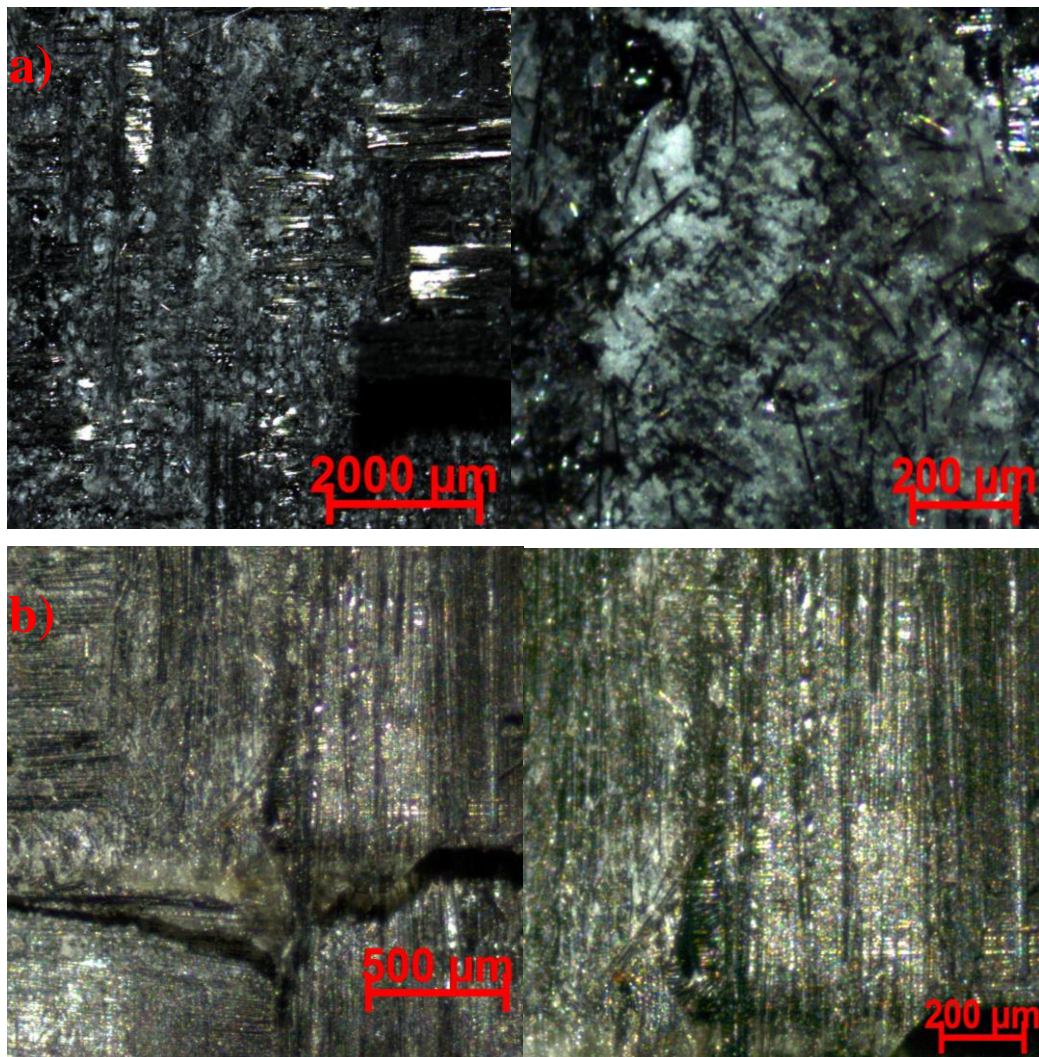


**Figure 5.5** : SBS fracture surface image of (a) marine epoxy and (b) aerospace epoxy NECs using optical microscopy.

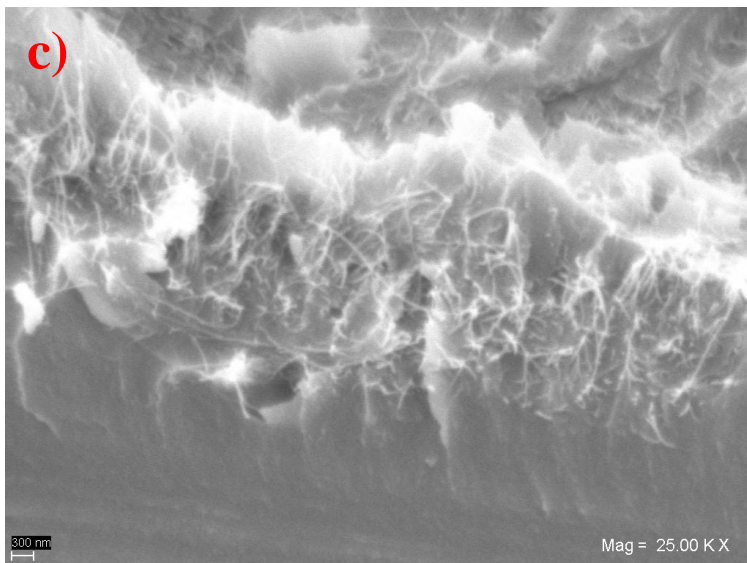
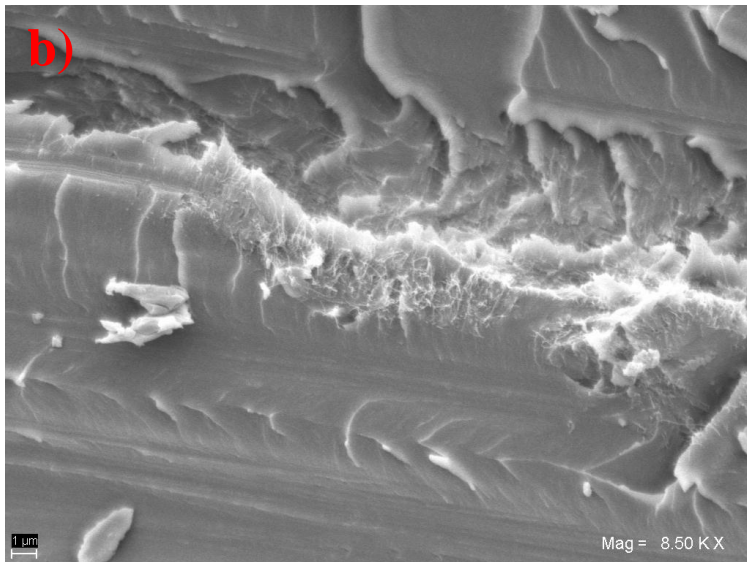


**Figure 5.6 :** SBS fracture surface of aerospace laminates, (a) epoxy fracture along tows, (b) low and (c) high magnification of pulled out of fracture surface in NECs laminates.

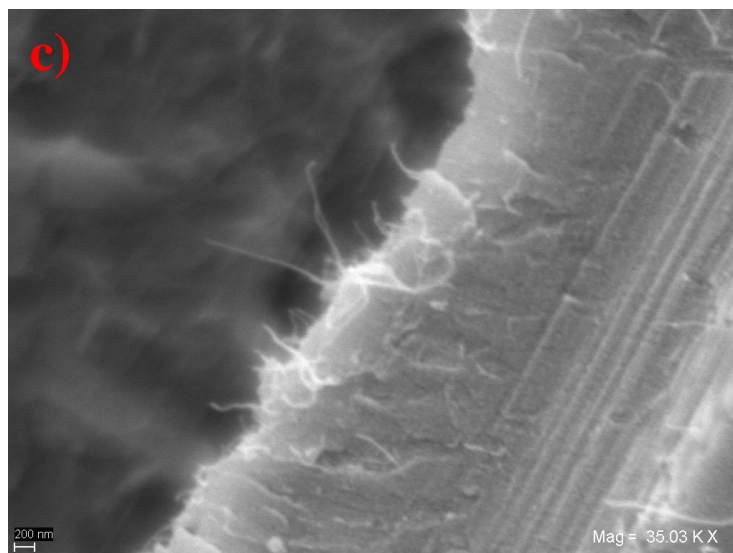
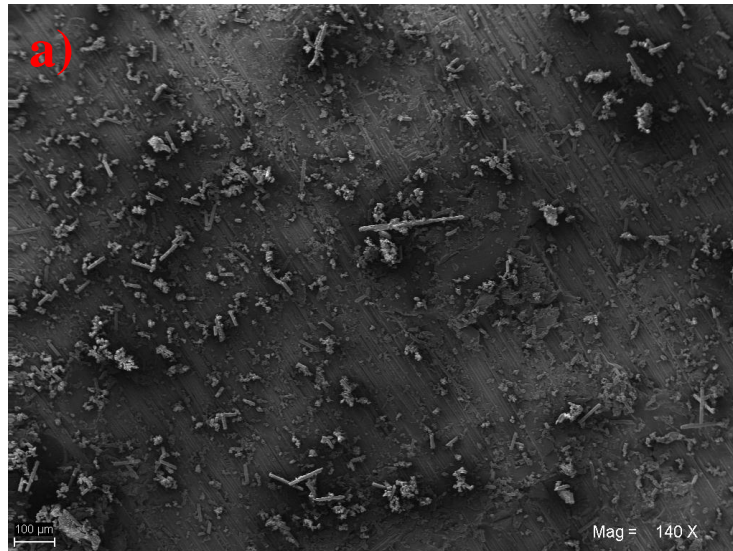


**Figure 5.7 :** SBS fracture surface of marine laminates, (a) epoxy fracture along tows, (b) low and (c) high magnification of pulled out of fracture surface in NECs laminates.

In the stitch structure, extra CNTs pulled out mechanism can be seen and it was observed in this study (**Fig. 5.8**). In contrast first study, in the second study a little ILSS improvement was seen. It can be explained that interface shows tougher properties depending on stitch height (in the first study long CNTs caused wetting problems). In literature it is reported that 20 $\mu$ m long CNTs array has provided 50% increase of SBS strength while the increasing the sample thickness, and in the study, A-CNTs sequences have been placed between each ply [21]. In this study also degree of stitch effect (placed mid plane) will be investigated.

The SBS test data were analyzed using Minitab 16 software and response table for signal to noise ratios are given in the **Table 5.3**. The rank shows effect of factors on SBS. Epoxy type is the most effective factor chosen in this study, and than fabrication method, amount of CNTs (0.04 and 0.06 wt% in epoxy), nano-stitch, 0.1 wt% CNTs and finally dispersion method come, respectively.

**Table 5.3 :** Response table for signal to noise ratios (larger is better).

Level	Epoxy Type	Fabrication Method	Nano-Stitch	Dispersion Method	Amount of CNTs		
1	35,16	32,39	31,89	32,14	31,92	31,74	31,81
2	28,91	31,68	32,18	31,93	32,15	32,33	32,26
Delta	6,26	0,71	0,29	0,22	0,24	0,6	0,45
Rank	<b>1</b>	<b>2</b>	<b>5</b>	<b>7</b>	<b>6</b>	<b>3</b>	<b>4</b>

To investigate the effects of levels, Taguchi response graph was plotted and is shown in **Fig. 5.9**. In the graph, the highest points show the effective level. According to the analysis, the highest improvement is achieved when the specimen is manufactured with 0.11wt % dispersed CNTs (E2+F2+G2) in IPA(D1) and RTM6 epoxy(A1), and nano-stitch (C2) using vacuum infusion process (B1). In contrast, composite production without A-CNTs in epoxy and stitched CNTs with marina epoxy using customized hand lay-up method has shown the lowest performance for interlaminar shear strength. In order to obtain the highest ILSS an extra manufacturing was done and the results are investigated.

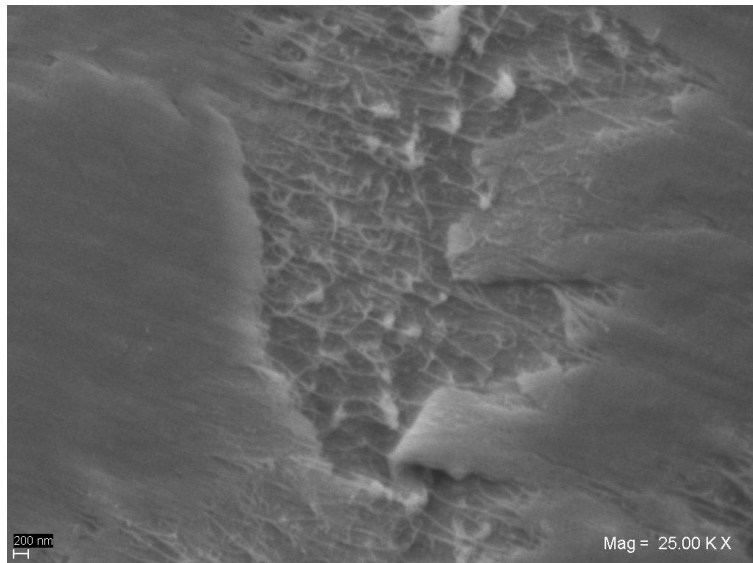
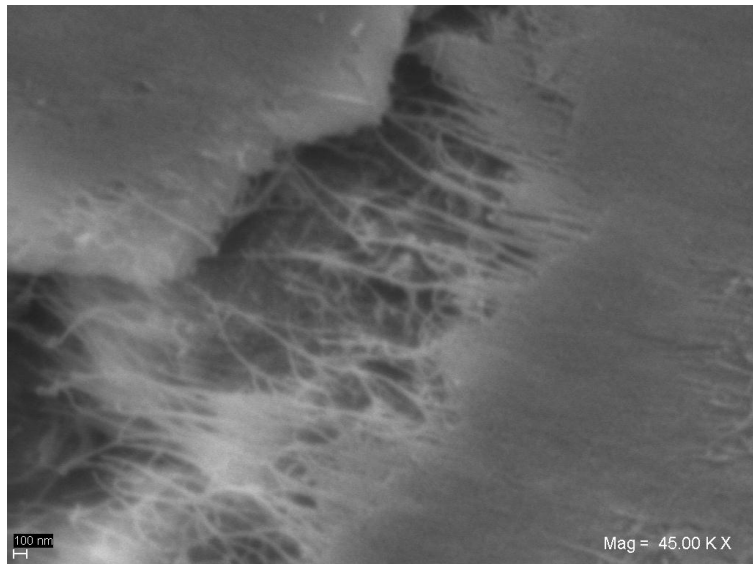
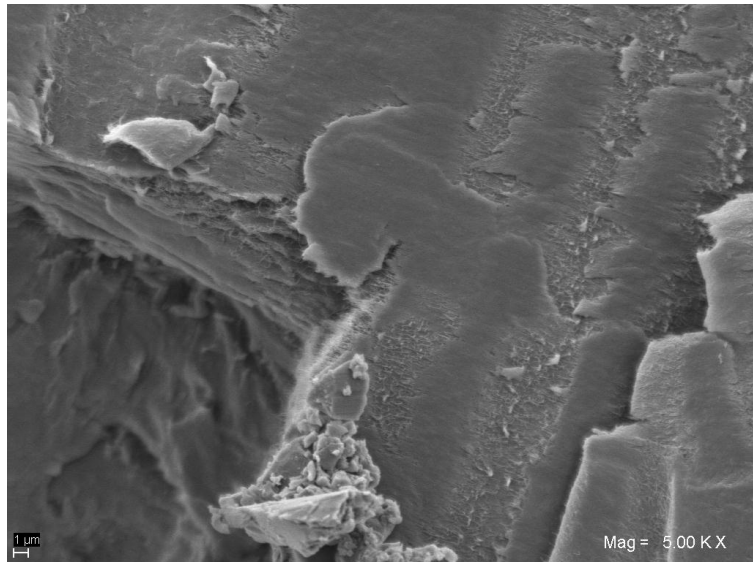


**Figure 5.8 :** Pull-out mechanism of S-NECs.

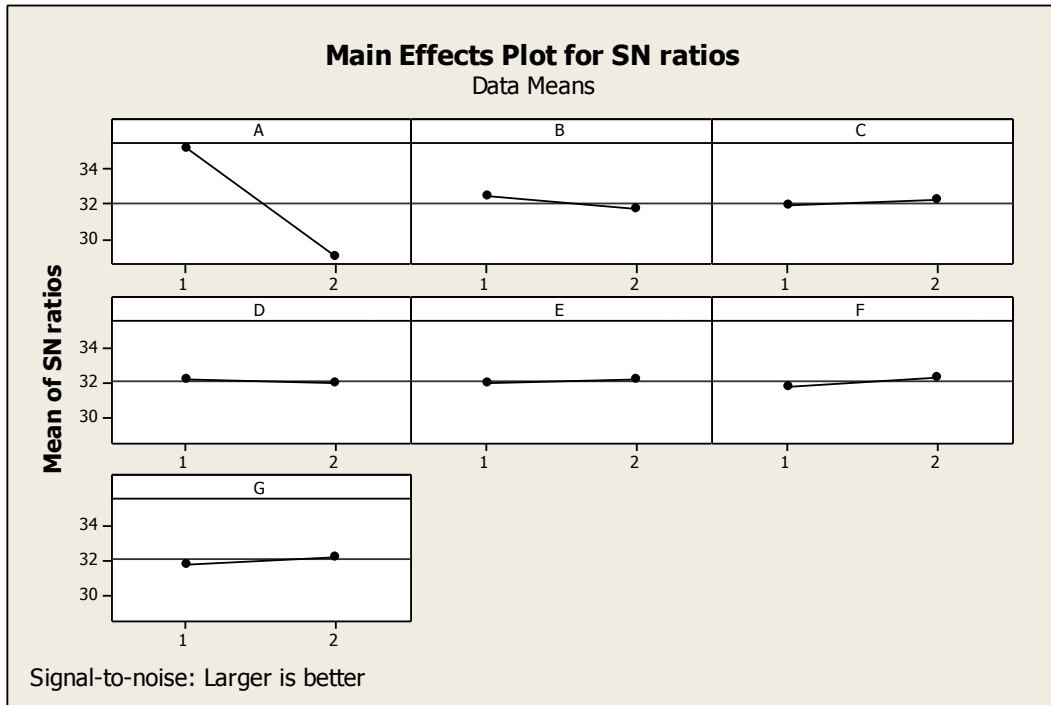


**Figure 5.9 :** Main effects plots for S/N ratios.

The ninth experiment results showed highest SB strength with 63.3 MPa average as expected and the SB strength-Time graph is given in **Fig. 5.10**. In this experiment, the load suddenly decreases to about by half. All SB strength results are given in **Fig. 5.11** as diagram.

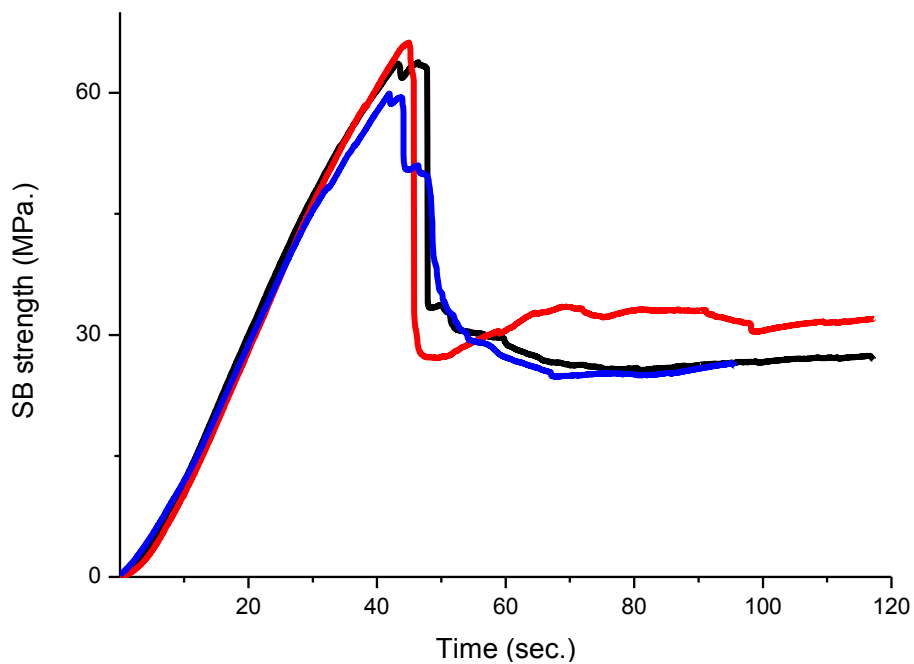


**Figure 5.10 :** SB strength versus time for ninth experiment.

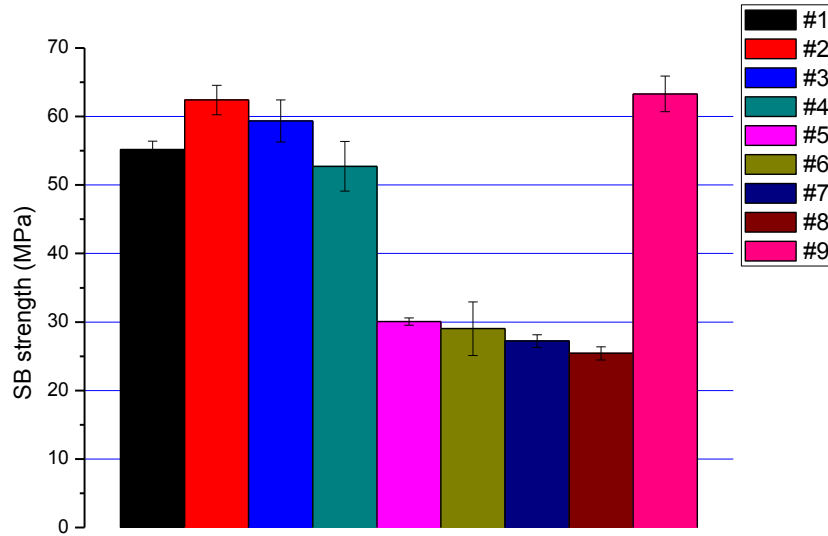


**Figure 5.11 :** Chart illustration of results of Taguchi L8 orthogonal array design.

## 5.2 Electrical Conductivity Analysis

Electrical conductivity (through the thickness) results are given in **Table 5.4** and **Fig. 5.12**.

**Table 5.4 :** Electrical conductivity results of Taguchi L8 orthogonal array design.

Epoxy type	Fabrication method	Nano-Stitch	Dispersion method	Amount of CNTs			Electrical conductivity (S/cm) Z
1	1	1	1	1	1	1	0.016072
1	1	1	2	2	2	2	0.060699
1	2	2	1	1	2	2	0.187615
1	2	2	2	2	1	1	0.168354
2	1	2	1	2	1	2	0.010336
2	1	2	2	1	2	1	0.023034
2	2	1	1	2	2	1	0.010344
2	2	1	2	1	1	2	0.013631

The NECs fabricated with carbon nanotube/carbon fiber reinforcement showed improved out-of-plane electrical conductivity as compared to first experiment. The enhanced out-of-plane conductivity shows that CNTs are added into the matrix-rich

regions. The average out-of-plane electrical conductivity of carbon fiber/RTM6 was 0.016 S/cm. The highest conductivity was observed in third experiment with 0.1 wt% CNTs loading and stitched mid-ply and was shown 11.6 fold enhancement. While the RTM 6 epoxy showing improvement, west marine epoxy showed unstable behavior. Only sixth specimen showed little improvement about 1.4 fold. It may be due to differences in viscosity. Better CNTs dispersion was observed in RTM 6 epoxy. The electrical investigation will be continue.

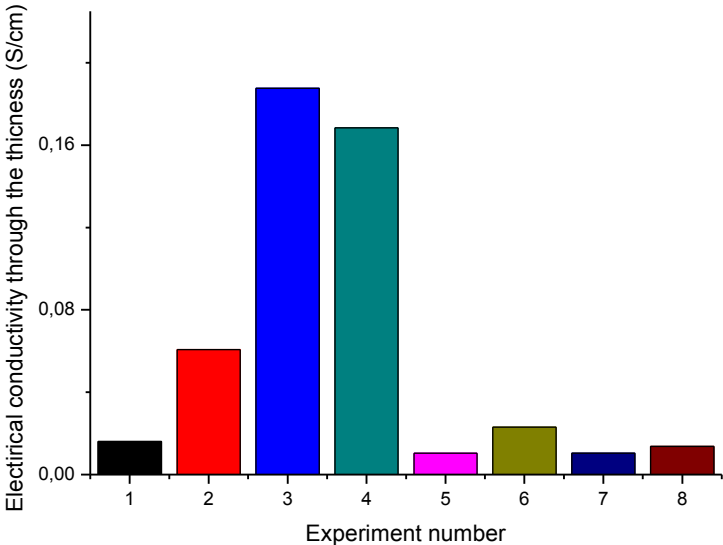


**Figure 5.12 :** Electrical conductivity through the thickness.



## 6. CONCLUSIONS AND FUTURE WORK

Nano engineered composite laminates with aligned and stitched CNTs were successfully fabricated and interlaminar shear strength property was investigated by using short beam shear test with the following main contributions;

- a. Synthesis of millimeter and micrometer-scale A-CNTs and PA-CNTs with a modified CVD process and their characterization and micro device fabrication.
  - i. Synthesis conditions in a 2'' tube furnace were optimized to produce A-CNTs. Easy delamination recipe was optimized for composite applications.
  - ii. A-CNTs were characterized by scanning electron microscopy, transmission electron microscopy, Raman spectroscopy and thermal gravimetric analysis to achieve information about morphological and thermal properties of CNTs. SEM images showed orientation and length of A-CNTs. High purity CNTs was determined using Raman spectroscopy.
  - iii. Substrate was prepared for patterned CNTs synthesis by using photolithography to fabricate nano-particle exchanger.
  - iv. Micro device was fabricated with PA-CNTs and A-CNTs. Adhesion property was investigated using different methods. Mold and flow channel were designed and fabricated. Nano-particle and gas exchange transfer will studied with this context.
- b. Fabrication and testing of nano-filler and stitched nano engineered composites
  - i. In order to limited experiment number and determine the effect level, in this study Taguchi L8 orthogonal array was used and it was analyzed using Minitab 16 software. 7 parameters were investigated using 8 experiments results.
  - ii. Customize prepreg was manufactured with different CNTs loading to use for stitch application. Nano engineered laminates were manufactured using vacuum infusion and hand lay-up methods.

- iii. Electrical conductivity was investigated using two-probe method and the studies will be continue on this issue. Highest electrical conductivity improving was about 12-fold.
- iv. Short beam shear test was performed to determine interlaminar shear strength and fracture analysis was carried out using scanning electron microscopy to understand effect of CNTs in composite. Highest ILSS improving was about 18-fold.
- v. The fuzzy fiber was created successfully and structure health monitoring system will be studied.

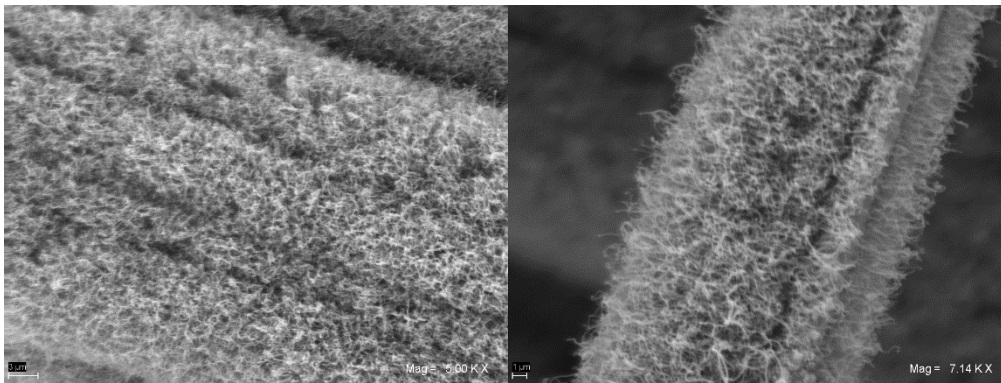


**Figure 6.1** : Fuzzy fiber SEM image.

## REFERENCES

- [1] **Qian, H., et al.**, (2010), Carbon nanotube-based hierarchical composites: a review. *Journal of Materials Chemistry*, **20**(23): p. 4751.
- [2] **Iijima S.**, (1991) Helical microtubules of graphitic carbon, *Nature*, (354): p. 56-58.
- [3] **Shanov, V.**, et al., (2013), *CVD growth, characterization and applications of carbon nanostructured materials*. *Surface and Coatings Technology*, **230**: p. 77-86.
- [4] **Chen, K.-R.**, (2013), *Optical-Electronic Properties of Carbon-Nanotubes Based Transparent Conducting Films*. *Advances in Chemical Engineering and Science*, **03**(01): p. 105-111.
- [5] **Liu, L., W. Ma, and Z. Zhang** (2011), *Macroscopic carbon nanotube assemblies: preparation, properties, and potential applications*. *Small*, **7**(11): p. 1504-20.
- [6] **Wicks, S.S.**, et al., (2014) *Multi-scale interlaminar fracture mechanisms in woven composite laminates reinforced with aligned carbon nanotubes*. *Composites Science and Technology*, **100**: p. 128-135.
- [7] **Georgousis, G.**, et al., (2015) *Strain sensing in polymer/carbon nanotube composites by electrical resistance measurement*. *Composites Part B: Engineering*, **68**: p. 162-169.
- [8] **Pozegic, T.R.**, et al., (2014) *Low temperature growth of carbon nanotubes on carbon fibre to create a highly networked fuzzy fibre reinforced composite with superior electrical conductivity*. *Carbon*, **74**: p. 319-328.
- [9] **Kumar, M. and Y. Ando**, (2010) *Chemical Vapor Deposition of Carbon Nanotubes: A Review on Growth Mechanism and Mass Production*. *Journal of Nanoscience and Nanotechnology*, **10**(6): p. 3739-3758.
- [10] **De Volder, M.F.**, et al., (2013) *Carbon nanotubes: present and future commercial applications*. *Science*, **339**(6119): p. 535-9.
- [11] **Belin, T. and F. Epron**, (2005) *Characterization methods of carbon nanotubes: a review*. *Materials Science and Engineering: B*, **119**(2): p. 105-118.
- [12] **Erik T. Thostenson, Z.R., Tsu-Wei Chou**, (2001) *Advances in the science and technology of carbon nanotubes and their composites: a review*. *Composites Science and Technology*, **61**: p. 1899-1912.
- [13] **See, C.H.**, (2007) *A Review of Carbon Nanotube Synthesis via Fluidized-Bed Chemical Vapor Deposition*. *Ind. Eng. Chem. Res.*, **46**.

- [14] **Chee Howe See, A.T.H.**, (2007) *A Review of Carbon Nanotube Synthesis via Fluidized-Bed Chemical Vapor Deposition*. *Ind. Eng. Chem. Res.*, **46**: p. 997-1012.
- [15] **Treacy, M.M.J., Ebbesen, T. W., & Gibson, J. M.**, (1996) *Exceptionally high Young's modulus observed for individual carbon nanotubes*. *Nature*, **381**: p. 678-680.
- [16] **Wong, E.W., Sheehan, P. E., & Lieber, C. M.**, (1997) *Nanobeam mechanics: Elasticity, strength, and toughness of nanorods and nanotubes* *Science*, **277**: p. 1971-1975.
- [17] **Xie, S.S., Li, W. Z., Pan, Z. W., Chang, B. H., & Sun, L. F.**, (2000) *Mechanical and physical properties on carbon nanotube*. *Journal of Physics and Chemistry of Solids*, **61**(7): p. 1153-1158.
- [18] **Enkeleda D., Z.L.**, et al., (2009), *Carbon Nanotubes: Synthesis, Properties, and Applications*. *Particulate Science and Technology*, **27**: p. 107–125.
- [19] **Allen, R.J.**, et al., (2013) *Mechanical testing and modelling of a vertically aligned carbon nanotube composite structure*. *Composites Science and Technology*, **77**: p. 1-7.
- [20] **Viets, C., S. Kaysser, and K. Schulte**, (2014) *Damage mapping of GFRP via electrical resistance measurements using nanocomposite epoxy matrix systems*. *Composites Part B: Engineering*, **65**: p. 80-88.
- [21] **Song, Y.**, et al., (2014) *Multiscale Laminated Composite Materials*. *Changing Engineering Design* p. 627-647.
- [22] **Yamamoto, N., R. Guzman de Villoria, and B.L. Wardle**, (2012) *Electrical and thermal property enhancement of fiber-reinforced polymer laminate composites through controlled implementation of multi-walled carbon nanotubes*. *Composites Science and Technology*, **72**(16): p. 2009-2015.
- [23] **Dong, L.**, et al., (2014) *Preparation of continuous carbon nanotube networks in carbon fiber/epoxy composite*. *Composites Part A: Applied Science and Manufacturing*, **56**: p. 248-255.
- [24] **Ma, P.-C.**, et al., (2010), *Dispersion and functionalization of carbon nanotubes for polymer-based nanocomposites: A review*. *Composites Part A: Applied Science and Manufacturing*, **41**(10): p. 1345-1367.
- [25] **Inam, F.**, et al., (2010) *Multiscale Hybrid Micro-Nanocomposites Based on Carbon Nanotubes and Carbon Fibers*. *Journal of Nanomaterials*, **2010**: p. 1-12.
- [26] **Khan, S.U. and J.-K. Kim**, (2012) *Improved interlaminar shear properties of multiscale carbon fiber composites with bucky paper interleaves made from carbon nano-fibers*. *Carbon*, **50**(14): p. 5265-5277.
- [27] **Ma, P.-C. and Y. Zhang**, (2014) *Perspectives of carbon nanotubes/polymer nanocomposites for wind blade materials*. *Renewable and Sustainable Energy Reviews*, **30**: p. 651-660.

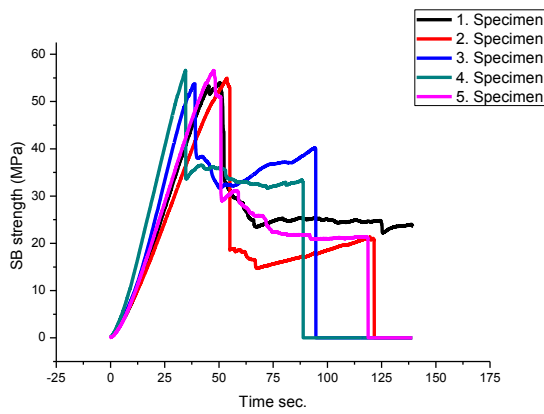
- [28] **Garcia, E.J., B.L. Wardle, and A. John Hart**, (2008) *Joining prepreg composite interfaces with aligned carbon nanotubes*. Composites Part A: Applied Science and Manufacturing, **39**(6): p. 1065-1070.
- [29] **Gojny, F.H.**, et al., (2005) *Influence of nano-modification on the mechanical and electrical properties of conventional fibre-reinforced composites*. Composites Part A: Applied Science and Manufacturing, **36**(11): p. 1525-1535.
- [30] **Wichmann, M.H.G.**, et al., (2006) *Glass-fibre-reinforced composites with enhanced mechanical and electrical properties – Benefits and limitations of a nanoparticle modified matrix*. Engineering Fracture Mechanics, **73**(16): p. 2346-2359.
- [31] **Green, K.J.**, et al., (2009) *Multiscale fiber reinforced composites based on a carbon nano-fiber/epoxy nanophased polymer matrix: Synthesis, mechanical, and thermomechanical behavior*. Composites Part A: Applied Science and Manufacturing, **40**(9): p. 1470-1475.
- [32] **Qiu, J.**, et al., (2007) *Carbon nanotube integrated multifunctional multiscale composites*. Nanotechnology, **18**(27): p. 275708.
- [33] **Giurgiutiu, V.**, (2015) *Structural health monitoring (SHM) of aerospace composites*. p. 449-507.
- [34] **Sánchez, M.**, et al., (2013) *Effect of the carbon nanotube functionalization on flexural properties of multiscale carbon fiber/epoxy composites manufactured by VARIM*. Composites Part B: Engineering, **45**(1): p. 1613-1619.
- [35] **Schadler, L.S., S.C. Giannaris, and P.M. Ajayan**, (1998) *Load transfer in carbon nanotube epoxy composites*. Applied Physics Letters, **73**(26): p. 3842.
- [36] **Gohardani, O., M.C. Elola, and C. Elizetxea**, (2014) *Potential and prospective implementation of carbon nanotubes on next generation aircraft and space vehicles: A review of current and expected applications in aerospace sciences*. Progress in Aerospace Sciences, **70**: p. 42-68.
- [37] **Vankanti, V.K. and V. Ganta**, (2014) *Optimization of process parameters in drilling of GFRP composite using Taguchi method*. Journal of Materials Research and Technology, **3**(1): p. 35-41.
- [38] **Christopher T. Kingston, B.S.**, (2003) *Fabrication of Carbon Nanotubes*. ANALYTICAL LETTERS, 2003. **36**(15): p. 3119–3145.
- [39] **Siddiqui, N.A., S.U. Khan, and J.-K. Kim**, (2013) *Experimental torsional shear properties of carbon fiber reinforced epoxy composites containing carbon nanotubes*. Composite Structures, **104**: p. 230-238.
- [40] **Siddiqui, N.A.**, et al., (2011) *Manufacturing and characterization of carbon fibre/epoxy composite prepregs containing carbon nanotubes*. Composites Part A: Applied Science and Manufacturing, **42**(10): p. 1412-1420.

- [41] **Yokozeki, T.**, et al., (2007) *Mechanical properties of CFRP laminates manufactured from unidirectional prepregs using CSCNT-dispersed epoxy*. Composites Part A: Applied Science and Manufacturing, **38**(10): p. 2121-2130.
- [42] **ASTM D2344/D2344M – 13**, *Standard Test Method for Short-Beam Strength of Polymer Matrix Composite Materials and Their Laminates*. 2013.
- [43] **Fan, Z., M.H. Santare, and S.G. Advani**, (2008) *ILSS of glass fiber reinforced epoxy composites enhanced with MWNTs*. Composites Part A: Applied Science and Manufacturing, **39**(3): p. 540-554.

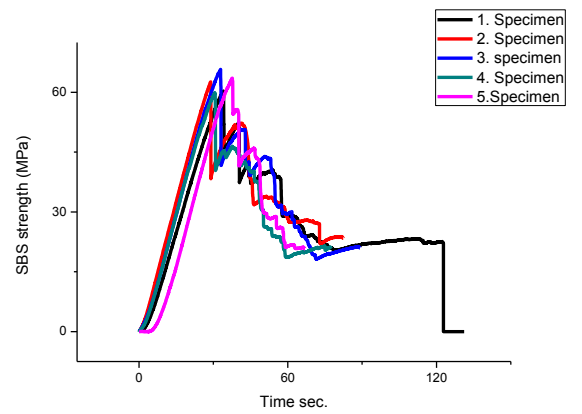
## APPENDICES

### APPENDIX A : SBS results

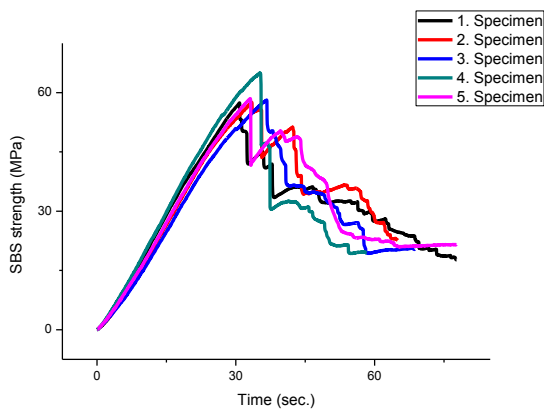
#### APPENDIX A



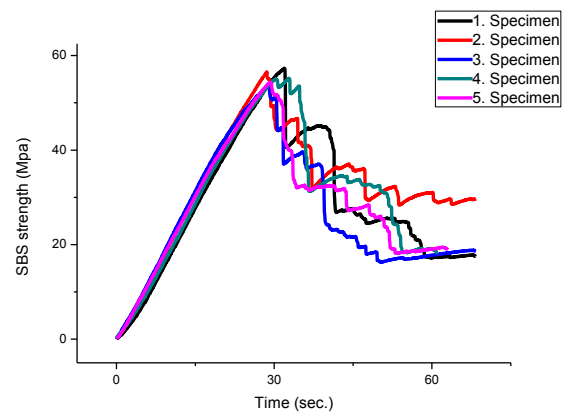
(a)



(b)

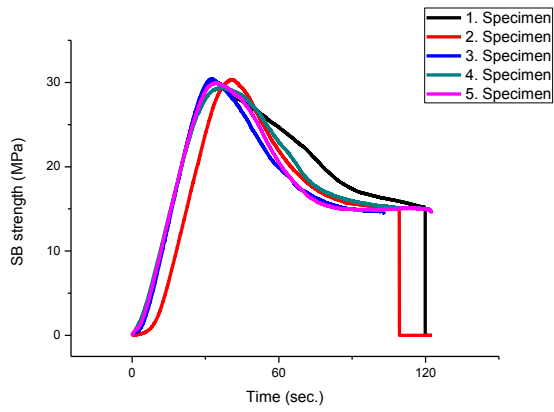


(c)

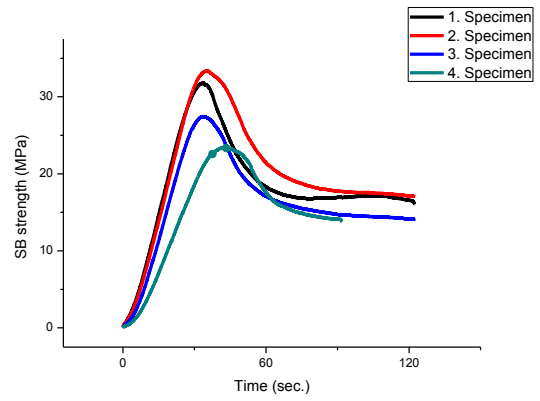


(d)

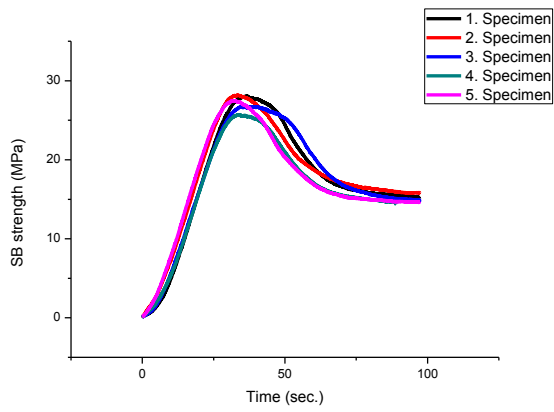
**Figure A.1** : Aerospace type epoxy experimental design results (a)First. (b)Second. (c)Third. (d)Fourth.



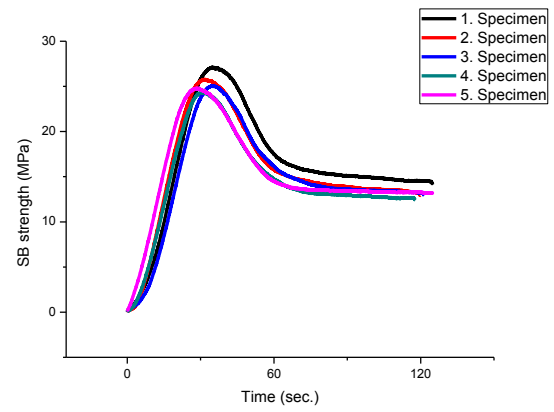
(a)



(b)



(c)



(d)

**Figure A.2** : Marine type epoxy experimental design results (a)Fifth. (b)Sixth. (c)Seventh. (d)Eighth.



## CURRICULUM VITAE

**Name Surname:** İdris GÜRKAN

**Place and Date of Birth:** 06/11/1987

**E-Mail:** [idrisgrkn@gmail.com](mailto:idrisgrkn@gmail.com)

### EDUCATION:

**B.Sc.:** Materials Science and Engineering/GYTE

### PUBLICATIONS, PRESENTATIONS AND PATENTS ON THE THESIS:

- \* **Gürkan, İ.**, Cebeci, H., 2015, Multiscale fibre reinforced composites with a carbon nanotube/epoxy nano-phased polymer matrix attached: Synthesis and interlaminar shear strength property investigation, *International Conference on Advances in Composite Materials and Structures*, 13-15 April 2015, Istanbul, Turkey, oral presentation.
- \* **Gürkan, İ.**, Çakıroğlu, D., Cebeci, F. Ç., Kavrar, D., Ergenc, A. F. Cebeci, H., 2014, Synthesis and Characterization of Arrays and Patterns of Vertically Aligned Carbon Nanotubes for Fabrication of a Micro-Device as a Nano-exchanger, *10th Nanoscience and Nanotechnology Conference*, 17-21 June 2014, Istanbul, Turkey, Nanotubes Session, poster presentation.
- \* Kavrar, D., **Gürkan, İ.**, Cebeci, H., 2014, Investigation the Effects of Carbon Nanotube Orientation on the Mechanical Properties of PDMS Polymer Nano-composites: Strain Hardening Evaluation, *10th Nanoscience and Nanotechnology Conference*, 17-21 June 2014, Istanbul, Turkey, Nano Materials Session, poster presentation.
- \* Nak H., **Gürkan İ.**, Ergenc A. F., Cebeci H., 2014, Carbon Nanotube Production System by Chemical Vapor Deposition: Control and Automation, *TOK 2014*, 11-13 September 2014 Kocaeli, Turkey, oral presentation.
- \* Ateşcan, Y., **Gürkan, İ.**, Kavrar, D., Cebeci, H., 2013, 'Impact Resistance of Hierarchical Composites Reinforced with Carbon Nanotubes, *Nano-TR Student Conference 2013*, 22 October 2013 Istanbul, Turkey, poster presentation.
- \* Kavrar, D., **Gürkan, İ.**, Çakıroğlu, D., Cebeci, F. Ç., Cebeci, H., 'Growth and Characterization of Vertically Aligned Multi-Walled Carbon Nanotubes, *Nano-TR Student Conference 2013*, 22 October 2013, Istanbul, Turkey, poster presentation